# Neurons derived from P19 embryonic carcinoma cells as a platform for biosensor applications – optimisation and characterisation

Dissertation

Zur Erlangung des Grades

Doktor der Naturwissenschaften

Am Fachbereich Biologie

Der Johannes Gutenberg-Universität Mainz

Hwei Ling Khor

geboren am 04.08.1977 in Singapore

Mainz, 2007

*Stuff is made out of dreams.*

*And life is made of many chanced encounters.*

# Table of Contents

# Abstract

P19 is a mouse-derived embryonal carcinoma cell line capable of differentiation toward ectodermal, mesodermal and endodermal lineages and could thus be differentiated into neurons. Different culture conditions were tested to optimise and increase the efficiency of neuronal differentiation since the population of P19-derived neurons was reported to be heterogeneous with respect to the morphology and neurotransmitters they synthesise. P19-derived neurons were cultured on microelectrode arrays as cell aggregates and as dissociated cells. Improved neuronal maturation was shown by the presence of microtubule associated protein 2, neurofilament and synaptophysin formation when initiation of neuronal differentiation was prolonged. High initial cell density cultures and coating of surfaces with polyethylenimine-laminin further improved neuronal maturation of differentiated P19 cells. Increased spontaneous activities of the P19-derived neurons were correspondingly recorded. Two to three hours recordings were performed between 17 and 25 days when extracellular signals were stabilised. It was found that P19-derived neurons developed network properties as partially synchronised network activities. P19-derived neurons appeared to give inhomogenous response to the 2 major neurotransmitters, γ-aminobutyric acid (GABA) and glutamate. The P19-derived neuronal networks obtained from optimised protocol in this thesis were predominantly GABAergic. The reproducible long term extracellular recordings performed showed that neurons derived from P19 embryonal carcinoma cells could be applied as a model for cell based biosensor in corporation with microelectrode arrays.

# 1.    Introduction

Beyond the investigation of single neurons, the analysis of their activity within small neuronal assemblies is a promising step forward to understand the function of networks within the central nervous system. Although the analysis of network behaviour may be achieved by multitude simultaneous patch-clamp recordings, it is very tedious and time consuming. Microelectrode arrays (MEAs) with dissociated neuronal cells or brain slices allow the convenient monitoring of spontaneous or stimulated electrical activities of excitable cells and enable the detection of neuroactive substance effects.

However, researchers face some difficulties when they start to utilise neuronal cells on MEAs: the serial preparation and cultivation of primary cells is labour intensive and requires highly skilled technicians beside high costs, long term scheduling and extensive animal care. Neuronal cell lines offer some clear advantages over freshly dissociated cells: they provide flexibility to the culturing process and represent a cell reserve that eliminates the need for timed pregnancy animals each time culture is initiated.

Cultured P19 embryonal carcinoma cells, a pluripotent cell type, can act as a renewable cell source which could be exploited for cell-based assay development. One of the major challenges faced for *in vitro* neuronal model cell types is the requirement for a source of cells that is both renewable and genetically stable in culture. Previous work has suggested that few neuronal cell lines express functional receptors[1, 2] such as $GABA_A$ receptors despite the expression of $GABA_A$ receptor subunits[3]. Reynolds *et al.*[4] had showed that $GABA_A$ receptor subunit mRNAs and GABA-induced currents were observed in P19-derived neurons.

## 1.1    Aim

1.  To optimise the differentiation of P19 embryonic carcinoma cells into the neuronal lineage.

    a.  To optimise the conditions for the extracellular recording of P19-derived neurons.

2.  To characterise the extracellular recording of P19-derived neurons in response to 2 major neurotransmitters L-Glutamate and GABA.

3.  To perform extracellular recording of olfactory receptor 5 transfected P19-derived neurons.

## 2. Literature Review

Biosensors incorporate a biological sensing element that converts a change in an immediate environment to signals conducive for processing. They have been implemented in environmental, medical, toxicological and defense applications.[1, 2, 5] Biosensors have 2 characteristics: they have a naturally evolved selectivity to biological or biologically active analytes and they have the capacity to respond to analytes in a physiologically relevant manner. There are at least three classes of biosensors, molecular, cellular and tissue. Molecular biosensors are based on antibodies, enzymes, ion channels or nucleic acids for detection of analytes. Cell based biosensors on the other hand have the added advantage of responding only to functional biologically active analytes. Cells express and sustain an array of potential molecular sensors. The receptors, channels and enzymes that are sensitive to an analyte are maintained in a physiologically relevant manner by native cellular machinery. Thus, cell based biosensors incorporating mammalian cells will have the advantage to offer insight into the physiological effect of an analyte.

In spite of the many advances in cell based biosensors, there are still many problems associated with them, such as analytical methods, reproducibility and reliance on primary, animal-derived cells.

## 2.1 Differentiation and Properties of Embryonal Carcinoma Cells P19-derived Neurons

Embryonic carcinoma cells resemble those comprising the inner cell mass of preimplantation blastocysts and a number of differentiated cell types, with characteristics of cells of the three germ layers, namely, ectodermal, mesodermal and endodermal that can be obtained reproducibly by different treatments.[6, 7]

Much is unknown about the determination events that commit unspecialized cells to differentiate into more specialised cell types that appear later during embryonic development. Lines of embryonal carcinomic cells can be isolated from

teratocarcinomas and maintained in an undifferentiated state when kept in exponential growth phase in tissue culture. If left undisturbed at high density, they differentiate *in vitro* into a variety of cell types including epithelium, neurons, muscle and cartilage. The value of the embryonic carcinoma cells in studying determination has been limited by the complexity of their differentiation patterns; any one determination event is obscured from study by others that occur simultaneously.

The P19 cell line was isolated by implanting a 7-day-old mouse embryo under the testis capsule of an adult which resulted in the formation of a tumour. The tumour cells were grown in culture and one clone, P19, was established as a line.

Treatment of P19 cells with retinoic acid (RA) in the range of $10^{-8} - 10^{-6}$ M induced their differentiation into a limited variety of cell types which appear to be similar to those derived from neuroectoderm.[8, 9] RA-treated P19 cell cultures have been shown to contain neurons, astroglia, microglia and cells resembling vascular smooth muscle[9, 10]. P19 derived neurons express a variety of neuronal markers such as the 68 000 and 160 000 molecular weight neurofilament proteins, tetanus toxin binding sites, synaptophysin and HNK-1 surface binding sites which marks for gycoproteins present on embryonic neurons[11]. Differentiation of cells was initiated after only one hour of RA treatment. The upregulation of retinoic acid receptor genes was more pronounced in the G1 phase of the cell cycle than in the S phase and continuous presence of RA was necessary to sustain this induction (up to 17 hours). Aggregation of the cells also enhanced the rate of RA mediated induction[12].

Although, it is a clonal cell line, P19 cells differentiate into populations of diverse neuronal cell types[10, 11, 13, 14]. Neurons initially comprised 30 – 70 % of the cells in the population.

Neuronal maturation (Figure 2.1) was defined as an integration of several aspects such as increased levels of expression of synaptic proteins, an increase in the level of evoked release and a more uniform distribution of post synaptic potential amplitude, segregation of axons and dendrites and morphological maturation of the synapse such
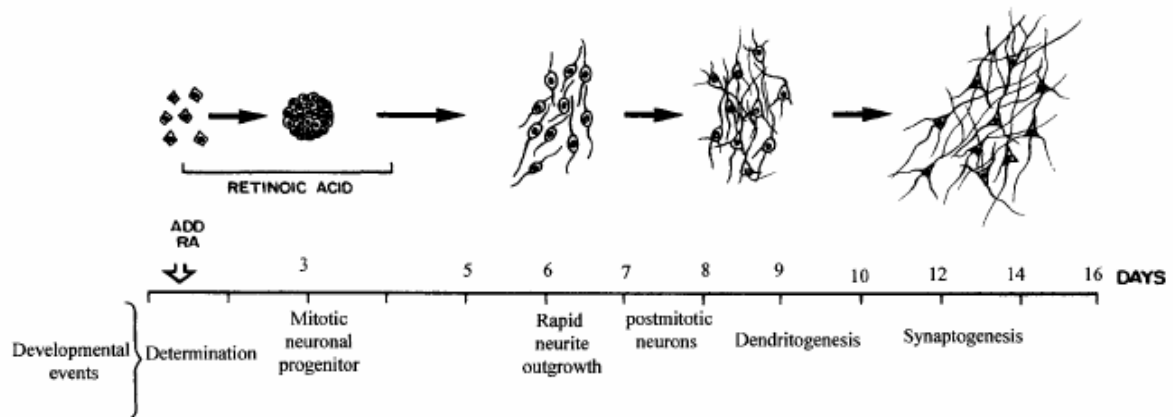
**Figure 2.1 A schematic view of cellular morphology during an interval beginning with the start of induction and ending 12 days later.[15]**

as clustering of synaptic vesicles near release sites. A variety of neurotransmitters, and associated gene transcripts and enzymes are expressed in P19-derived neurons.[11, 13, 14, 16] Work to characterise the neurotransmitters present in RA-treated P19 cell cultures indicated that the enzyme choline acetyltransferase (ChAT) could be detected biochemically, and that acetycholine was synthesized also[16]. The neurons from the RA treated cultures developed functional GABA receptors that are blocked by bicuculline and bezodiazpines.[4, 17] High affinity uptake sites for GABA were present on neuronal cells in RA-treated cultures. Some neurons contained the enzymes of the catecholamine synthetic pathway, although catecholamine was not detected chemically[11]. GABA is the predominant neurotransmitter but neuropeptide Y and somatostatin are also found in many neurons[14]. Functional ionotropic glutamate receptors of both NMDA and AMPA/kainite types (please see section 2.2.2.1) are also expressed in P19-derived neurons[18-20]. These receptors are hallmarks of neurons of the central nervous system and are not expressed in most of the commonly used neuronal cell lines.

## 2.2    Synaptic Transmission

A synapse is a specialised zone of contact at which one neuron communicates with another. The average neuron forms about 1000 synaptic connections and receives more, perhaps as many as 10 000 connections. Although many of these connections

are highly specialised all neurons make use of one of the two basic forms of synaptic transmission: electrical or chemical. The strength of both forms of synaptic transmission can be enhanced or diminished by cellular activity. This plasticity in nerve cells is crucial to memory and other higher brain functions.

## 2.2.1    Electrical synapses

At electrical synapse the pre- and postsynaptic cells communicate through special channels called gap junctions channels that serve as conduit between the cytoplasm of the two cells. The current that depolarises the postsynaptic cell is generated directly by the voltage gated ion channels of the presynaptic cell. As such, electrical synapses provide instantaneous signal transmission. Gap junctions can be found between glial cells as well as neurons. In glia, the gap junctions seek to mediate both intercellular and intracellular communication. Electrical stimulation of neuronal pathways in brain slices can trigger a rise of intracellular $Ca^{2+}$ levels in certain astrocytes, producing a wave of intracellular $Ca^{2+}$ throughout the astrocyte network. Although the exact function of such $Ca^{2+}$ waves are not known, their existence suggests that glial cells play an important role in signaling in the central nervous system.

## 2.2.2    Chemical synapses

Chemical neurotransmitters act either directly or indirectly in controlling the opening of ion channels in the postsynaptic cell (Figure 2.2). Receptors that gate ion channels directly are integral membrane proteins named ionotropic receptors. Many such receptors contained 5 sub-units, each of which is thought to comprise of 4 membrane spanning α–helical regions. Upon binding of neurotransmitter, the receptor undergoes a conformational change that results in the opening of the channel.

Indirect gating is mediated by activation of metabotropic receptors. They act by altering intracellular metabolic reactions. The receptor activates a GTP-binding protein which in turn activates a second messenger cascade that modulates channel activity. Many such second messengers activate protein kinases, enzymes that

phosphorylate different substrate proteins. In many cases, the protein kinases directly phosphorylate ion channels, leading to their opening or closing. The typical metabotropic receptor composed of a single subunit with 7 membrane spanning α–helical regions that bind ligand within the plane of the membrane.
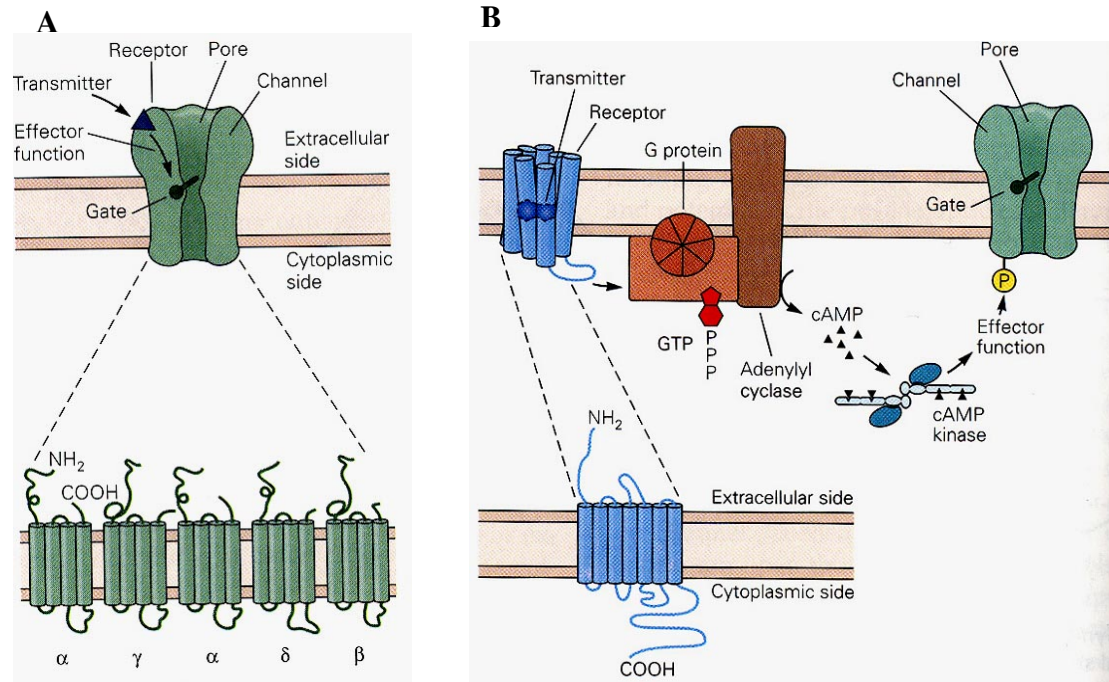


**Figure 2.2 Neurotransmitters act either directly (A) or indirectly (B) on ion channels that regulate current flow in neurons[21].**

The ionotropic receptors produce relatively fast synaptic actions lasting only milliseconds. They are commonly found in neural circuits that mediate rapid behaviours, such as the stretch receptor reflex. The metabotropic receptors produce slower synaptic actions lasting seconds to minutes. These slower actions can modulate behaviour by altering the excitability of neurons and the strength of the synaptic connections of the neural circuitry mediating behaviour. Such modulating synaptic pathways often act as crucial reinforcing pathways in the process of learning.

## 2.2.2.1 Neurotransmitters

In the invertebrate central nervous system, γ-aminobutyric acid (GABA) is the most widely distributed inhibitory neurotransmitter. It acts on 3 receptors, $GABA_A$, $GABA_B$ and $GABA_C$ receptors. $GABA_A$ and $GABA_C$ receptors are an ionotropic receptor that gates $Cl^-$ channel (Figure 2.3A, C). The $GABA_B$ receptor is a metabotrophic receptor that activates a second messenger cascade, which often activates $K^+$ and $Ca^{2+}$ channels.

$GABA_A$ receptors are well known targets for certain classes of environmental toxins and pharmaceutical compounds. The GABA-gated channel is the target for three types of drugs that are at once clinically important and socially abused: the benzodiazepines, barbiturates and alcohol. The benzodiazepines are anti-anxiety agents and muscle relaxants that include diazepam (Valium), lorazepam (Ativan) and clonazepam (Klonopin). The barbiturates comprise a group of hypnotics that includes phenobarbital and secobarbital. The four classes of compounds, GABA, bezodiazepines, barbiturates and alcohol act at different sites to increase the opening of the channel and hence enhance inhibitory synaptic transmission. The $GABA_A$ receptor channels can be composed of a variable of polypeptide subunits ($\alpha$1-6, $\beta$1-3, $\gamma$1-3, $\varepsilon$, $\delta$, $\pi$ and $\theta$). The $\alpha$, $\beta$ and $\gamma$ subunit classes are responsible for most of the $GABA_A$ receptor mediated fast inhibition in the mature nervous system. GABA can bind to any of the $\alpha$, $\beta$ and $\gamma$ subunits. The extracellular ligand binding domain of the subunits is followed by four hydrophobic transmembrane domains (labeled 1, 2, 3 and 4) (Figure 2.3B). Two molecules of GABA are needed to activate their respective channels.

In addition, it was shown that GABA has also an excitatory action in immature central neural system neurons which over time switches to the well established inhibitory action of the adult [22, 23]. A family of cation-chloride cotransporters has been identified to tightly control the chloride gradient across neurons, namely, the $Na^+$ -$K^+$ -$2Cl^-$ cotransporter (NKCC1) which is driven by sodium and potassium gradients, raises $Cl^-$ concentration and the $K^+$-$Cl^-$ cotransporter (KCC2) which couples the outward movement of $Cl^-$ and $K^+$ across the cell membrane. Immature neurons express
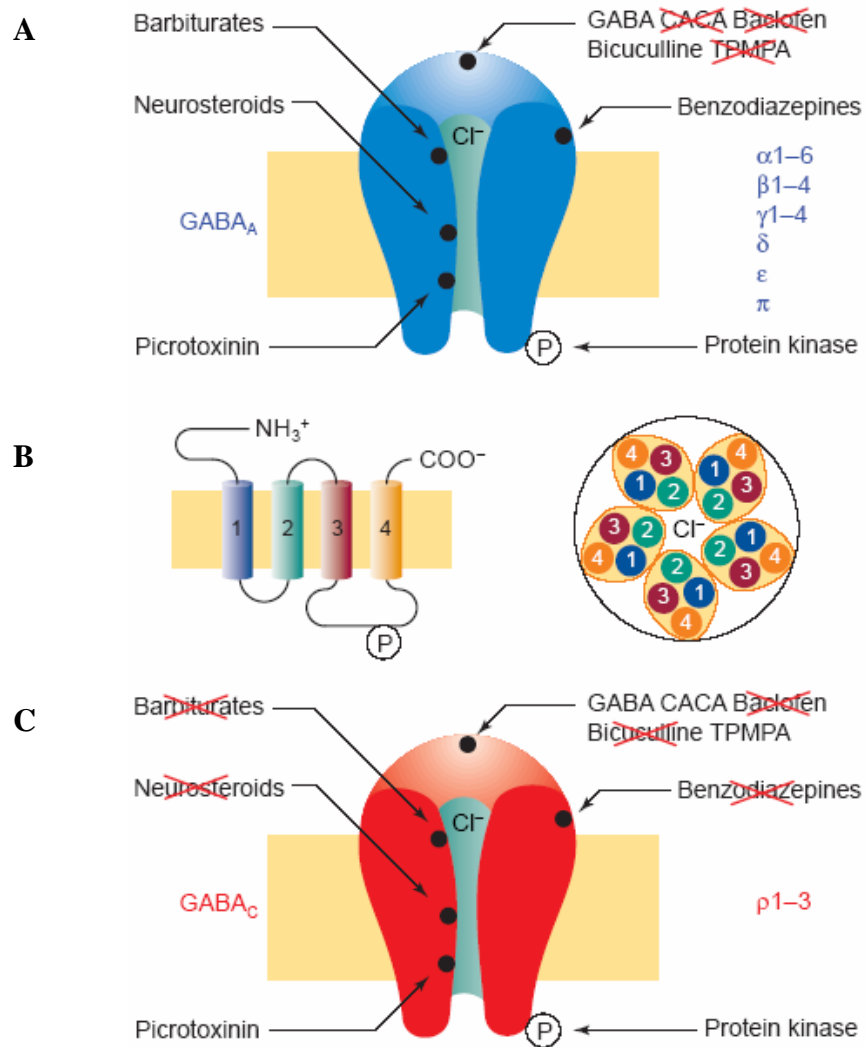
**Figure 2.3 Multiplicity of ionotropic GABA receptors [24]. (A) Pentameric GABA$_A$ receptors are composed of several types of related subunits. Each subunit has 4 transmembrane domains. The "2" domain lines the Cl$^-$ channel pore. GABA responses are blocked competitively by bicuculline and non-competitively by picotoxinin. Protein kinases modulate the GABA responses. (B) Each subunit comprises four transmembrane domains (1 – 4). The large intracellular loop between 3 and 4 contains consensus sites for phosphorylation by protein kinases. (C) GABA$_C$ receptors are composed exclusively of ρ (ρ1-3) subunits. The GABA$_C$ receptor is also a Cl$^-$ pore and is activated by agonist CACA (cis-4-aminocrotonic acid). It is blocked competitively and non-competitively by TPMPA (1,2,5,6-tetrahydropyridine-4-yl(methyl-phosphinic acid) and picotoxinin respectively. The red crosses indicate the non acting substances.**
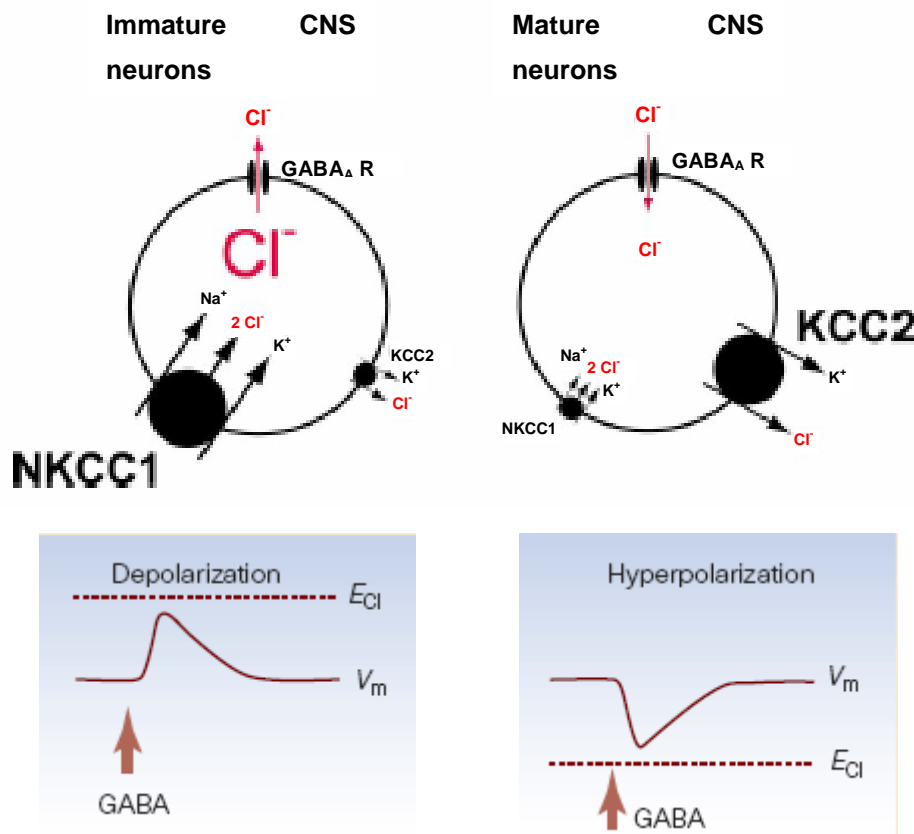
**Figure 2.4 Developmental regulation of chloride homeostasis in neurons [22, 23].** **(A)** Immature neurons express primarily NKCC1 and to a lesser extent KCC2, resulting in a high intracellular concentration of Cl⁻. Levels of intracellular Cl⁻ are high, and the equilibrium potential for Cl⁻, $E_{Cl}$, is positive relative to the membrane potential, $V_m$. **(B)** In mature neurons the expression of NKCC1 decreases and KCC2 increases. This results in a low intracellular Cl⁻ concentration. $E_{Cl}$ is negative relative to $V_m$ and the activation GABA$_A$ receptor inhibits the cell.

primarily NKCC1 and to a lesser extent KCC2, resulting in a high intracellular concentration of Cl⁻ so that GABA$_A$ activation causes Cl⁻ efflux and depolarization. In mature neurons the proportion of the cotransporters reverses and this results in a low intracellular Cl⁻ concentration so that GABA$_A$ receptor activation causes Cl⁻ influx and thus hyperpolarisation. In the developing cerebral cortex, GABA depolarises immature neurons to the point where calcium enters through both voltage-gated and N-methyl-D-aspartate receptor activated channels. The increased $Ca^{2+}$ controls gene expression and neurotrophin signaling and thus may control axonal connections. In the hippocampus, GABA depolarization induces a synchrony of cell firing. The large, rhythmic synaptic events and associated oscillations in intracellular $Ca^{2+}$ may provide

a natural trigger for plasticity of synaptic connections and thus establish and pattern the neural network.

The amino acid L-Glutamate is the major excitatory transmitter in the brain and spinal cord. Glutamate mediates physiological responses such as synaptic plasticity and long term potentiation and plays a role in neurodegenerative conditions such as stroke and epilepsy[25, 8]. Excessive exposure to glutamate can kill central neurons, resulting in a $Ca^{2+}$ overload in cells.[23, 26, 27] The glutamate gated channels conduct both $Na^+$ and $K^+$ with nearly equal permeability. The glutamate receptors can be divided into two broad categories: the ionotropic receptors that directly gate channels and metabotropic receptors that indirectly gate channels through second messengers (Figure 2.5). There are three major subtypes of ionotropic glutamate receptors: α-amino-3-hydroxy-5-methylisoxazole-4-propionic acid (AMPA), kainate and N-methyl-D-aspartate (NMDA). Ligand binding triggers $Na^+$ and/ or $Ca^{2+}$ influx and a surge in $Ca^{2+}$ concentration. The NMDA glutamate receptor is selectively blocked by APV (2-amino-5-phosphonovaleric acid). The AMPA and kainate receptors are blocked by the drug CNQX (6-cyano-7-nitroquinoxaline-2,3-dione). The metabotropic glutamate receptor can be selectively activated by trans-(1S,3R)-1-amino-1,3-cyclopentaedicaboxylic acid (ACPD). The action of glutamate on ionotropic receptors is always excitatory while activation of metabotropic receptors can be excitatory or inhibitory. Many excitatory synapses possess both NMDA and AMPA type glutamate receptors.

The glutamate receptor channels are thought to be tetramers composed of different types of closely related subunits ( Figure 2.6). The subunits have 3 transmembrane domains and a re-entrant loop. The AMPA and NMDA receptors have different pore properties that have been attributed to a single amino acid residue in the pore forming M2 region ( Figure 2.6). All NMDA receptor subunits contain the neutral but polar residue asparagine at a certain position in the M2 region. In most types of AMPA receptor subunits this residue is the uncharged polar amino acid glutamine. The glutamine containing AMPA receptors have similar permeability properties to those of the NMDA receptors in that they readily conduct $Ca^{2+}$.
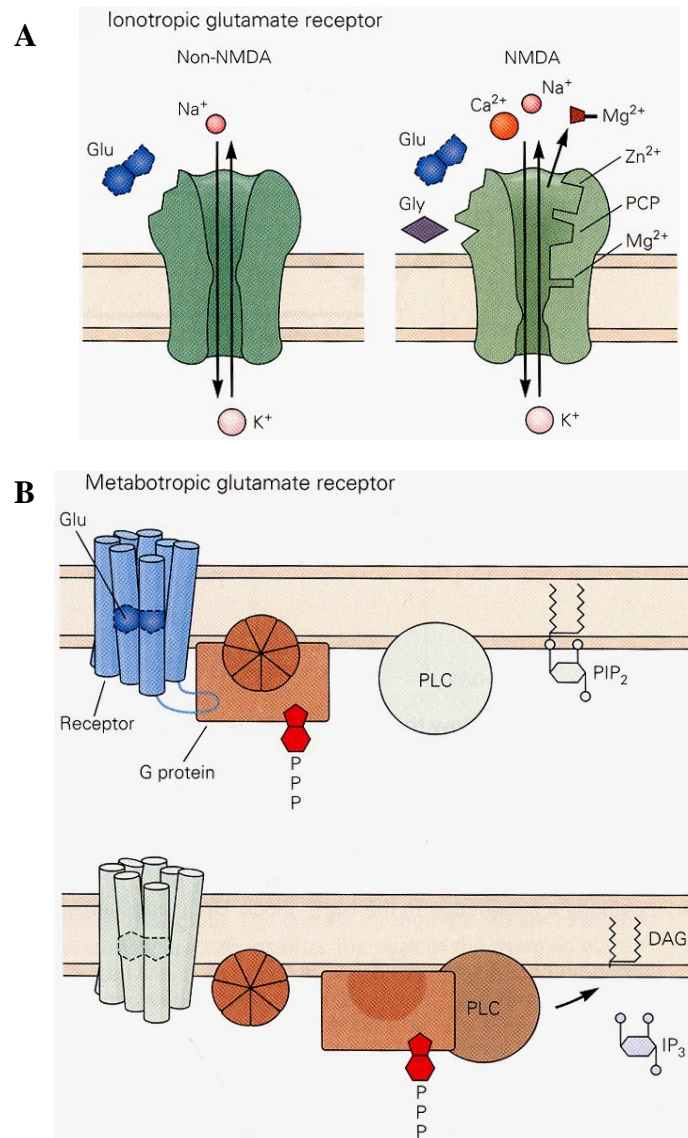
**Figure 2.5 Three classes of glutamate receptors regulate excitatory synaptic actions in neurons in the spinal cord and brain[28].** **(A) Two types of ionotropic glutamate directly gate ion channels. The non-NMDA receptors bind glutamate agonists kainite or AMPA and regulate a channel permeable to $Na^+$ and $K^+$. The NMDA receptor regulates a channel permeable to $Ca^{2+}$, $K^+$ and $Na^+$ and has binding sites for glycine, $Zn^{2+}$, phencyclidine (PCP), $Mg^{2+}$. (B) The metabotropic glutamate receptors indirectly gate channels by activating a second messenger. The binding of glutamate to some metabotropic glutamate receptors stimulates the activity of the enzyme phospholipase C (PLC), leading to the formation of two second mesessengers derived from phosphatidylinositol 4,5-biphosphate ($PIP_2$): inositol 1,4,5-triphosphate ($IP_3$) and diacylglycerol (DAG).**

The NMDA receptor channel comprises of the essential NR1 subunit and one or more of the modulatory NR2 subunits, NR2A – NR2D. It controls a cation channel of high conductance (50 pS) that is permeable to $Ca^{2+}$ as well as $Na^+$ and $K^+$. Opening of the channel requires extracellular glycine as a cofactor and its opening depends on membrane voltage and chemical transmitter. Extracellular $Mg^{2+}$ binds to a site in the pore of the open channel and blocks current flow. At the resting membrane potential (-65 mV) $Mg^{2+}$ binds tightly to the channel. But when the membrane is depolarized, $Mg^{2+}$ is expelled from the channel by electrostatic repulsion, allowing $Na^+$ and $Ca^{2+}$ to enter. Therefore, maximal current flows through the NMDA-type channel when glutamate is present and the cell is depolarized. Blockade of NMDA receptors produces symptoms that resemble hallucinations associated with schizophrenia. Most cells have both NMDA and non-NMDA glutamate receptors. However, due to the presence of $Mg^{2+}$ in the NMDA receptor channels during resting membrane potential, they do not contribute significantly to the excitatory post synaptic potential (EPSP). NMDA type receptor opens and closes relatively slowly in response to glutamate, thus contributing to the late phase of EPSP.

At developmentally early time points, many excitatory synapses are thought to be postsynaptically silent, possessing functional NMDA but lacking functional AMPA receptors. Mechanisms such as long term potentiation exist that recruit functional AMPA receptors to these silent synapses.[29, 30] During bouts of synaptic activity, AMPA receptor mediated depolarization of the postsynaptic membrane facilitates activation of NMDA receptors, that initiate $Ca^{2+}$-dependent signaling pathways that modulate the surface presence of AMPA receptors. Changes in AMPA receptors at the postsynaptic membrane cause changes in synaptic strength.[31]

AMPA receptors mediate the vast majority of the fast excitatory synaptic transmission and consist of a combination of four subunits GluR1 – GluR4.[32] Only AMPA receptors that lack the GluR2 subunit are permeable to $Ca^{2+}$. The deactivation and "intrinsic" desensitisation of AMPA receptors is defined as the decrease in responsiveness to a prolonged pulse of glutamate. Gating of AMPA channels is rapid in cochlear nucleus neurons, in inhibitory interneurons of the neocortex and the hippocampus, while it is slower in hippocampal granule cells and pyramidal neurons, and neocortical pyramidal neurons. Cyclothiazide (CTZ) is a complete blocker of

desensitisation of AMPA channels and is able to increase glutamate release.[33-35] It is a non-competitive AMPA antagonist that acts as a positive allosteric modulator by stabilising a non-desensitised agonist bound state of the receptor complex.[36] It has been recently found that CTZ can also directly inhibit GABA$_A$ receptors.[37] It has the unique characteristic in acting simultaneously on two prominent synaptic transmission systems: it significantly enhances excitatory glutamatergic neurotransmission while suppressing inhibitory GABAergic neurotransmission. The net effect of CTZ on a neural network will be a significant tilt of the excitation-inhibition balance toward hyperexcitation. CTZ has been known to increase presynaptic glutamate release. CTZ acts as a modulator of AMPA and GABA$_A$ receptors and is not associated with significant cell death.[38] Chronic treatment (5 µM, 48 hours) and acute treatment (20 – 50 µM, 1 – 2 hours) with CTZ has been shown to cause a permanent alteration of the functional output of neural networks after the treatment.
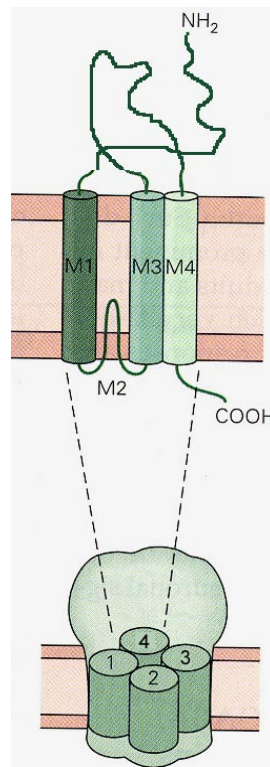


**Figure 2.6 The glutamate receptor channels are found to be tetramers composed of different types of closely related subunits. The subunits have 3 transmembrane domains and one region, M2, that forms a loop that dips into the membrane. Figure modified from Kandel et al.[28]**

## 2.2.3    Olfactory Receptors

Olfactory receptor cells transform the concentration profile of volatile odours in the air into a train of action potentials that can be conveyed to the olfactory bulb. Olfactory transduction takes place in the cilia of the olfactory receptor cells which forms a dense mat in the mucus lining the nasal cavity. Odour molecules dissolve in the mucus film and bind to one of a large family of receptors (R) in the ciliary membrane which then activates a G protein-coupled cascade resulting in the synthesis of cyclic adenosine monophosphate (cAMP) from adenosine triphosphate (ATP) by adenylyl cyclase (AC) (Figure 2.7). The olfactory receptors are members of the seven transmembrane domain, G protein-coupled receptor (GPCR) superfamily.

The consequent rise in cAMP concentration leads to the opening of cyclic nucleotide-gated channels (CNG) conducting $Na^+$ and $Ca^{2+}$ into the cilia, indicating the electrical response to odour stimulation. $Ca^{2+}$ in turn opens $Ca^{2+}$ activated $Cl^-$ channels and since intracellular concentration of $Cl^-$ is high, it leads to $Cl^-$ efflux and thus further depolarization. In contrast to these excitatory actions, $Ca^{2+}$ feeds back negatively upon the receptor current by reducing the affinity of the CNG channel to cAMP through calcium-calmodulin (Ca-CaM) binding. Ca-CaM in turns activates CaM kinase (CaMK) which phosphorylates AC and reduces cAMP production. A $Na^+$-$Ca^{2+}$ exchanger extrudes the $Ca^{2+}$ which entered during the odour response and returns intraciliary $Ca^{2+}$ concentration to pre-stimulus levels so that the $Ca^{2+}$ activated $Cl^-$ channel closes and the response is terminated.
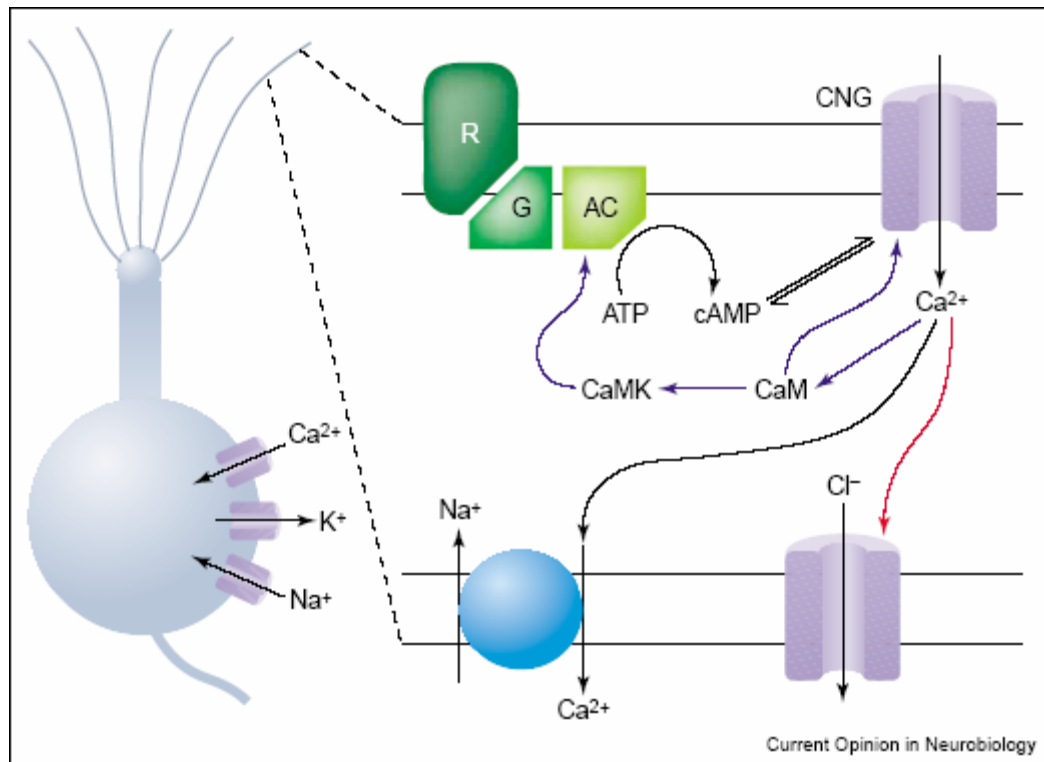
**Figure 2.7 A schematic diagram that illustrates the olfactory transduction.[39] Blue and red arrows indicate the inhibitory and excitatory actions of $Ca^{2+}$ respectively.**

## 2.3    Electrophysiology of P19-derived Neurons

Most neuroblastoma cell lines are not a suitable model for studying neuronal development because they neither become post-mitotic nor express ionotropic glutamate receptors of both the NMDA and AMPA/kainite types. Few neural cell lines also express functional $GABA_A$ receptors, the capacity to rapidly screen for compounds that affect $GABA_A$ receptor function is presently limited.[2, 3] Therefore, P19 embryonal carcinoma cells with the capability to be differentiated into the neuronal lineage and amenable to genetic modification were explored for the application as a cell based biosensor.

P19 neurons were shown to be functional following implantation into the rat brain[40]. Grafted P19-derived neurons had been shown by intracellular recordings to survive and mature *in vivo* capable of displaying mature, stable neuronal electrophysiological characteristics after four weeks.[40, 41] Membrane input resistance decreased and a

resting membrane potential of up to -68 mV was established. Active properties (action potentials) developed rapidly following the establishment of the resting membrane potential and decrease in input resistance, resulting in the earliest action potential with a small amplitude, long duration and without any associated after hyperpolarisation. The appearance of functional voltage-dependent $Na^+$ channels capable of generating action potential resulted later in the capability to elicit significant after-hyperpolarisation showing the presence of $K^+$ channels. Only the combination of both tetrodotoxin (TTX) and low $Ca^{2+}$/high $Mg^{2+}$ completely blocked spiking activity indicating that both TTX sensitive $Na^+$ channels and $Ca^{2+}$ channels participate in spike generation. P19-derived neurons reached a final stage of development electrophysiologically similar to the adult forebrain neurons including cortical and hippocampal pyramidal neurons.

## 2.4    Microelectrode Array

The quick and reliable measurement of harmful substances in the environment, of medically relevant metabolites and pharmacological substances, and of compounds important to the food industry, necessitates the development of a great variety of sophisticated sensor systems. However, the analytical demands for a chemical sensor such as selectivity, sensitivity, accuracy, stability and rapidity are not easily achieved for every compound of interest. Biosensors have therefore evolved to expand the sensing domain and accelerate crucial reactions. Within this group, whole cell-based sensors are receiving increasing attention because they have the potential to perform unique sensory functions by relying on the response amplification and reliability provided by populations of living sensor units.[1, 2, 5, 42]

Electrical activity of electrogenic cells in neuronal and cardiac tissues can be recorded by means of microelectrode arrays (MEA) that offer the possibility for non-invasive extracellular recording from as many as 60 sites simultaneously.[5, 43, 44] Since its introduction thirty years ago, the technology and the related culture methods have been continually improved and have found their way into many academic and industrial laboratories. This technology has attracted increased interest due to the

industrial need to screen selected compounds against ion channel targets in their native environment at the organic, cellular and sun-cellular level.[5]

Recording experiments using MEAs are useful to gain information about interactions between electrogenic cells at different locations in the same tissue, which may be used to analyse the spatio-temporal dynamics of activity or the representation of information in neuronal networks. They can also monitor changes of electrical activity over periods of time not accessible with individual conventional electrodes such as glass capillary or tungsten electrodes *in vitro*. The culture of random networks of neurons on MEAs were used to perform reliable biochemical sensing[45-50] although the density of synaptic formations in such artificial networks have been found to be lower than that found in physiological environments.

Nerve cells which have a diameter of $10 - 100$ μm are surrounded by an electrically insulating membrane. The thin phospholipid bilayer of about 5 nm thick separates the intracellular electrolyte with about 100 mM KCl from the environment with about 100 mM NaCl. The electrical current through the membrane is mediated by specific protein channels for sodium and potassium ions with a conductance of about $10 - 100$ pS.[51] In the generation of action potentials only small amounts of ions are actually involved in the potential change and these are all in the vicinity of the cell membrane.[43] The mechanism of action potential propagation ensures that the action potential is transmitted unattenuated along the membrane itself. Effectively, this means that some sections of the membrane must be net positive with respect to the extracellular fluid as the action potential passes over that section of membrane whilst adjacent sections retain their normally negative potential relative to the outside (Figure 2.8). The ionic distribution around the membrane can be considered as an electrostatic travelling dipole charge of the membrane. The extracellular electrode should detect the action potential first as a negative charge at the membrane followed by a positive charge as that section of the membrane recovers. This results in a different waveform for the detected extracellular signal in comparison with the intracellular signal. Theoretical electrostatic modeling of the membrane has shown that the extracellular voltage close to the active membrane, for a cell in a volume conductor can be related to the second differential of the intracellular voltage signal

with respect to time.[52] In practice, with the MEA the measured signal will be modified by the proximity of the external electrode and dependent on the cell-electrode interface impedance.
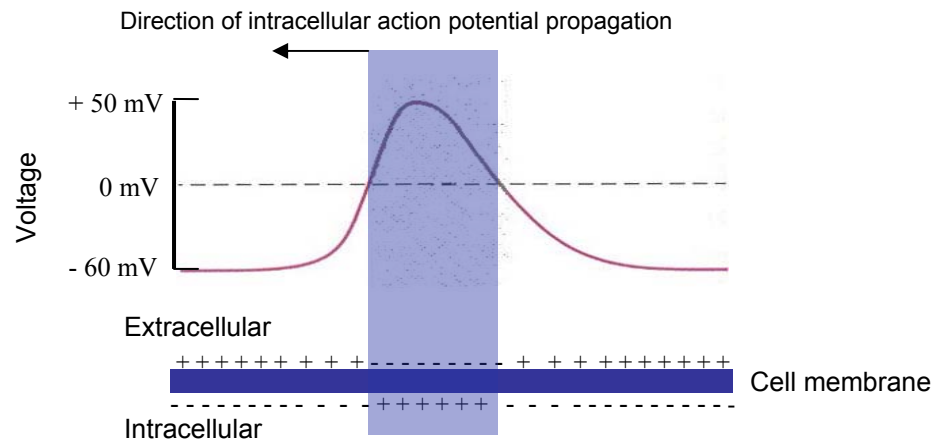


**Figure 2.8 Some sections of the membrane must be net positive with respect to the extracellular fluid as the action potential passes over that section of membrane whilst adjacent sections retain their normally negative potential relative to the outside. The ionic distribution around the membrane can be considered as an electrostatic travelling dipole charge of the membrane.**

With MEAs extracellular potential of cellular sources are recorded at the two-dimensional surface of a conductive cell population where electrogenic cells are in contact with the planar substrate (Figure 2.9A). Such a system in principle consists of three main components: 1) the cell population with the signal sources, 2) the interface between the cells and the electrodes and 3) the substrate with the embedded microelectrodes that are connected either to filter amplifiers and recording software or stimulation sources. The sources of the recorded signals are compartments of single neurons namely, dendrites or axon hillocks. By summation of the simultaneous activity of a population of cells a continuous potential field is generated. Its spatial modulation reflects the distribution, orientation, polarization and density of signal sources. The extracellular voltage change of a neuron recorded by a MEA closely approximates the first derivative of the intracellular action potential (Figure 2.9B).
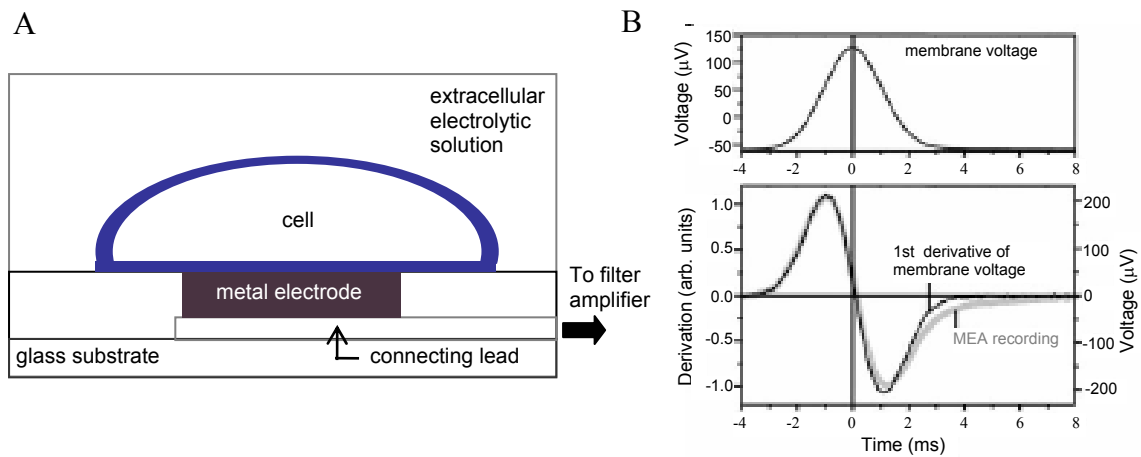
**Figure 2.9 Extracellular potential of cellular sources are recorded at the two-dimensional surface of a conductive cell population where electrogenic cells are in contact with the planar substrate. (A) A single cell cultured on a planar electrode. (B) Comparison of intracellular (top) and extracellular (bottom) voltage.[5]**

Neuronal networks are intrinsically non-linear dynamic systems which create complex electrophysiological spatio-temporal patterns through rapid communication between neurons in the network. Spontaneous network activity generated by neuronal cultures is used as a basic dynamic platform on which changes in activity represent detection events. Knowledge of complex and still unknown sensory coding is consequently not required. Neurons are homeostatic systems that constantly regenerate molecules and may be considered renewable receptor platforms. A network of such neurons should provide reliability and greater reproducibility. Neuronal networks are fault tolerant and maintain activity patterns despite the loss of network components and alteration of the circuitry. In this manner, a spontaneously active neuronal ensemble might be engineered to sense a variety of chemical compounds with the potential to provide sensitivity, accuracy and long term on line performance.

# 3.    Materials and Methods

## Protocol 1: Growth and maintenance of P19 cells in culture

P19 cells (ATCC, VA, USA, CRL-1825) culture must be maintained in the exponential growth phase. P19 cells grow rapidly with a generation time of 12-14 hours.

1. Cells are cultured in α-modified form of Eagle's minimal essential medium (MEM α medium, PAA Laboratories, Pasching, Austria, E15-862 with L-Glutamine) supplemented with 7.5 % (v/v) calf serum (New born calf, Cat. no.16010-159, Gibco[®], Invitrogen Corporation, CA, USA,) and 2.5 % (v/v) fetal bovine serum (Gibco[®]).

   For 500 ml
   a. 37.5 ml calf serum
   b. 12.5 ml fetal bovine serum
   c. MEM amino acid solution (PAA Laboratories, Cat. no. M11-002, without glutamine)
      i. Stock 50X concentration – 10ml in 500ml medium
   d. MEM vitamins (100X) (PAA Laboratories, Cat. no. N11-002)
      i. 5 ml in 500 ml medium

2. P19 cells are subcultured at intervals of 48 hours or less in order to maintain continuous exponential proliferation. Rinse the culture with $Ca^{2+}$ and $Mg^{2+}$ free PBS.

3. Add Trypsin-EDTA solution (10X concentration, Gibco[®]): 1mM EDTA + 0.025 % (w/v) trypsin in phosphate buffered solution (PBS) for a few minutes or until the cultures are seen detaching.

4. Centrifuge the cell suspension at 1000 rpm for a few minutes.

5. 1 culture flask can be approximately expanded into 3-5 flasks.

## Protocol 2: Induction of neuronal differentiation

1. Differentiation of P19 cells into the neuronal lineage was optimised according to 2 different induction conditions, IC1 and IC2.
   a. IC1: 1 day monolayer culture followed by a 1 day suspension culture
   b. IC2: 4 day suspension culture

2. Differentiate the P19 cells when they are 70 – 80 % confluent which is usually 2 days after the last passage. Do not allow them to be too confluent before the initiation of differentiation.

3. Sterile filter high grade ethanol.

4. Dissolve all trans-retinoic acid (RA) in ethanol to a stock solution of 3 mg/ml (0.01 M).
   a. 50 mg retinoic acid (Sigma-Aldrich Co., Saint Louis, USA, Cat. no. R2625)
   b. 16.7 ml ethanol
   c. Sensitive to light, wrap falcon tube with aluminum foil and store it at - 20 $^0$C
   d. Stock solution is stable for 1 month

5. For IC1 cultures, add 0.5 µM or 1 µM RA to culture flasks at one day after the previous passage and leave it alone for a day.

6. Trypsinise the cultures as in Protocol 1, step 3.

7. Prepare 60 mm bacteria grade petri dish (Greiner Bio-One GmbH, Frickenhausen, Germany, Cat. no. 633180) for the suspension culture. Add 10 ml MEM-α medium with supplements to each petri dish and leave them in the incubator.

8. Resuspend the cell pellet and count the equivalent volume for 1 x $10^6$ cells.

9. Take the volume of the cell suspension added to the petri dish into account to make up a final volume of 10 ml. Remove the equivalent volume of medium from each petri dish. Add $1 \times 10^6$ cells per petri dish.

10. Concentration of trans-retinoic acid added to the culture is $0.5 \times 10^{-6}$ M or $1 \times 10^{-6}$ M
    a. Vortex the stock solution to ensure that the precipitate is re-dissolved (Leaving the stock solution at room temperature for 15 min helps to re-dissolve it faster)

11. Add 0.5 μl (0.5 μM) or 1 μl (1 μM) of stock RA solution to every 10 ml medium and cell suspension.

12. Rock the suspension gently to ensure even mixing of cells and RA. Leave the petri dishes undisturbed in the incubator for 1 day (IC1 cultures) and 4 days (IC2 cultures).

13. After 1 day (IC1 cultures) and 4 days (IC2 cultures), remove and centrifuge the suspension at 1000 rpm for 5 min at room temperature. Wash the petri dish 1 X to ensure that most of the cell aggregates are removed.

14. Remove media and rinse the pellet once with 37 $^0$C PBS. Centrifuge the aggregates again.

15. Prepare 40 ml aliquots of B-27 (50X, Gibco®, Cat. no. 17504) and L-glutamine (200 mM, Gibco®, Cat. no. 25030-032) supplemented Neurobasal medium (Gibco®, Cat. no. 21103). Constituents of the Neurobasal medium and B-27 can be found in Brewer et al.[53]
    For 49.1 ml Neurobasal medium add
    a. 800 μl B27 supplement
    b. 100 μl L-glutamine

16. For IC1A cultures, resuspend the aggregates in supplemented Neurobasal medium in step 14 and seed approximately 40 aggregates / $cm^2$ on poly-D-lysine (PDL) (Sigma-Aldrich Co., Cat. no. P6407) coated surfaces (Protocol 3). 10 -12 samples were seeded.

17. Add 0.05 % Trypsin to reduce cell aggregate size (IC1S and IC2S cultures). Add 3 ml 0.05 % trypsin and 15 µl DNAse I (200X stock, Roche Diagnostics GmbH, Mannheim, Germany, Cat. no. 1284932) for every 3 - 4 petri dishes of aggregate suspension. Incubate in water bath at 37 $^0$C for 5 min with gentle rocking.

18. Centrifuge at 1000 rpm at room temperature for 10 min.

19. Remove medium and add supplemented Neurobasal medium. Use a fire polished glass pipette to break up the aggregates into single cells, about 40 – 50 times of pipetting.

20. Seed the single cells on to coated substrates (see Protocol 3 for preparation of coated substrates) at either 20 000 cells/$cm^2$ (IC1S-20K) or 40 000 cells/$cm^2$ (IC1S-40K, IC2S-40K). 10 – 12 samples in each experimental group were seeded.

21. The age of the neuronal cultures was then annotated as the number of days post seeding.

22. On the 5$^{th}$ day, change half the medium with Neurobasal Medium supplemented with B-27 only. Glutamine encourages glial cell growth and contributes to neuronal mortality.

23. Medium is changed every 2 days after 12 - 14 days of culture or when medium is yellow.

## Protocol 3: Coating Substrates

1. Clean substrates before coating:

    i. 12 mm diameter glass coverslips (Paul Marienfeld GmbH & Co. KG, Lauda-Königshofen, Germany) were left in Ethanol – HCl solution (90 % / 10 %) for 2 – 3 hours

    ii. They were then rinsed in ethanol and dried with an air gun.

2. The cleaned coverslips were autoclaved and dried in an oven.

3. All coating solutions were sterile filtered with 0.22 μm PVDF syringe filters (Rotilabo®, Carl Roth GmbH, Karlsruhe, Germany, Cat. no. P666.1).

4. Coating solutions

    a. Poly-D-lysine (PDL) (Sigma-Aldrich Co., Cat. no. P6407) coated substrates: 70 – 150 kDa, 0.1 mg/ml in PBS

    b. P19 laminin fragment (LN) (Sigma-Aldrich Co., Cat. no. C6171) coated substrates: 10 μg/ml in PBS

    c. PDL–LN coated surfaces: 200 μg/ml PDL in PBS

    10 μg/ml LN in PBS

    d. Polyethylenimine (MW 70 000, Polysciences Europe GmbH, Eppelheim, Germany, Cat. no. 9002-98-6) – laminin (PEI-LN) coated surfaces:

    1 mg/ml PEI in PBS

    10 μg/ml LN in PBS

5. The autoclaved glass coverslips were placed in 12-well plates.

6. The glass coverslips were coated with 80 μl solutions in step 4 overnight at room temperature under the lamina flow bench.

7. The coated glass cover slips were rinsed 3 times with sterile MilliQ water (Millipore Corporation, MA, USA) and allowed to dry under the lamina flow hood.

8. PDL-LN and PEI-LN samples were coated with the final layer of laminin fragment and incubated at 37 $^0$C for an hour.

9. PDL-LN and PEI-LN samples were then rinsed in sterile MilliQ water 3 times and allowed to dry under the lamina flow hood.

## Protocol 4: Immunostaining

1.  Media was removed and samples were washed once with warm PBS.

2.  Samples were fixed by incubating with 4 % paraformaldehyde, 3 % sucrose solution (pH 7.4) for 20 minutes at 4 $^0$C.
    a.  Preparation of fixative solution (50 ml)
        i.   25 ml deionised water
        ii.  2 g paraformaldehyde
        iii. Heat to 60 $^0$C, stir
        iv.  Add 4 - 5 drops of 1N NaOH
        v.   Add 1.5 g sucrose
        vi.  Add PBS and adjust pH to 7.4, making the final volume of 50 ml

3.  The samples were rinsed 3 times, 5 min each with cold PBS. The fixed samples can be stored at 4 $^0$C for up to 2 weeks.

4.  The samples were incubated with 5 % goat serum (Dianova, Hamburg, Germany) in PBS at room temperature for 30 min to block unspecific binding.

5.  Wash 3 times with PBS.

6.  Incubate with 0.6 % Triton X-100 (Sigma-Aldrich Co.) in PBS at 4 $^0$C for 20 min.

7.  Wash 3 times with PBS and tap the remaining liquid off the samples.

8.  Dilute primary antibodies in PBS added with 1 % goat serum and 0.15 % Tween20 (Sigma-Aldrich Co.).

9.  Incubate diluted primary antibodies for a specified time shown in Table 3.1.

10. Wash 3 times with PBS and tap the remaining liquid off the samples onto a piece of paper.

11. Incubate the samples with secondary antibodies for a specified time shown in Table 3.2.

12. Wash 3 times with PBS.

13. To stain the nuclei, incubate with 0.25 μg/ml 4, 6-diamidine-2-phenylindol-dihydrochloride (DAPI) (Roche Diagnostics GmbH) in PBS for 5 min at room temperature.

14. Wash 3 times with PBS.

15. The samples were mounted with Fluorescence Mount Medium (DakoCytomation, CA, USA) and sealed with nail polish.

16. The samples were viewed either under a confocal laser microscope (Carl Zeiss LSM 510, Carl Zeiss AG, Cologne, Germany) or fluorescence microscope (Olympus IX70 and U-RFL-T power supply unit, Tokyo, Japan).

| Antigen | Anti-serum | Concentration | Incubation conditions | Manufacturer |
|---|---|---|---|---|
| Microtubule associated protein 2 (MAP2) | Rabbit IgG | 1:200 | 3 hours, 4 $^0$C | Chemicon Europe, Hofheim, Germany, Ab5622 |
| MAP2a/2b | Mouse IgG1 | 1:200 | 3 hours, 4 $^0$C | Abcam Ltd, Cambridge, UK, ab11268 |
| Neurofilament 160 kD (NF160) | Mouse IgG2a | 1:200 | 8 hours, 4 $^0$C | Abcam, ab7794 |
| Glial fibrillary acidic protein (GFAP) | Mouse IgG1 | 1:400 | 3 hours, 4 $^0$C | Chemicon, MAB360 |
| Glutamic acid decarboxylase 65/67 (GAD) | Rabbit IgG | 1 :600 | 12 hours, 4 $^0$C | Sigma-Aldrich Co., G5163 |
| Synaptophysin | Mouse IgG1K | 1:400 | 12 hours, 4 $^0$C | Chemicon, MAB5258 |
| Olfactory receptor 5 C-Terminus | Mouse IgG2b | 1:500 | Overnight, 4 $^0$C | Lemker[54] |

**Table 3.1 List of primary antibodies used.**

| Antigen | Anti-serum | Concentration | Incubation conditions | Manufacturer |
|---|---|---|---|---|
| Rabbit IgG | Donkey, Rhodamine conjugated | 1:100 | 1 hour, room temperature | Chemicon |
| Rabbit IgG | Donkey, Fluorescein conjugated | 1:100 | 1 hour, room temperature | Chemicon |
| Mouse IgG | Donkey, Rhodamine conjugated | 1:100 | 1 hour, room temperature | Chemicon |
| Mouse IgG | Donkey, Fluorescein conjugated | 1:100 | 1 hour, room temperature | Chemicon |

**Table 3.2 List of secondary antibodies used.**

## Protocol 5: Co-culturing P19-derived neurons with glial cells

1. Glial cells were either isolated from primary rat cortex or differentiated from P19 cells and seeded on to sterile PDL coated 12 mm diameter glass coverslips.

2. PDMS drops were contacted at 3 points of the 12 mm round coverslips leaving behind tiny rounded polydimethylsiloxane (PDMS) (Sylgard® 182, Dow Corning Corporation, Michigan USA) stands on the surfaces (Figure 3.1). Allow the PDMS to harden in an oven heated to 80 $^0$C for an hour.

3. Autoclave the prepared glass coverslips and coat them with PDL according to Protocol 3.

4. Primary glial cells were prepared from 18 day old embryos of pregnant CD rats (Charles River, Sulzfeld, Germany).

    a. The meninges of the embryonic brain was removed and the cerebral cortices were separated from the hippocampus. The cortices was then enzymatically treated with cystein activated papain (L-cystein: 0.2 mg/ml, papain: 2 U/ml, Sigma-Aldrich Co.) and DNAse I (10 mg/ml, Roche Diagnostics GmbH) in medium. The cortices were then triturated a few times carefully with a fire polished glass pasteur pipette and incubated for 30 minutes in a water bath at 37 $^0$C.

    b. The enzymes were removed by centrifugation at 1000 rpm for 5 minutes and washing the pellet with PBS. Repeat this one more time.

    c. The dissociated cortical pieces were resuspended in MEM (Gibco) supplemented with 20 mM glucose (Sigma-Aldrich Co.) and 10 % fetal bovine serum (Gibco) and triturated with a fire polished glass Pasteur pipette until the tissue pieces could not be seen any more.

5. Glial cells were also selected from RA treated P19 cells.

31

a. P19 cells were differentiated in the neuronal lineage as described in Protocol 2.

b. RA treated P19 cells were dissociated in MEM-a supplemented with 10 % fetal bovine serum instead of supplemented neurobasal medium and seeded at 80 000 cells/cm$^2$ on PDL coated glass coverslips.

c. Medium was changed 2 days later to MEM supplemented with 20 mM glucose, 5 % fetal bovine serum and 5 % horse serum.

6. After 2 weeks, a confluent monolayer of flattened cells with few or no neurons could be observed due to the medium used for the selection of glial cells survival.

7. Prepare this monolayer culture of glial cells 2 weeks before the culture of P19-derived neurons.

8. The coverslips with the glial cell culture were placed upside down with the cell side facing the P19-derived neurons (Figure 3.1). The co-culture was performed in supplemented Neurobasal medium as in Protocol 2.
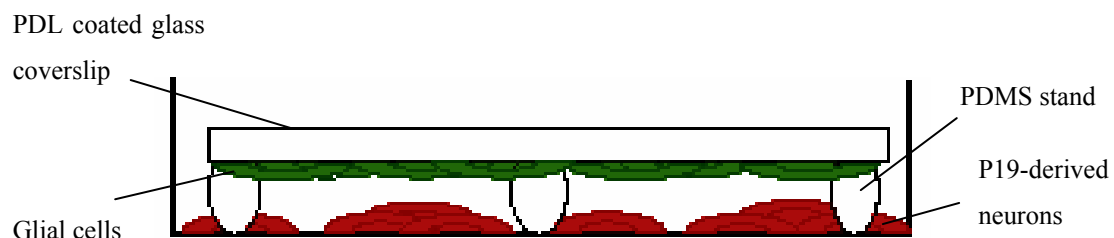


**Figure 3.1 Schematic diagram of co-culture system, drawn not to scale.**

## Protocol 6: Microelectrode array recording

1. Before coating the multielectrode arrays (MEAs) (Multi Channel Systems MCS GmbH, Reutlingen, Germany) according to Protocol 3, step 4 they were plasma cleaned with 90 % argon, 10 % oxygen for 3 minutes. It is recommended to plasma clean the MEAs after every 3 – 5 uses.

2. The MEAs were filled with deionised water and autoclaved.

3. P19-derived neurons were seeded on coated MEAs and topped up with 2 ml medium.

4. MEA cultures were maintained at 37.5 $^0$C during recording.

5. The MEAs (Figure 3.2) consist of a 20 mm high dish with 60 electrodes aligned in an 8 x 8 planar array. The electrodes are 30 μm in diameter and are made of titanium nitride, isolated by silicon nitride. The inter-electrode distance is 200 μm. The culture area of the MEA is enclosed by a 19 mm diameter glass ring and is 2.84 cm$^2$.

6. To reduce evaporation and prevent infection during recording, a cover for the MEA cultures was fabricated according to Potter *et. al* [55]. The covers (Figure 3.2) were machined from solid polytetrafluoroethylene (PTFE) Teflon$^®$ round stock to fit the MEAs tightly with a rubber O-ring. A fluorinated ethylene-propylene membrane (Teflon$^®$ FEP film, 12.7 μm thickness, specified permeabilities to $CO_2$, $O_2$ and water vapour of 212, 95 and 78 μM/cm$^2$/day respectively by ASTM D-1434 and E-96 tests). The films were manufactured by Dupont, OH, USA.

7. All recordings were performed in the laminar flow bench.

8. The MEA is mounted on an integrated 60 channel pre- and filter-amplifier (gain 1200X) which is in turn connected to a computer with a PCL data acquisition card for real time signal monitoring and recording.

9. Recordings of the MEA culture was performed after the 5th day post seeding to check for spontaneous activity.

10. Signals from all 60 electrodes were sampled at 25 kHz, visualised and stored using standard software MC_Rack (MultiChannel Systems).

11. Spike detection was done by setting the threshold manually for each active electrode. The extracellular recorded signals were embedded in biological and thermal noise of $20 - 30$ µV peak to peak.

12. Electrode impedance had been reported to increase with time in culture.[43] The MEAs usually need to be replaced after 1 year's usage.
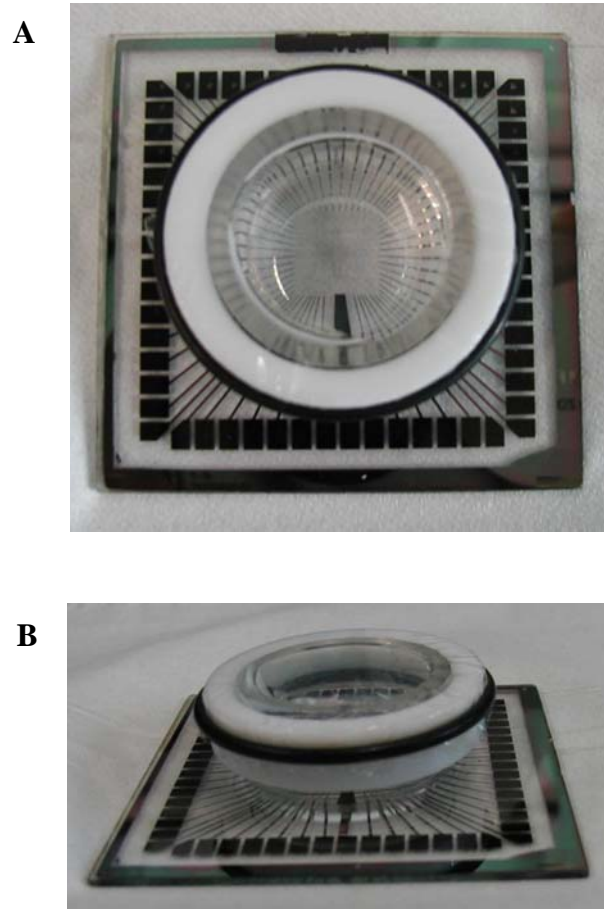


**Figure 3.2 MEA with 20 mm diameter glass ring fitted with a cover. (A) Top view, (B) Side view.**

## Protocol 7: Pharmacological Recordings

1. Half the media (1 ml) in the MEA cultures were changed 24 hours before recording with the test substances.

2. Before starting the recording, set up the incubation system (Figure 3.3A) and let it run for at least an hour. An empty MEA filled with just medium was fitted with a self made incubation chamber (Figure 3.3B) that was connected to the CTI-Controller 3700 (Leica microsystem GmbH, Wetzlar, Germany) maintaining a constant moist air stream of 5 % $CO_2$. The heating stage of the MEA was set to 37.5 $^0$C.

3. The MEA culture was removed from the incubator and fitted to the incubation system.

4. Two to three hours extracellular recordings consisting of the native state, the reference state, test substance application and wash state were performed. The native state is the original activity before any change in the medium was done during the long term recording. Reference state is the activity of the cultures when half the medium was changed.

5. Each state was recorded for between 20 – 30 minutes.

6. 10 % (200 μl) of the medium in the MEA cultures was removed. All test substances were from Sigma-Aldrich Co. unless otherwise stated. GABA (Cat. no. A5835), bicuculline Cat. no. B6889), muscimol (Cat. no. G019), glutamate (Cat. no. G8415) and cyclothiazide (Cat. no. 9847). Cyclothiazide was dissolved in dimethyl sulfoxide (DMSO) (Cat. no. D2650). A stock solution of the test substances was prepared and diluted in the culture medium that was removed taking into account that the final volume should remain the same.

7. The medium containing the test substance was returned to the MEA culture after pipetting it a few times for even mixing of the test substance. It was then

carefully added at 4 points of the MEA dish $90^0$ from each other to ensure that the test substance was evenly distributed in the culture medium.

8. Washing of the cultures was performed up to a maximum of 3 half medium changes to observe if the activity return to the reference state. Half medium changes have to be performed carefully and slowly to avoid wash induced damages to the neuronal culture.

9. Mean spike rate (MSR) at 10s bins were computed with the supplied MC_Rack program and plotted with respect to time to observe the changes in activity over a long period of time. MSR data was presented together with the standard deviation. Statistical significance of the changes in MSR relative to the reference activity was performed with the paired Student's t-test at a significance level of $P = 0.05, 0.01$ and $0.001$.

10. To examine the effects of the drugs on activity, the MSR for the first 10 minutes and 20 - 30 minutes after the drug application after were analysed.

11. To examine effects of the drugs on activity relative to reference activity, activity after the addition of drugs was normalised with the reference activity. Statistical significance of the change relative to the reference activity was performed with the paired Student's t-test at a significance level of $P = 0.05$, $0.01$ and $0.001$.

12. The prolongation effect of cyclothiazide on activity was calculated by the time it takes for MSR to reduce by 1 spike/s, $\tau$.

$$\tau = \frac{T}{MSR_{max} - MSR_{min}}$$

T = time for MSR to reach baseline activity. T is calculated by the intercept of the linear fit to the drop in MSR after CTZ application and the linear fit to the baseline activity; $MSR_{max}$ is the maximum mean spike rate during CTZ application; $MSR_{min}$ is the mean spike rate of the baseline activity.
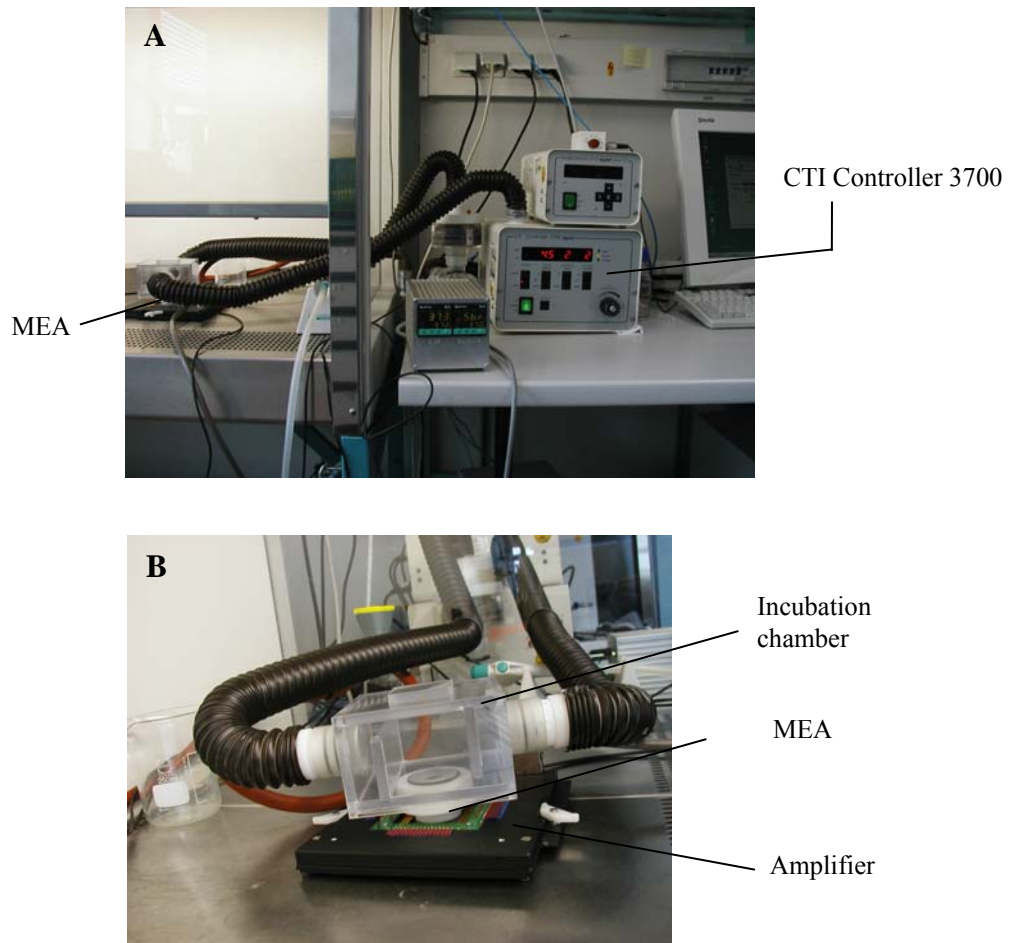
**Figure 3.3 MEA connected to the acquisition and incubation system (A). (B) a close up of the incubation chamber.**

## Protocol 8: Virus Infection

1. Recombinent Semliki forest virus (SFV) particles containing the OR5 gene was obtained from Eva Lemker (Max Planck Institute for Biochemistry, Munich, Germany).

2. Prior to infection the recombinant virus was activated by chymotrypsin treatment.

    a. 10 ml of virus stock suspension is incubated with 250 μl α-chymotrypsin (stock: 20mg.ml) (Roche Diagnostics GmbH, Mannheim, Germany) at room temperature for 20 minutes.

    b. Inactivate chymotrypsin by adding 250 μl aprotinin (stock: 10 mg/ml) (Sigma-Aldrich Co., Saint Louis, USA).

3. P19-derived neurons grown for 17 days on 3 MEAs and 6 sibling glass coverslips. Culture medium was removed and the cultures were washed once with PBS.

4. A small volume of the activated viral particles just enough to cover the cultures was added and incubated at 37 $^0$C, 5 % $CO_2$ for 1 hour.

5. Medium was removed and fresh culture medium was added. The cultures were returned to the incubator.

6. Recording was performed after 4 – 15 hours.

7. Glass coverslip cultures were fixed and stained after 15 hours.

## Protocol 9: DNA cloning

1. T-REx$^{TM}$ System (Invitrogen Corporation, CA, USA) was applied according to manufacturer's instructions as a mammalian expression system for the expression of OR5 in P19-derived neurons.

2. T-REx$^{TM}$ System consists of an inducible expression plasmid, pcDNA$^{TM}$ 4/TO and a regulatory plasmid, pcDNA6/TR$^{©}$. The expression of the gene of interest is controlled by the strong human cytomegalovirus immediate-early (CMV) promoter and two tetracycline operator 2 (TetO$_2$) sites. pcDNA6/TR$^{©}$ encodes for tetracycline repressor under the control of human CMV.

3. pcDNA$^{TM}$ 4/TO and pcDNA6/TR$^{©}$ plasmids were inoculated and expanded in chemically competent E. coli cultures (One Shot$^{TM}$ TOP10F', Invitrogen Corporation).

4. Plasmids pTNT-OR5 and pcDNA$^{TM}$ 4/TO were double restricted by EcoRI and Not1 enzymes (New England Biolabs Inc, MA, USA) and ligated by DNA ligase (Rapid DNA Ligation Kit, Roche Diagnostics GmbH, Cat. No. 11 635379 001).

5. DNA samples were diluted in loading buffer (HyperLadder I, Bioline GmbH, Luckenwalde, Germany) and ran in 1 % agarose gel in TAE buffer at 250 V.

6. Before transfecting into the cells, plasmids were sent to Sequiserve (Vaterstetten, Germany) for sequencing to ensure that the OR5 gene was correctly encoded.

7. Minimum concentration of blasticidin and Zeocin$^{TM}$ needed to select transfected P19 cells was determined to be 5 μg/ml and 50 μg/ml, respectively by exposing P19 cell cultures to different concentration of both antibiotics in duplicates.

## Protocol 10: Transfection of P19-derived neurons: electroporation and calcium phosphate precipitation

1. Plasmids were linearised (Sap I) before transfection.

2. Optimisation of electroporation (Electro Square Porator ECM$^{®}$ 830, BTX Instrument Division of Genetronics, Inc., CA, USA) conditions (Table 3.3) for P19 cells were first performed with eGFP plasmids supplied by Prof. Wolfrum (Institute for Zoology, Johannes Gutenberg University, Mainz, Germany). Cells in 10 different areas at the bottom of culture flasks were counted. Condition 3 was found to yield the highest transfection efficiency.

3. P19-derived neurons were tranfected with a combination of electroporation and calcium phosphate precipitation (CalPhos$^{TM}$ Mammalian Transfection Kit, Clontech Laboratories, Inc., CA, USA) methods. Cultures were incubated with the calcium phosphate/DNA precipitates for 3 hours. Transfection was performed immediately after the P19 cells were treated in RA supplemented suspension culture for 4 days.

   a. Group 1 consisted of first electroporating pcDNA $^{TM}$ 4/TO/OR5 plasmids in to the RA treated P19 cells and then introducing pcDNA6/TR$^{©}$ plasmids by calcium phosphate method 2 days later.

   b. Group 2 consisted of first electroporating pcDNA6/TR$^{©}$ plasmids, followed by transfecting with pcDNA $^{TM}$ 4/TO/OR5 plasmids via calcium phosphate method 2 days later.

   c. Group 3 consisted of transfecting the cells first with pcDNA6/TR$^{©}$ plasmids and then pcDNA $^{TM}$ 4/TO/OR5 plasmids a day later by calcium phosphate method.

4. For each group in step 2, P19-derived neurons were seeded on triplicates of PEI-LN coated MEAs and glass coverslips.

5. The transfection of the RA treated P19 cells with both plasmids were performed within 3 days post seeding when they are still mitotic.

6. Control cultures were transfected with pcDNA $^{TM}$ 4/TO/lacZ instead of pcDNA $^{TM}$ 4/TO/OR5. 48 hours after transfection, cells expressing the lacZ gene product, β-galactosidase, was stained using the β-Gal Staining Kit (Cat. no. K1465-01, Invitrogen Corporation).

7. Antibiotics, blasticidine and Zeocin$^{TM}$, at the concentration which was previously optimised were added to the cultures 48 hours after tranfection with both plasmids.

8. Recording of the MEA cultures was done between 17 – 19 days post seeding. 24 hours before the first recording, 1 μg/ml tetracycline was added to them to induce the higher expression of OR5.

**Electroporation Data (done on 220307)**

(All done with 4mm gap Cuvette, 25ug DNA, PBS, pulse interval 1.5ms)

| Sample | 1 | 2 | 3 | 4 | 5 | 6 | 7 | 8 | 9 |
|---|---|---|---|---|---|---|---|---|---|
| cell count ( x10^6) | 15 | 15 | 10 | 10 | 10 | 10 | 10 | 10 | 10 |
| volume (ul) | 400 | 400 | 400 | 400 | 400 | 400 | 400 | 800 | 800 |
| voltage (V) | 320 | 320 | 350 | 350 | 350 | 320 | 320 | 320 | 350 |
| pulse duration (ms) | 2 | 2 | 2 | 2 | 2 | 2 | 2 | 2 | 2 |
| pulse number | 1 | 3 | 3 | 1 | 2 | 1 | 2 | 1 | 1 |
| | | | | | | | | | |
| confluence after 24hrs | 70 | 70 | 30 | 50 | 40 | 50 | 40 | 60 | 50 |
| cell count after 24hrs (per view) | 214 | 153 | 35.3 | 111.8 | 52 | 131.25 | 128.4 | 81.25 | 94.6 |
| transfected count | 9.3 | 10.4 | 9.73 | 7.9 | 6.6 | 6.25 | 9.75 | 3.75 | 3.8 |
| efficiency (%) | 4.35 | 6.80 | 27.56 | 7.07 | 12.69 | 4.76 | 7.59 | 4.62 | 4.02 |

**Table 3.3 Optimisation of electroporation conditions.**

# 4.    Results

## 4.1    Optimisation of Neuronal Differentiation of P19 cells

It has been reported that P19 derived neurons display different phenotypes depending on their culture conditions.[9, 14, 16] In order to obtain reproducible and reliable extracellular recordings with MEAs, a high proportion of neurons growing on the MEA would be necessary. Retinoic acid-treated P19 cell cultures have been shown to contain neurons, astroglia, microglia and cells resembling vascular smooth muscle. Various differentiation protocols summarised in Figure 4.1 were consequently examined to obtain the highest population of neurons from P19 cells. Four culture parameters: duration of aggregate mediated differentiation, the concentration of retinoic acid (RA), seeding method and cell seeding density were varied to optimise the differentiation of P19 cells into neurons. Anti-mitotic agent, cytosine arabinoside (ARA-C), was also added to the differentiated cultures at a later time point to discourage the growth of non-neuronal cells. 5 μg/ml of ARA-C was added to the media at two different time points, two and five days post-seeding.

### 4.1.1    Aggregate seeding vs single cell seeding

#### 4.1.1.1    Morphology

Induction of neuronal differentiation was carried out under IC1: 1 day monolayer culture followed by a 1 day suspension culture (protocol from Lemker[54]). 0.5 μM or 1 μM RA was added to the cultures at the beginning of the induction. The efficiency of neuronal differentiation was compared between two seeding methods. The cells after 2 days of induction with RA were either seeded as single cells (IC1S) or aggregates (IC1A) on poly-d-lysine (PDL) coated glass cover slips and MEAs. IC1S cultures were seeded at two different cell seeding density of 20 000 cells/cm$^2$ (IC1S-20K) and 40 0000 cells/cm$^2$ (IC1S-40K). The addition of RA and allowing the cells to grow in suspension were necessary to induce the P19 cells into the neuronal lineage.
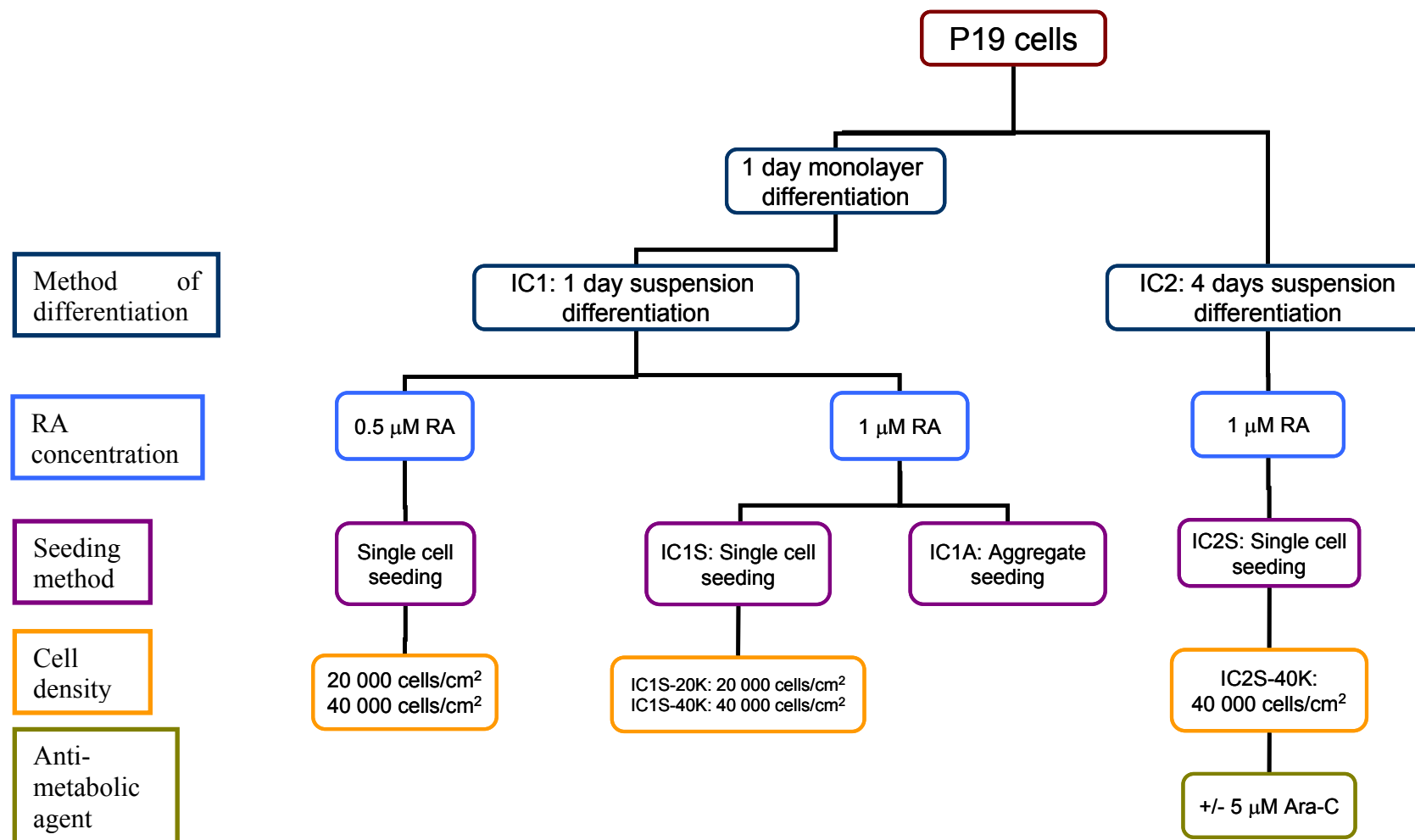
**Figure 4.1** Different culture conditions were tested to determine the best conditions to obtain the highest population of neurons

Undifferentiated P19 cells are polygonal in shape (Figure 4.2A) with a prominent nucleus and little cytoplasm. The nuclei of the undifferentiated P19 cells were granular. No visible differences were observed after the addition of RA for 24 hours in monolayer cultures (Figure 4.2B) in comparison to untreated P19 cultures of the same passage.
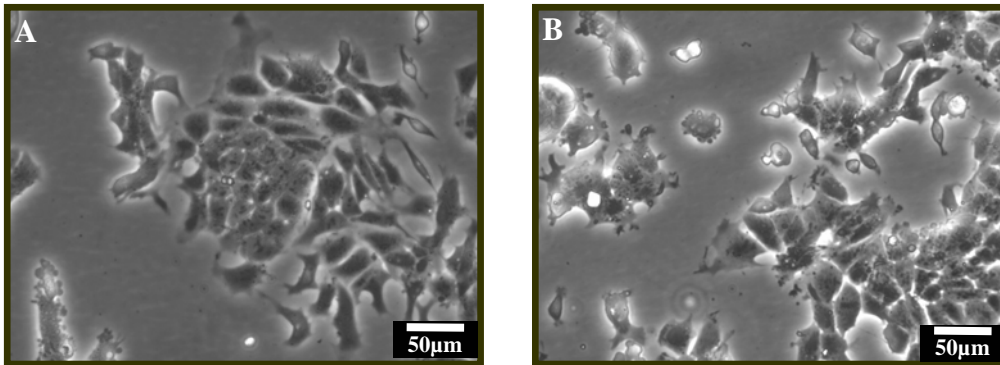


**Figure 4.2 Phase contrast micrographs of undifferentiated P19 cells (A) and adherent P19 cells treated with 1 μM RA (B) after 24 hours *in vitro*.**

The RA treated cultures (Figure 4.3) have different morphological characteristics in comparison to untreated P19 cultures (Figure 4.2A) even at 1 day post seeding. IC1S cultures regardless of the cell seeding density formed adherent cell clusters after 1 day post seeding despite breaking up the aggregates (Figure 4.3) prior to seeding. Long neuritic processes (arrow in Figure 4.3A) extended out of the cell clusters, some ending in a neighbouring cell cluster. The cell clusters were made up of a multilayer of cells growing on top of one another. Microvilli and filopodia from individual cells at the edge of the clusters could be seen spreading out of some of the cell clusters (Figure 4.3A).

After 7 days post seeding, IC1S cultures developed islands of cells with neuronal processes extending out of the islands to other islands or single neurons (Figure 4.3B). Thick neuritic bundles are formed extending from one cell cluster to another when cell clusters were greater than 100 μm in diameter. Clusters formed were usually between 100 μm to 500 μm. More non-neuronal cells were observed in the IC1S cultures after 14 days (Figure 4.3C). Neurons (arrows in Figure 4.3C) with their typical polarised morphology were growing on an underlying sheet of flattened cells.
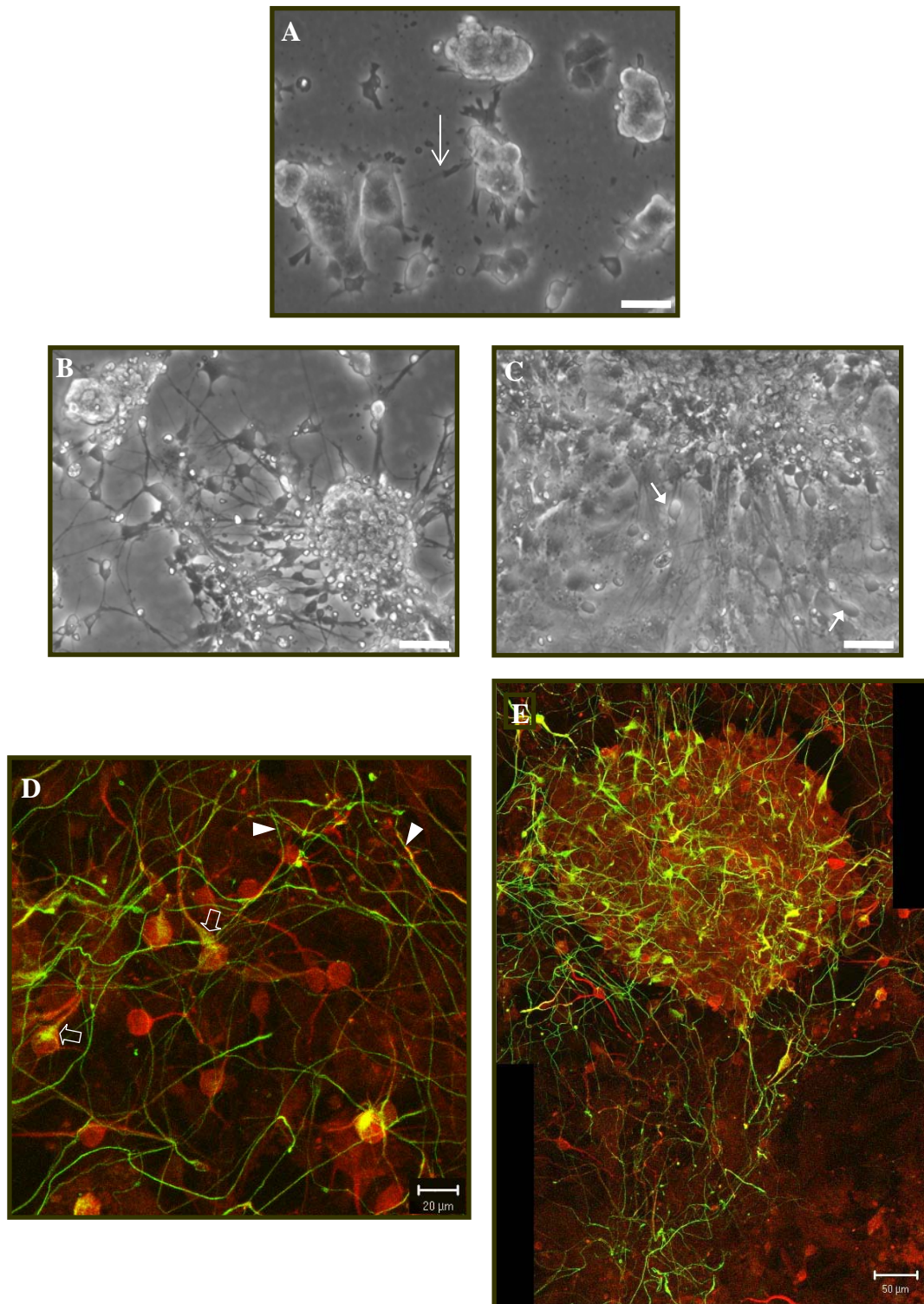
**Figure 4.3 Phase contrast micrographs of IC1S-40K cultures after (A) 1 day, (B) 7 days and (C) 14 days post seeding are shown here. Long neuritic processes (arrow in A) extended out of the cell clusters, some ending in a neighbouring cell cluster. IC1S cultures developed islands of cells with neuronal processes extending out of the islands to other islands or single neurons (B). Neurons (arrows in C) with their typical polarised morphology were growing on an underlying sheet of flattened cells. (D) and (E) are MAP2 (red) and NF160 (green) stained neurons after 14 days post seeding. (E) is made up of 2 confocal micrographs depicting one of the many cell clusters and its**

**surrounding. MAP2 positive processes in IC1S-40K cultures were long and sinuous. The long and smooth axons, some of them running along the MAP2 stained dendrites (D, arrowheads) could be seen touching the soma of the neurons. Some somas were also weakly stained against the anti-sera for NF160 (D, block arrows). (A) – (C) Bar, 50 μm. (C) Bar, 20 μm. (D) Bar, 50 μm.**

It was also observed that the concentration of RA tested did not have an influence on the neuronal differentiation of the P19 cells. Cell seeding density seemed to have a much larger effect on the development of a mature neuronal network instead. In general, cultures with an initial higher cell density developed longer neuritic processes and the neurons were more polarised. Neurons from lower density cultures were rounder and had shorter neuritc processes. There were fewer single neurons growing between cell clusters in cultures with a lower initial cell density even after 14 days post seeding (Figure 4.4A).

The aggregates formed during the 1 day suspension culture adhered to the surface after they were seeded on the PDL coated glass cover slips and MEAs (IC1A). Neurons migrated out from these aggregates (Figure 4.5A). Smaller clusters of cells as in IC1S cultures formed from neurons migrating out of the aggregates could be observed. Thick neuritic bundles extended out from the aggregates and cell clusters touching individual cells or other aggregates and cell clusters after 7 days (Figure 4.5A). After 14 days, the aggregates and cell clusters grew in size and the neuritic extensions increased in complexity (Figure 4.5B). The initially short neuritic extensions increased in length and formed branches, making contacts with one another, with cells and cell clusters.

Neurons can be further marked by the localisation of microtubule associated proteins (MAP) and neurofilament for the radial outgrowth of axons. MAPs promote the oriented poymerisation and assembly of the microtubules. Microtubule associated protein 2 (MAP2) present in developing dendrites could be detected in both IC1S and IC1A cultures after 4 days post seeding. MAP2 is present early in the development of neurons. Undifferentiated P19 cells were negative for MAP2 (Figure 4.6). The cell bodies of the neurons derived from P19 cells (Figure 4.3D, E, Figure 4.4B, C and Figure 4.5C, D) were strongly stained for MAP2 indicating successful differentiation.
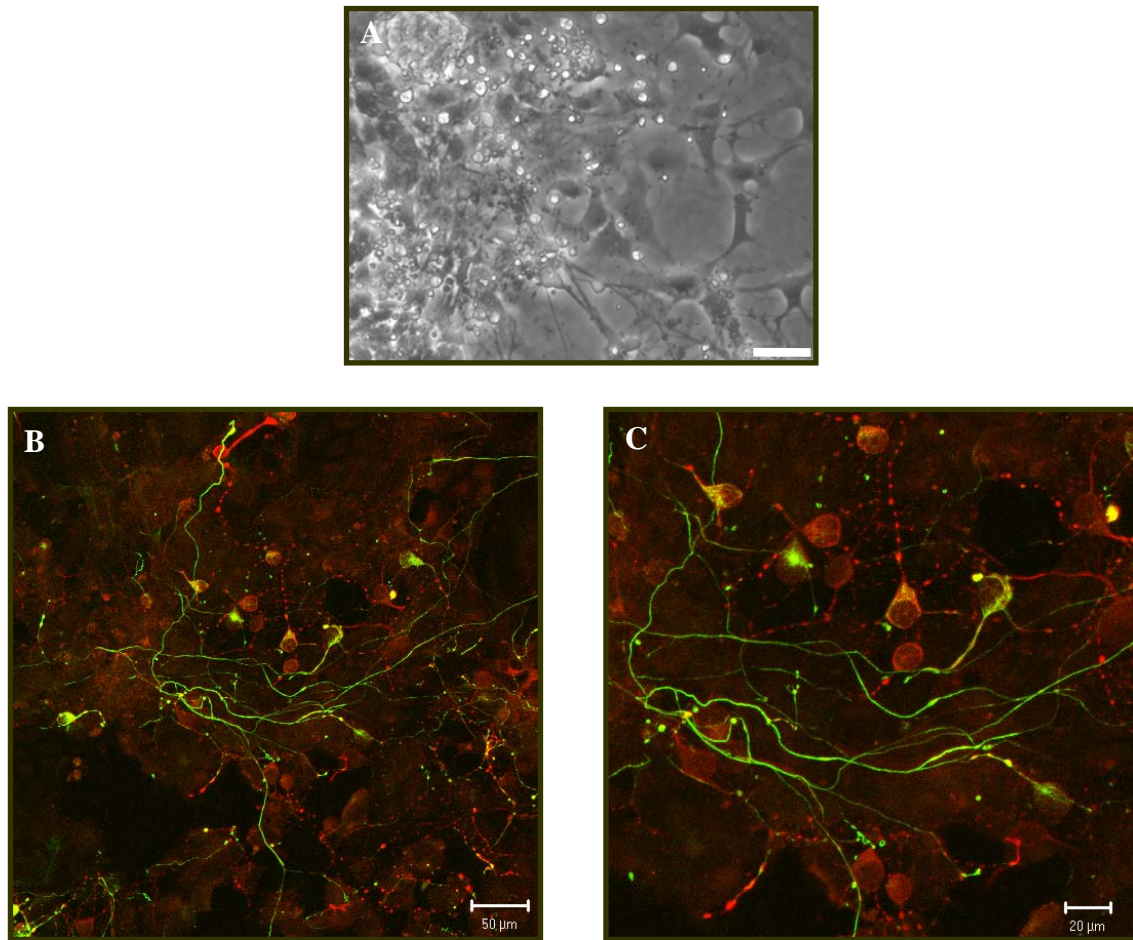
**Figure 4.4 Phase constrast micrographs of IC1S-20K cultures after 14 days post seeding (A). There were fewer single neurons growing between cell clusters in cultures with a lower initial cell density even after 14 days post seeding. IC1S-20K cultures showed varicosities on MAP2 stained processes (red). Long neurites stained for NF160 (green) were present also after 14 days post seeding. (C) is a higher magnification of (B). (A) Bar, 50 μm. (B) Bar, 50 μm. (C) Bar, 20 μm.**

IC1S-40K cultures of higher cell seeding density of 40 000 cells/cm$^2$ developed a more mature neuronal phenotype as compared to that of a lower cell seeding density of 20 000 cells/cm$^2$ (IC1S-20K). Neurons in IC1S-20K after 14 days post seeding (Figure 4.4C) stained less intensively for MAP2 in the neuritic processes in comparison to those for IC1S-40K (Figure 4.3D), with varicosities present in most MAP2 stained processes, indication of perhaps neurotransmitter storage in the neurites. The cell bodies of neurons in IC1S-40K cultures were more compact and rounder (Figure 4.3D) than those in IC1S-20K. MAP2 positive processes in IC1S-40K cultures were long and sinuous while those of IC1S-20K were short and varicose. The cell clusters that were observed in the phase contrast micrographs shown before were
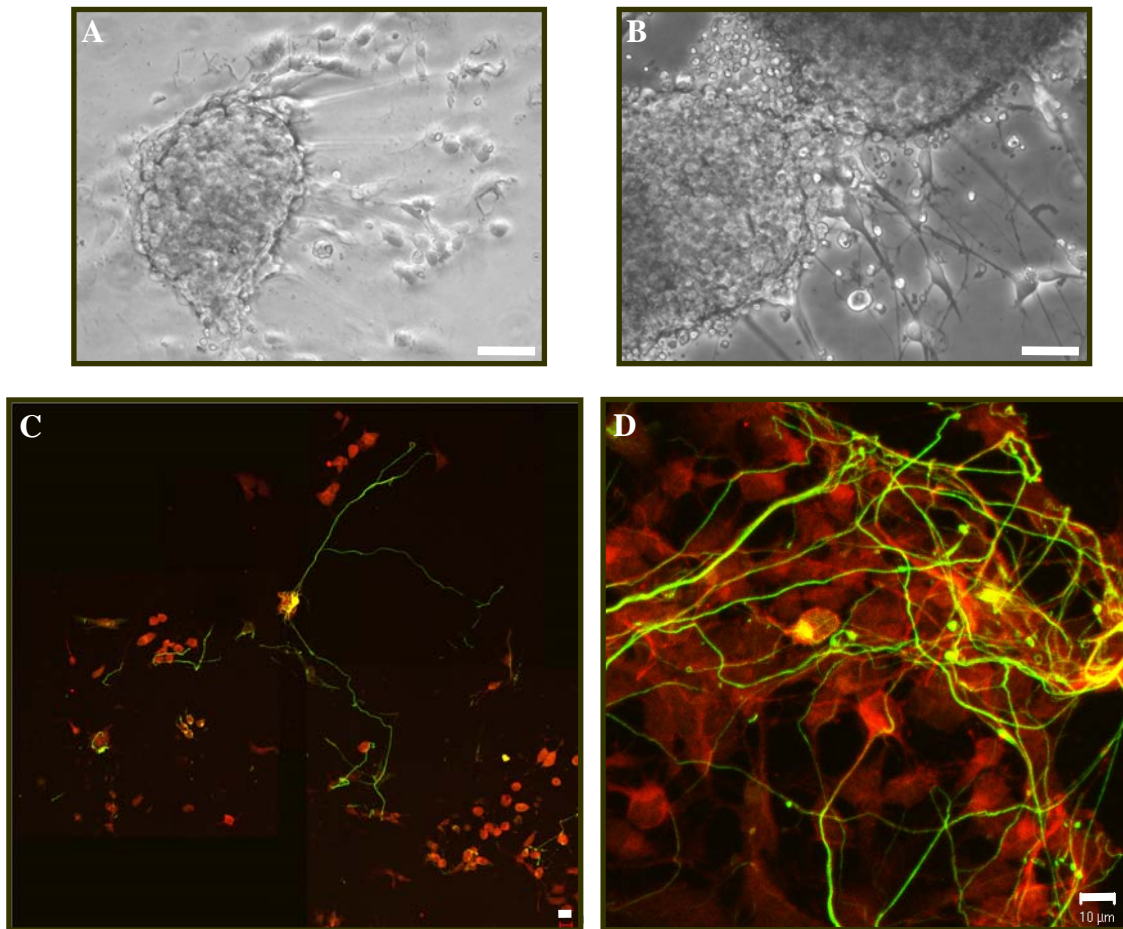
**Figure 4.5 Phase contrast micrographs of IC1A cultures after 7 days (A) and 14 days (B) post seeding. Neurons stained for MAP2 (red) were observed after 7 days (C) and 14 days (D) post seeding. Adhered aggregates grew in size as the culture continued and neurons grew out of these aggregates. Sinuous neurites stained for NF160 (green) developed later and were well formed throughout the IC1A cultures with long extensions after 14 day (D) post seeding. (C) is made up of 3 micrographs of 3 neighbouring areas. (A), (B) Bar, 50 μm. (C) Bar, 20 μm. (D) Bar, 10 μm.**

also stained positive for MAP2, showing that neurons were also present in these clusters (Figure 4.3E). Neurons were less homogenously distributed in IC1A cultures (Figure 4.5C). MAP2 stained neurons could be found too in the cell clusters formed in IC1A cultures (Figure 4.5D). MAP2 expression is necessary for both neurite extension and cessation of cell division.[56]

Neurofilaments (NF) are the most abundant fibrillar components in axon. Unlike microtubules the much thinner NF are very stable and almost totally polymerised in the cell. 160 kDa neurofilament proteins (NF160) are usually expressed in late stage neuronal development. A well formed network of axons expressing NF160 which are

10 nm in diameter were present in IC1S-40K cultures after 14 days post seeding (Figure 4.3D, E). The long and smooth axons, some of them running along the MAP2 stained dendrites (Figure 4.3D, arrowhead) could be seen touching the soma of the neurons. Some somas were also weakly stained against the anti-sera for NF160 (Figure 4.3D, block arrow).
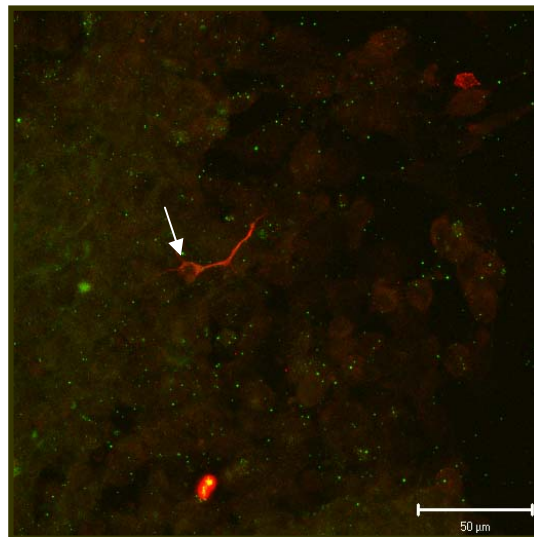


**Figure 4.6 Undifferentiated P19 cells did not stained for MAP2. A single differentiated cell (arrow) could be observed in the undifferentiated P19 cell culture stained positive for MAP2. Few if any neurons are present in the untreated P19 cell culture. Bar, 50 μm.**

The cell clusters which were present in all cultures as observed earlier in the phase contrast pictures, had a rich network of axons stained positive for NF160 entering and leaving its periphery (Figure 4.3E). Neurons that stained positive for MAP2 could be observed within and at the periphery of the cell clusters. On the other hand, a lower density of axons stained for NF160 were present in IC1S-20K cultures (Figure 4.4 B) than in IC1S-40K cultures after 14 days post seeding. Formation of NF160 stained axons were detected in IC1A cultures after 7 days post seeding (Figure 4.5C). A dense network of axons stained against NF160 were found only within the aggregates and cell clusters (Figure 4.5D) with some formation of axons outside of these aggregates and cell clusters after 14 days post seeding.

## 4.1.1.2  Microelectrode array recording

Neurons derived from P19 cells under IC1S-40K conditions were the most developed as observed in their morphologies. Immunohistology demonstrated that neurons differentiated under IC1S-40K conditions were able to form more complex neuritic networks. Electrophysiological activities of the IC1S-40K and IC1A cultures were subsequently monitored to select the most appropriate model for the application as a cell based biosensor.

P19-derived neurons differentiated under IC1 conditions were plated on 2 microelectrode arrays (MEA) previously coated with PDL as single cells at a seeding density of 40 000 cells/cm$^2$ (MEA40) and as cell aggregates (MEA-CA) similar to the cultures grown on cover slips. The extracellular recordings were done until 34 days after RA treatment.

Spontaneous firing was first detected between 17 and 19 days after RA treatment for both MEA-CA and MEA40 (Figure 4.7). Average spike rates of less than 10 spikes/s were recorded from the 2 MEA cultures. After 20 days post seeding the neurons in both cultures were hard to make out (Figure 4.8). Recordings for MEA-CA were more robust though different electrodes at times were activated during the time period monitored. Recordings for MEA40 were only few and sporadic during the time period studied. Spikes recorded from both MEAs had the typical form of the first derivative of an action potential (Figure 4.9B and Figure 4.10B) with an initial small positive peak and a large negative peak. The voltage minimum of the spikes recorded ranged from -20 to -70 µV (Figure 4.9 and Figure 4.10).

Recordings could only be obtained from 1 or 2 electrodes from MEA40 during the experimental time period (Figure 4.7). Activity was observed until day 27 post seeding for MEA40. MEA-CA spike rates peaked between 25 – 27 days with the highest spike rate detected after 26 days. The P19-derived neurons in MEA-CA appeared to be firing at random at day 25 day with increasing co-ordination of firing from day 26 to day 27 (Figure 4.11). By the 32$^{nd}$ day, average spike rate decreased to less than 2 spikes/s.

Although the P19-derived neurons were able show spontaneous activity after differentiation under IC1S-40K and IC1A conditions, the average spike rates and the number of active electrodes were very low. The differentiation of the P19 cells in the neuronal lineage have to be further optimised for extracellular recording with MEA as the recordings did not appear to stabilise and the firing activity of the neuronal network in both cultures was not robust due its low firing rate and the presence of a low number of active electrodes.
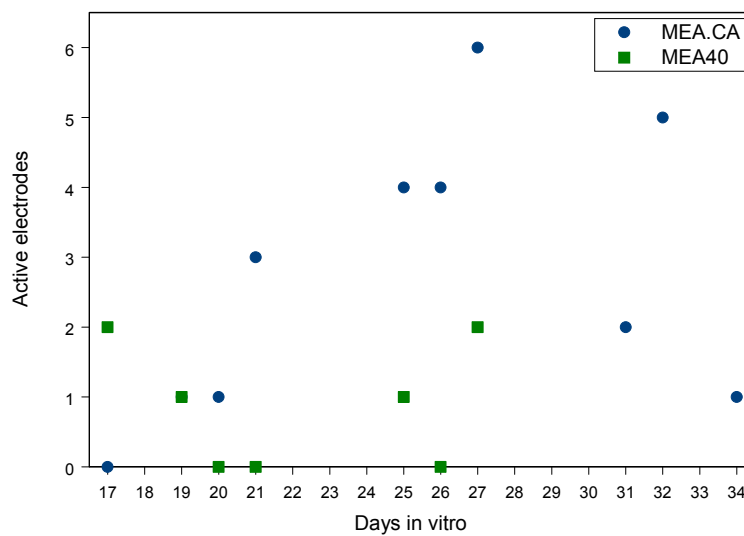


**Figure 4.7 Number of active electrodes during the culture time. Six or less electrodes were active throughout the culture time for both MEA40 and MEA-CA. Recordings for MEA-CA were more robust though different electrodes at times were activated during the time period monitored. Recordings for MEA40 were only few and sporadic during the time period studied.**
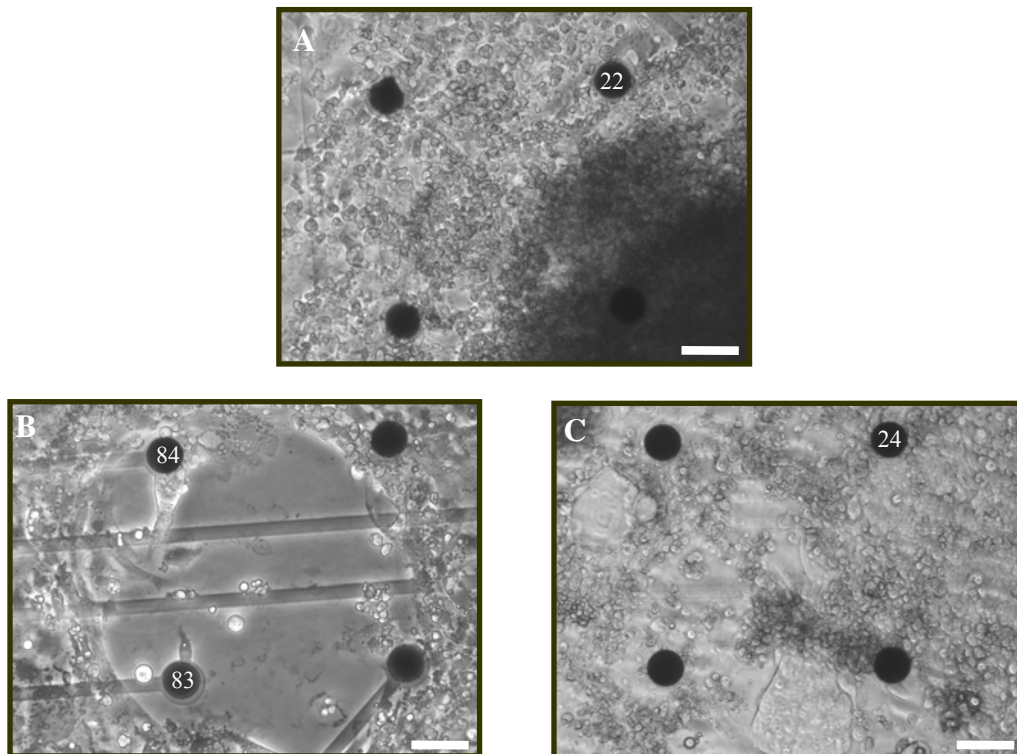
**Figure 4.8 Light microscopic images of MEA40 (A) and MEA-CA (B), (C) with numbered electrodes indicated after 35 days post seeding. The neurons in both cultures were hard to make out after 20 days post seeding. Signal recordings from electrodes 22, 83 and 24 were presented in the following graphs. Bar, 50 μm.**

**A**



**B**
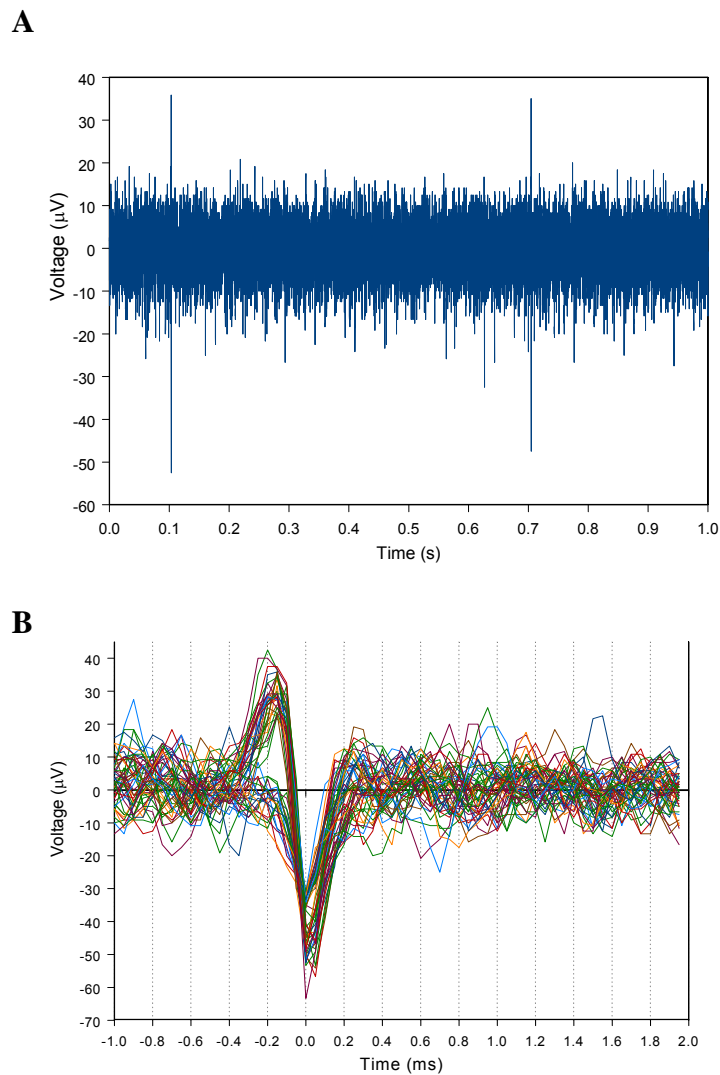


**Figure 4.9 MEA recording from electrode 22 of MEA40 after 27 days post seeding (A) and the waveform of the spikes recorded (B). Spikes recorded from MEA40 had the typical form of the first derivative of an action potential with an initial small positive peak and a large negative peak. The largest voltage minimum of the spikes recorded was - 63 μV.**

**A**



**B**
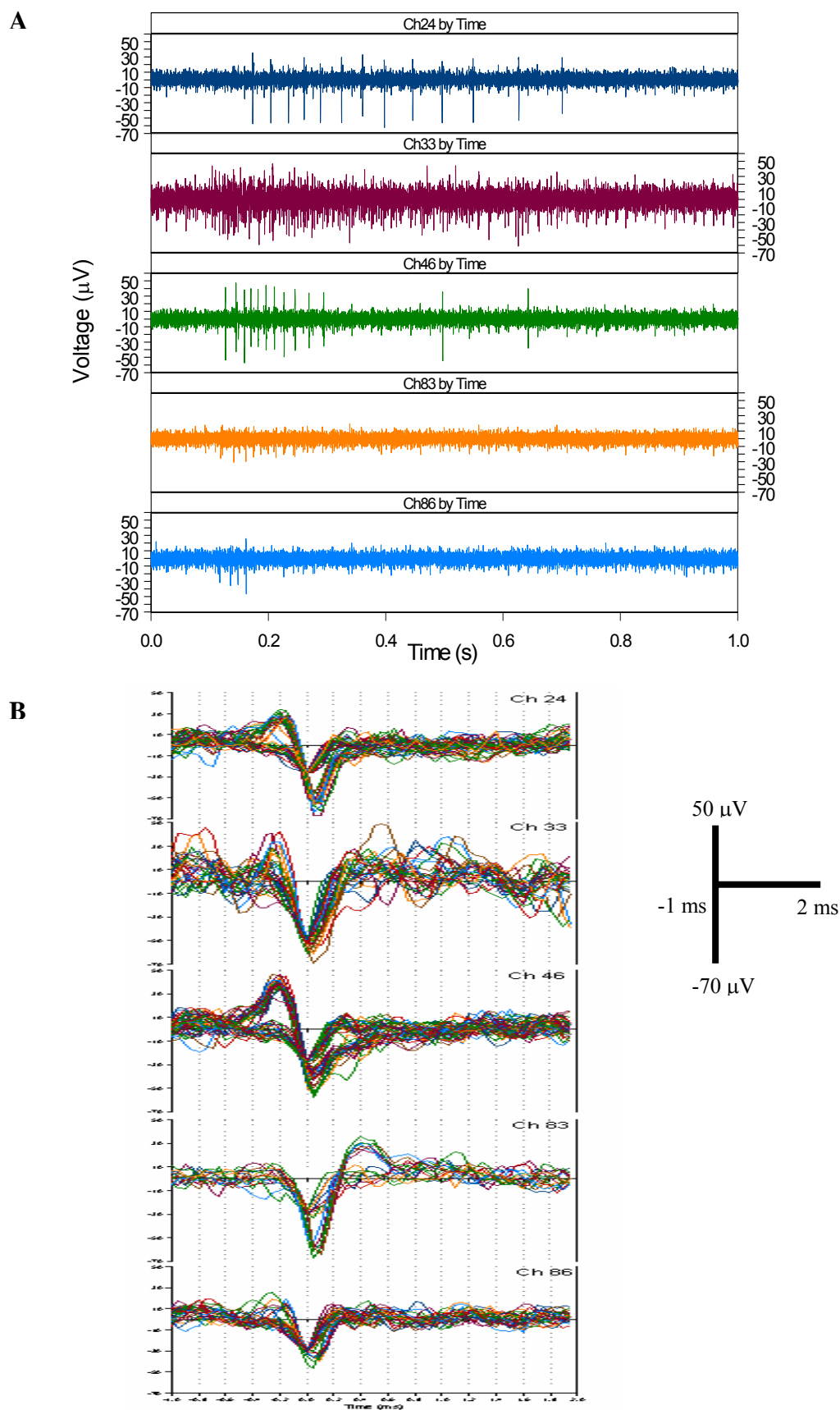


**Figure 4.10 MEA recording of MEA-CA with 5 electrodes detecting activity at the 23rd second (A) after 32 days post seeding. The waveforms of the 50 spikes recorded from the respective**

electrodes are shown in (B). Spikes recorded from both MEAs had the typical form of the first derivative of an action potential with an initial small positive peak and a large negative peak. The voltage minimum of the spikes recorded ranged from -20 to -70 µV.
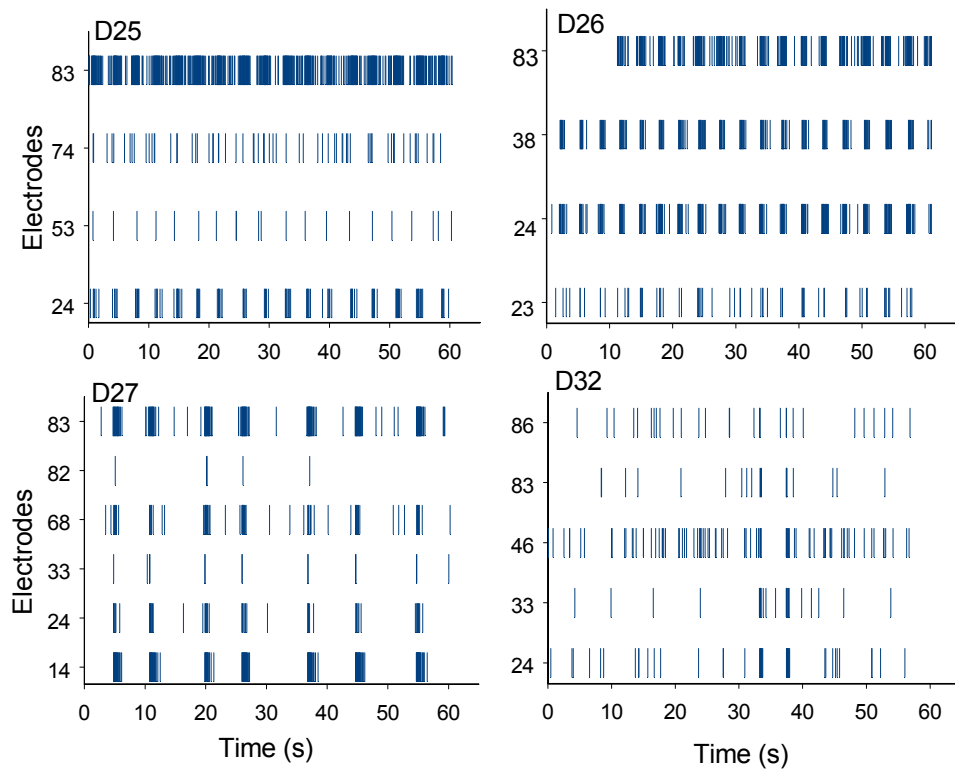


**Figure 4.11 Raster plots of MEA-CA from day 25 to day 32 post seeding. The P19-derived neurons in MEA-CA appeared to be firing at random at day 25 day with increasing co-ordination of firing from day 26 to day 27.**

## 4.1.2 Four day suspension differentiation vs one day suspension differentiation

### 4.1.2.1 Morphology

P19-derived neurons have been demonstrated previously that they were able to fire spontaneously. Recordings from less than 7 electrodes could so far be obtained. This could be due to the inadequate number of neurons present. To have a reliable model for extracellular recordings, it would be necessary to be able to record from as many electrodes as possible.

P19 cells were induced to differentiate this time over a prolong period of four days in suspension in the presence of RA, without first undergoing a one day monolayer culture  in the presence of RA. This culture condition is termed IC2 as shown in Figure 4.1. The concentration of RA used here is 1 µM since it was shown in previous sections that the effects of 0.5 µM and 1 µM were insignificant.

Larger aggregates were formed when the P19 cells were kept in suspension culture for four days compared to one day (Figure 4.12). Much cell debris was observed in the suspension culture after four days.
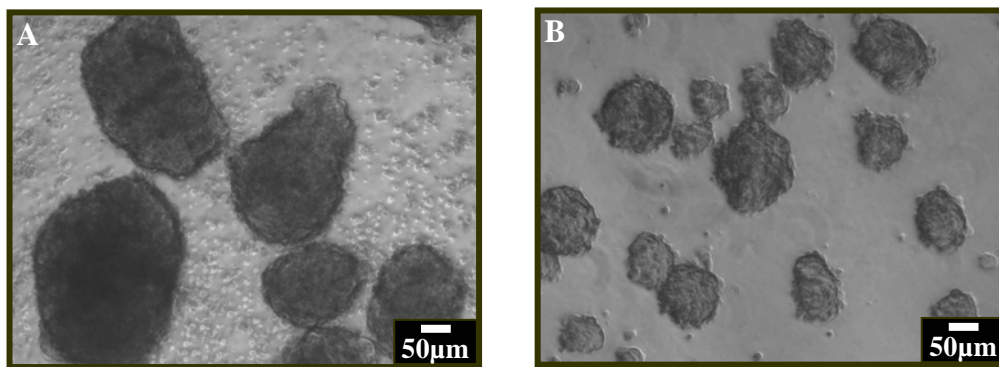


**Figure 4.12 Larger aggregates were observed after 4 days (A) than 1 day (B) suspension culture.**

After 4 days in cell suspension in the presence of 1 µM RA, the resulting cell aggregates were broken up and seeded as single cells with a cell density of 40 000 cells/cm$^2$ (IC2S-40K). Adherent cell clusters after 1 day post seeding were formed as in IC1S cultures despite breaking up the aggregates (Figure 4.13) prior to seeding. Long neuritic processes (arrows in Figure 4.13A) could be seen as before extending out of the cell clusters, some ending in a neighbouring cell cluster.

Neuron-like cells whose processes grew rapidly appeared first. The number of cells increased as the cultures progressed. Neuron-like cells from P19 cells treated in IC2S-40K developed longer processes more rapid than those from IC1 cultures. At just 2 days post seeding, neuron-like cells from IC2S-40K were polarised and had developed processes longer than one cell body length whereas those from IC1 were rounded and had processes shorter than 1 cell body length.

After 7 days post seeding, IC2S-40K developed islands of cells with neuronal processes extending out of the islands to other islands or single neurons (Figure 4.13B). Thick neuritic bundles were also formed extending from one cell cluster to another when cell clusters were greater than 100 μm in diameter. Clusters formed were usually between 100 μm to 500 μm. These cell clusters appeared to grow in size as the cultures were prolonged and were distributed throughout the cultures sometimes interconnected to one another by neuritic bundles (Figure 4.13C and Figure 4.16). Neurons treated under IC2S-40K appeared to develop an elaborate neuronal network after 7 days post seeding (Figure 4.13B). Cultures from IC1A and IC1S did not develop such elaborate neuronal network at this time point.
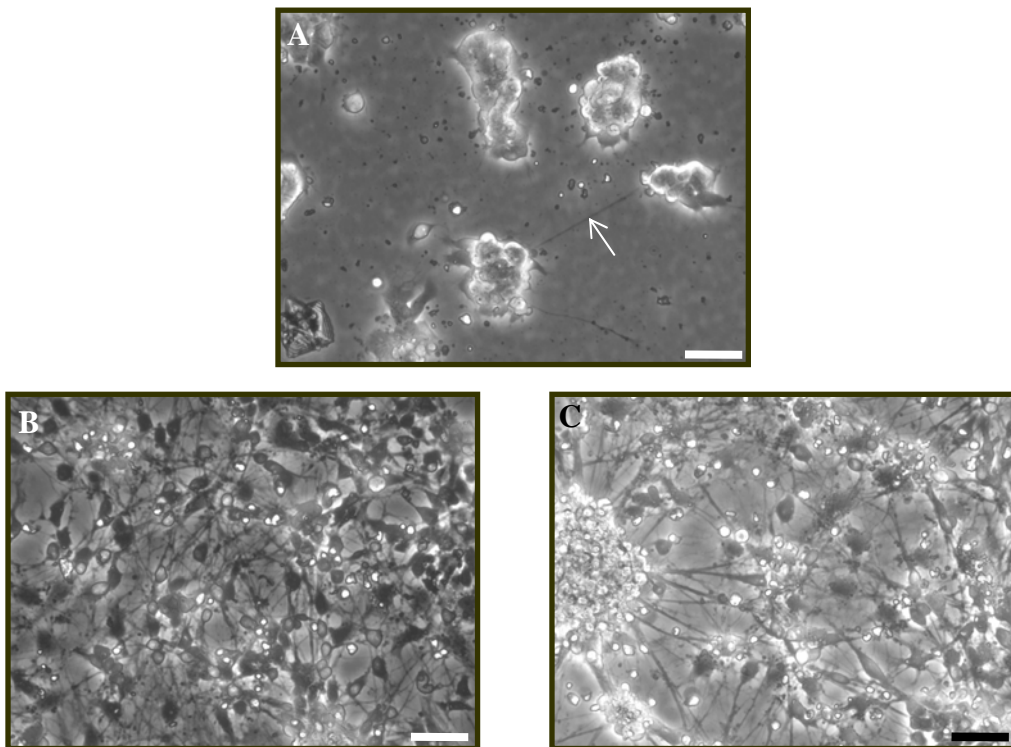


**Figure 4.13 IC2S-40K cultures after 1 day (A), 7 days (B), 14 days (C) post seeding. (A) – (C) Bar, 50 μm.**

Synaptophysin, a 38-kD protein, is a common transmembrane protein to all synaptic vesicles. It is found in the secretory vesicles of nerve terminals and could function in exocytosis. Synaptophysin (green) was found in a punctuate manner in IC2S-40K cultures after 14 days of RA treatment especially in regions of high cell confluence (Figure 4.14). Synaptophysin appeared to be found apposition to the dendritic

extensions and at a lower density on the somas of neurons, that is in agreement with the fact that synaptophysin is a membrane protein found in vesicles which in turn are present at synaptic terminals. Synaptophysin was not detected on IC2S-40K cultures 11 days after RA treatment which seems in contradictory with work found elsewhere [11].
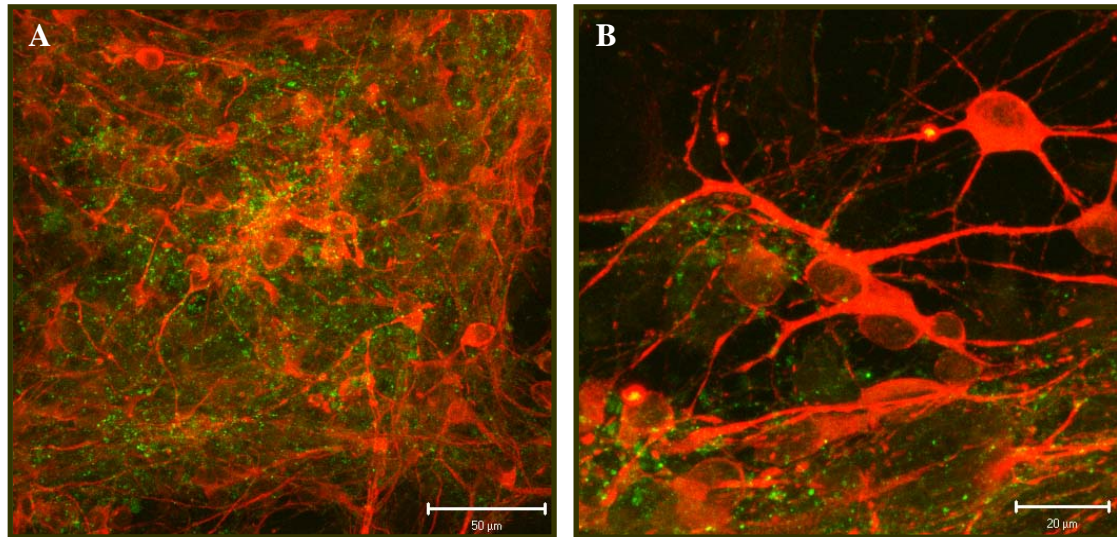


**Figure 4.14   Synaptophysin (green) was observed in IC2S-40K cultures after 14 days post seeding. Dendrites of P19-derived neurons were strongly stained for MAP2 (red). (A) Bar, 50 μm. (B) Bar, 20 μm.**

γ-aminobutyric acid (GABA) is a major inhibitory transmitter in the brain and spinal cord. Some neurons were stained positive for glutamic acid decarboxylase (GAD), the enzyme responsible for GABA synthesis, in IC2S-40K cultures 21 days after RA treatment. GAD immunoreactivity was found in cell bodies and dendrites of neurons (Figure 4.15, arrows). The dendrites had intensely GAD positive varicosities which were found in close proximity to the cell somas. The GAD positive varicosities in the dendrites were indicative of GABA storage. The cells stained positive for GAD were also stained positive for MAP2. Not all neurons positive for MAP2 were GABAergic. Cultures at 14 days post seeding appeared not to have GABAergic cells which contradicted results published elsewhere [14, 16]. They reported that GABAergic neurons could be found 10 days after RA treatment. Undifferentiated P19 cells were not stained for both synaptophysin and GAD.

More non-neuronal cells were observed in the cultures after 14 days. These non-neuronal cells could be observed growing beneath the neurons as shown in Figure 4.16. They appeared as flattened or endothelial-like cells. Many of these non-neuronal cells were mature astrocytes that contained glial fibrillary acidic protein (GFAP), an intermediate filament (Figure 4.17). There was also a higher cell turn over rate as the cultures mature as evident by the small bright points in Figure 4.13C and Figure 4.16
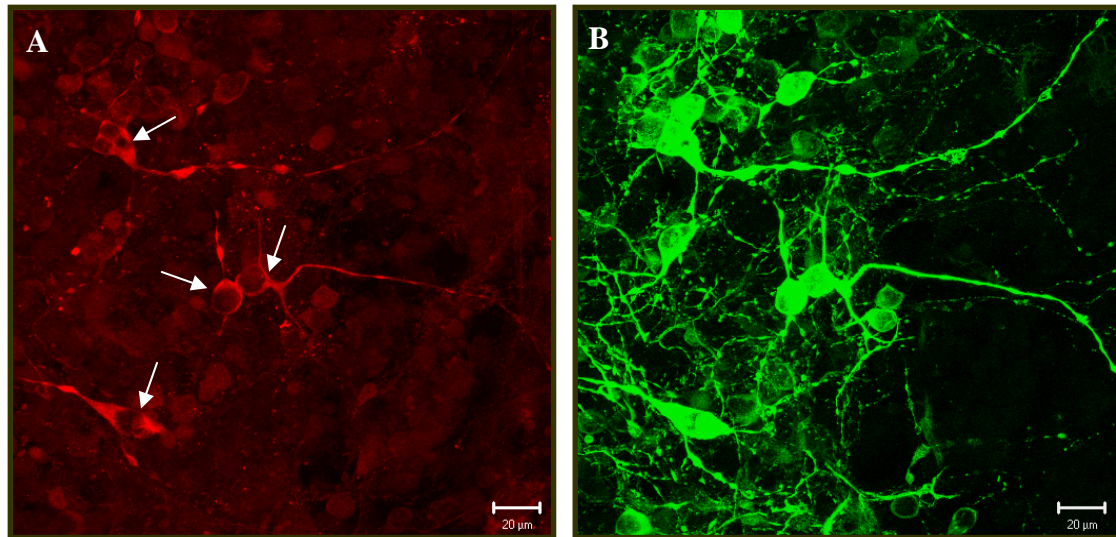


**Figure 4.15 (A) A few P19-derived neurons were stained positive for GAD (red). (B) MAP2 stained neurons (green) in the same area in (A). (A), (B) Bar, 20 μm.**

which were dead cells that rounded up above the viable cells. Cultures under IC2 developed a more mature neuronal network than cultures under IC1 after 14 days post seeding. IC2 produced a wide and elaborate neuronal network with good interconnectivity between neurons. Many neurons present in cultures under IC1 were still immature with their rounded phase bright cell bodies and short neuritic processes.
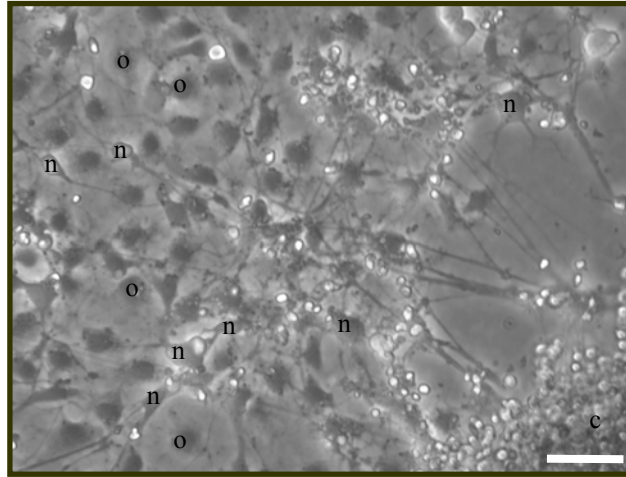
**Figure 4.16 IC2S-40K cultures after 14 days post seeding showing clearly the non-neuronal cells (o) growing beneath the neurons (n). The non-neuronal cells (o) appeared as flattened or endothelial-like cells, while the neurons (n) had a polarised appearance. Cell clusters (c) of 100 - 500 $\mu$m could be found distributed in the whole culture. Bar, 50 $\mu$m**
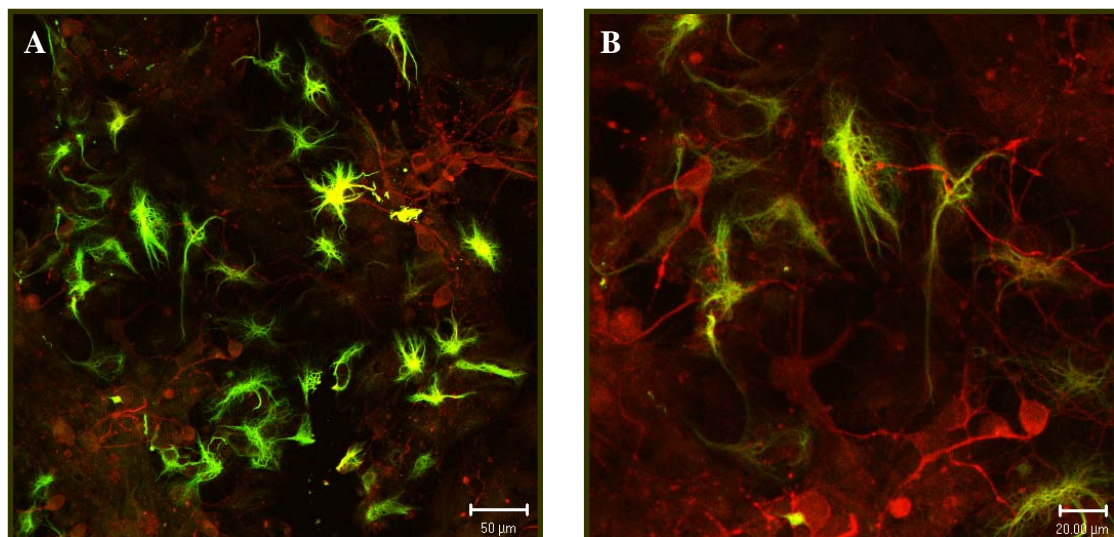


**Figure 4.17 Presence of astrocytes (green) stained for glial fibrillary acidic protein (GFAP) was observed among the neurons (red) after 14 days post seeding. (A) Bar, 50 $\mu$m. (B) Bar, 200 $\mu$m.**

Non-neuronal cells growing beneath the neurons continued to proliferate as the cultures were prolonged (Figure 4.18) and overgrow the post mitotic neuronal population. In order to discourage the growth of non-neuronal cells, 5 $\mu$g/ml cytosine arabinoside (Ara-C) was added to the culture. Ara-C is a nucleotide analogue which when incorporated into the DNA of cycling cells prevents further DNA synthesis and so is toxic to proliferating cell populations. Ara-C is added to the cultures at two

different time points, 2 days post seeding (T1) and 5 days post seeding (T2). Two days after the addition of Ara-C at T1, many cells were found to be seen floating in the media for all cultures. When Ara-C was added at T1, widespread necrotic clusters of cells were observed in all cultures less than one week after its addition. The number of non-neuronal cells was reduced in IC2 cultures 1 week after the addition of Ara-C (Figure 4.18B) but the remaining neurons did not stay viable after 2 weeks post seeding. On the other hand, if Ara-C was added at T2, the cultures were surviving longer after its addition. In general, IC2 cultures did not react well to the addition of Ara-C as largely necrotic cell clusters with neuritic bundles remained shortly 1 week after its addition. After 18 days post seeding (Figure 4.18C), many of the neurons' somas have many vacuoles within and a bubbly outer membrane (Figure 4.18C, arrow) indicative of apoptosis. They possessed neurites that have a rough appearance.
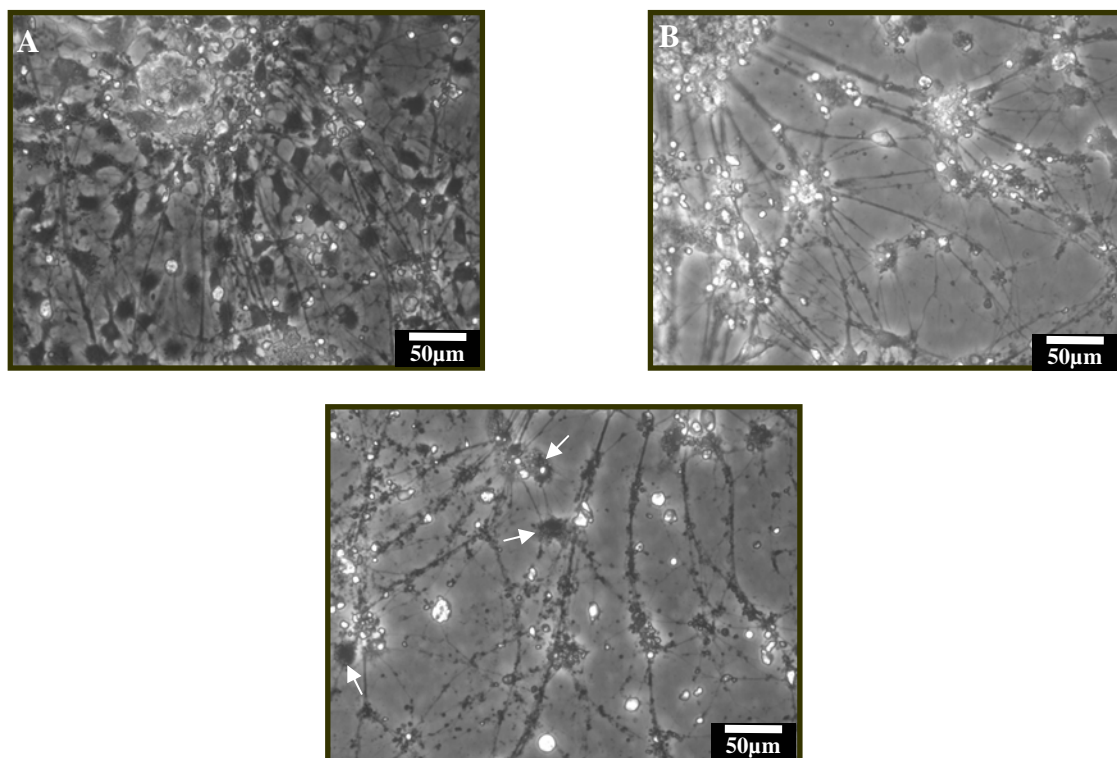


**Figure 4.18 (A), (B) and (C) were phase contrast pictures of IC2 cultures after 1 μM RA and seeded at 40 000 cells/cm$^2$.  (A) Non neuronal cells continued to proliferate under a network of neurons after 18 days post seeding. (B) Non neuronal cells were reduced after the addition of 5 mg/ml Ara-C on the fifth day post seeding after 14 days post seeding.  (C) Neuritc processes with few surviving neurons (arrows) after addition of Ara-C on the fifth day post seeding could be observed after 18 days post seeding.**

Co-culture of P19-derived neurons with astrocytes (Figure 4.19) was performed to reduce the gial population in RA treated P19 cells. The astrocytes were grown first on glass cover slips and then placed with the cell side down in RA treated P19 cells cultures. Mophological differences between co-cultures and sibling P19-derived neuronal cultures were not observed. Raster plots of the both cultures after 21 days post seeding (Figure 4.20) did not yield better extracellular recordings in co-cultures. The number of active electrodes and spontaneous activity did not improve in the co-cultures.
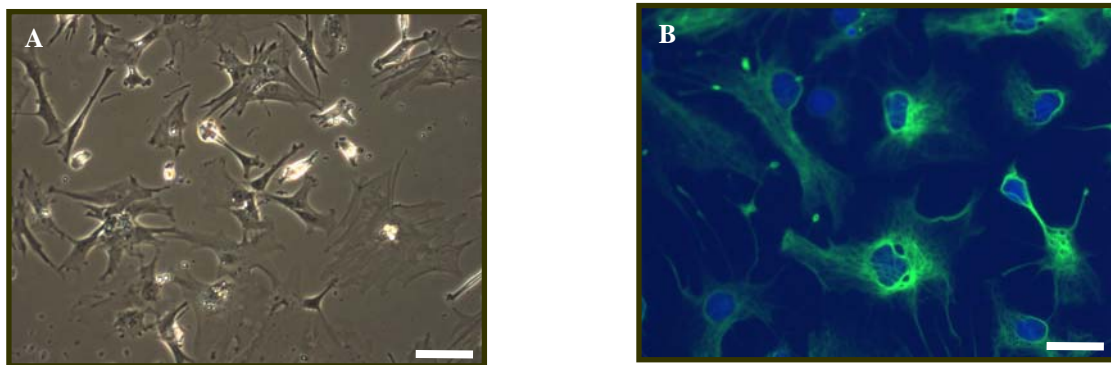


**Figure 4.19 Astrocytes isolated from 18 days embryos of pregnant CD rats. (A) Optical micrographs after 11 days *in vitro*. (B) Immunoflorescence staining of the astrocytes after 11 days *in vitro* against GFAP (green). The nuclei were stained blue. (A) Bar, 50 μm. (B) Bar, 25 μm.**
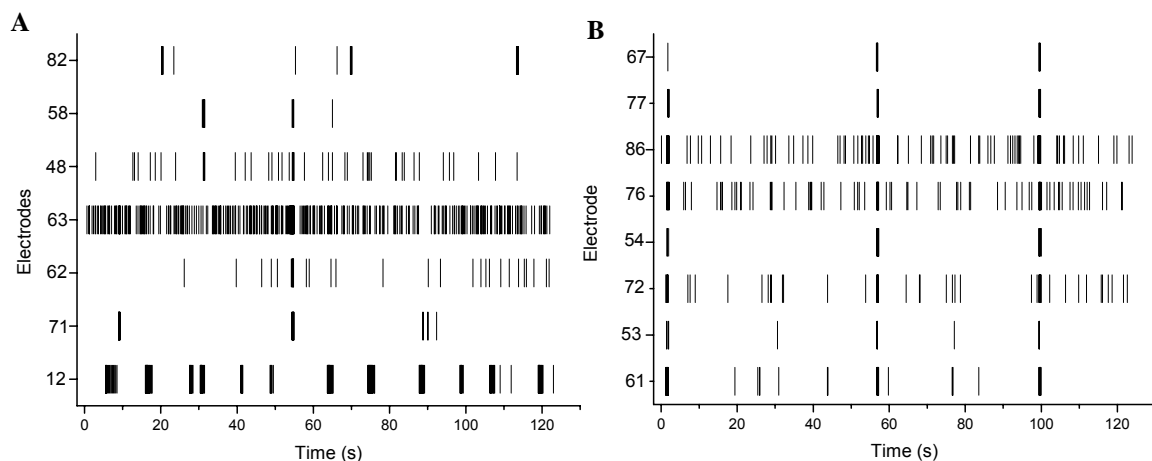


**Figure 4.20 Raster plots of (A) P19-derived neuron only cultures and (B) co-cultures after 21 days post seeding. Spontaneous firing of co-cultures remained random and sporadic. The number of active electrodes did not improve significantly in the co-cultures.**

The non-neuronal cells appeared to be present in a relatively high number in the IC2S-40K cultures. To reduce the non-neuronal cell population, P19 cells should not be allowed to be passaged too many times. A master stock of passage 1 P19 cells was frozen and they were allowed to be expanded *in vitro* up to the maximum of four passages before the differentiation. Thereafter, the culture is restarted from the master stock. It was found that in this way the number of non-neuronal cells in IC2S-40K cultures was kept low.

Neurons in IC2S-40K cultures were shown to be able to form a more mature neuronal phenotype in terms of  more sophisticated neuritic networks, synaptic formations 14 days after RA treatment and their capability of synthesising and storing GABA.

## 4.1.3    Cell culture surface coating

### 4.1.3.1    Morphology

Up till now only PDL was applied on the culture surfaces for the attachment of the RA treated P19 cells. Different types of coated surfaces were next explored in this section to improve the adherence of P19-derived neurons on the MEAs as well as to further enhance the maturation of the neurons obtained. P19 cells were differentiated into neurons according to method IC2S-40K.

The culture surfaces were coated with 3 different combinations of polymers. Laminin (LN) only, Poly-d-lysine-laminin (PDL-LN) and polyethyleneimine-laminin (PEI-LN) were coated on glass coverslips and MEAs prior to seeding the differentiated P19 cells. The molecular weight of PEI used was 70 000 while that of PDL used was 70 – 150 kDa.

Laminin is the major noncollagenous glycoprotein component of basement membranes and is a mediator of cell adhesion, migration, growth and differentiation. Cys-laminin A chain, a fragment between 2091 – 2108 of the laminin molecule, was

used in this study. This IKVAV containing segment of laminin has been found to promote neurite formation [57-59].

It was found that the initial attachment of neurons on laminin only coated cover slip surfaces was bad. Few neurons were attached. The 16 amino acid long laminin fragment has been known not to adsorb well to glass surfaces. Therefore, to coat this laminin fragment on glass surfaces, a polyelectrolyte would be first needed to cover the glass surfaces. PDL and PEI were both positively charged.

P19-derived neurons cultured on PDL-LN and PEI-LN coated surfaces were stained positive for synaptophysin after just 8 days post seeding in contrast to P19-derived neurons cultured on PDL coated surfaces which were not stained positive for synaptophysin after 11 days. Large cell clusters in PDL-LN coated cultures were observed detaching from the surface. There appear to be much lesser non-neuronal cells after 14 days post seeding in both PDL-LN and PEI-LN coated cultures (Figure 4.21A and Figure 4.22A, B). Punctuate synaptophysin were found apposition to dendrites stained positive for MAP2, following along the contours of the dendritic extensions (Figure 4.21B, C and Figure 4.22C, D). Cell clusters present in both cultures were densely stained positive for synaptophysin (Figure 4.21B and Figure 4.22E). PEI-LN coated cultures appeared to have a higher density of synaptophysin in regions outside the cell clusters when compared to PDL (Figure 4.14) and PDL-LN cultures. There appeared to be larger clustering of synaptophysin in PEI-LN cultures as observed by the larger sizes of synaptophysin positive structures in these cultures. These synaptophysin clusters indicated that the clustering of synaptic vesicles most probably at synaptic terminals occurred for the release of neurotransmitters.
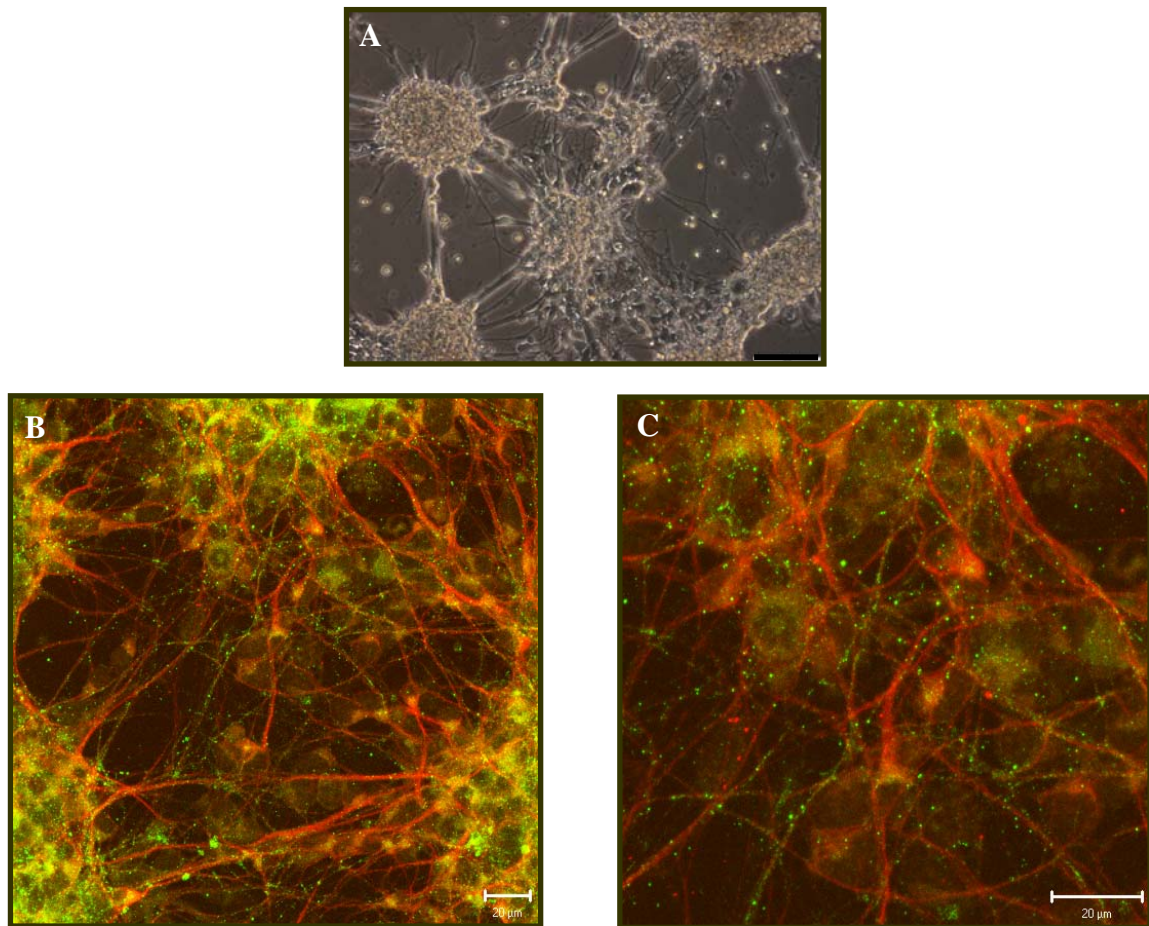
**Figure 4.21 (A) P19-derived neurons cultured on PDL-LN coated coverslips after 14 days post seeding. Synaptophysin (green) was observed in PDL-LN coated cultures after 14 days post seeding (B). Dendrites of P19-derived neurons were strongly stained for MAP2 (red). (C) is larger magnification of (B). (A) Bar, 100 μm. (B) and (C) Bar, 20 μm.**
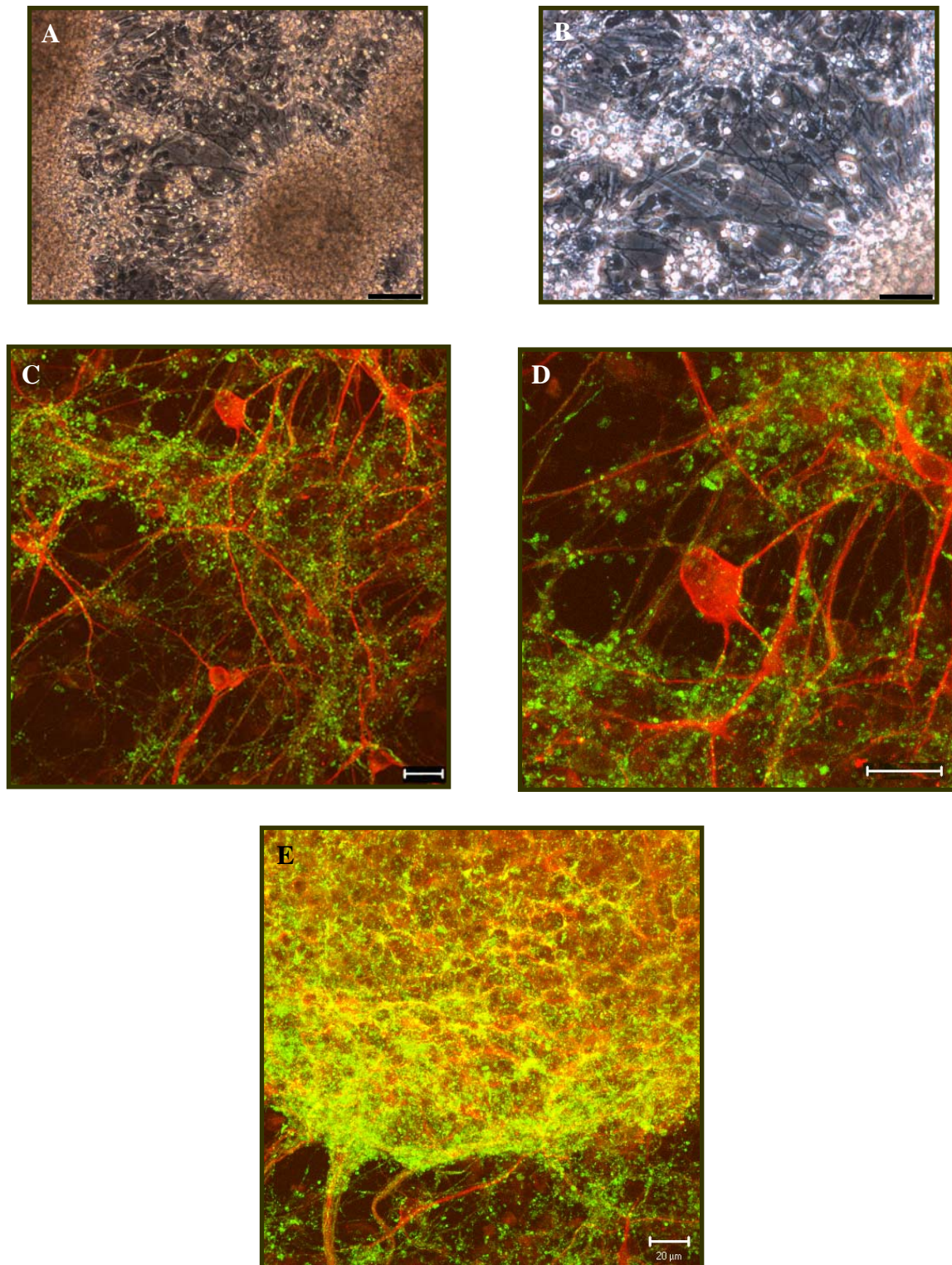
**Figure 4.22 (A), (B) P19-derived neurons cultured on PEI-LN coated coverslips after 14 days post seeding. Synaptophysin (green) was observed in PEI-LN coated cultures after 14 days post seeding (C) and (D). (D) is a larger magnification of (C). Dendrites of P19-derived neurons were strongly stained for MAP2 (red). (A) Bar, 100 μm. (B) Bar, 50 μm. (C), (D) and (E) Bar, 20 μm.**

### 4.1.3.2 Microelectrode array recording

The maturation of P19-derived neurons was improved on PEI-LN coated surfaces as shown by the earlier occurrence of synaptophysin post seeding and the high density of synaptophysin after 14 days post seeding. A complex network of neurites was observed and non-neuronal cells were reduced after 14 days post seeding. Cell clusters formed after 14 days post seeding remained adhered to the PEI-LN surfaces whereas some of those formed on PDL-LN surfaces were observed to detach.

2 MEAs were coated with PEI-LN and seeded at 50 000 cells/cm$^2$ (PEI-LN50K) and 150 000 cells/cm$^2$ (PEI-LN150K) each. P19-derived neurons were cultured within a culture area of diameter 19 mm constrained by glass O-rings on the MEAs up to 25 days post seeding. Recordings obtained from the cultures showed consistency within the same batch of differentiated P19 cells. Good signal to noise ratios (> 2.5) were obtained from the cultures such that spike analysis could be done. It was observed that MEA cultures pre-coated with PEI-LN had generally lower background signals and better signal to noise ratios when compared to PDL or PDL-LN coated cultures. This indicated that there was better cell-electrode coupling in PEI-LN coated surfaces in addition to the improved neuronal phenotype obtained.

Spontaneous firing in PEI-LN50K cultures was detected on the 15$^{th}$ day post seeding. There were only 1-3 electrodes active between 15 and 25 days post seeding with the highest activity on the 22$^{nd}$ day (Figure 4.23). Recording from electrode 77 showed the most robust firing of 2 active electrodes and is further analysed in Figure 4.23.The peak to peak amplitude ($V_{PP}$) of spikes recorded from electrode 77 of PEI-LN50K average at 30.6 ± 2.3 µV (± standard deviation, SD) on the 22$^{nd}$ day post seeding with an average amplitude minimum ($V_{min}$) of -19.4 ± 1.4 µV (± SD) (Figure 4.23B). Spike rate was low over a recording period of 2 minutes, with a probability of inactivity at 93 % of the time (Figure 4.23C). Slightly over a quarter of the spikes had a spike interval of less than 500 ms (Figure 4.23).

The spontaneous firing of P19-derived neurons was more robust when they were seeded at 3 times the initial cell density of PEI-LN50K cultures. The number of active
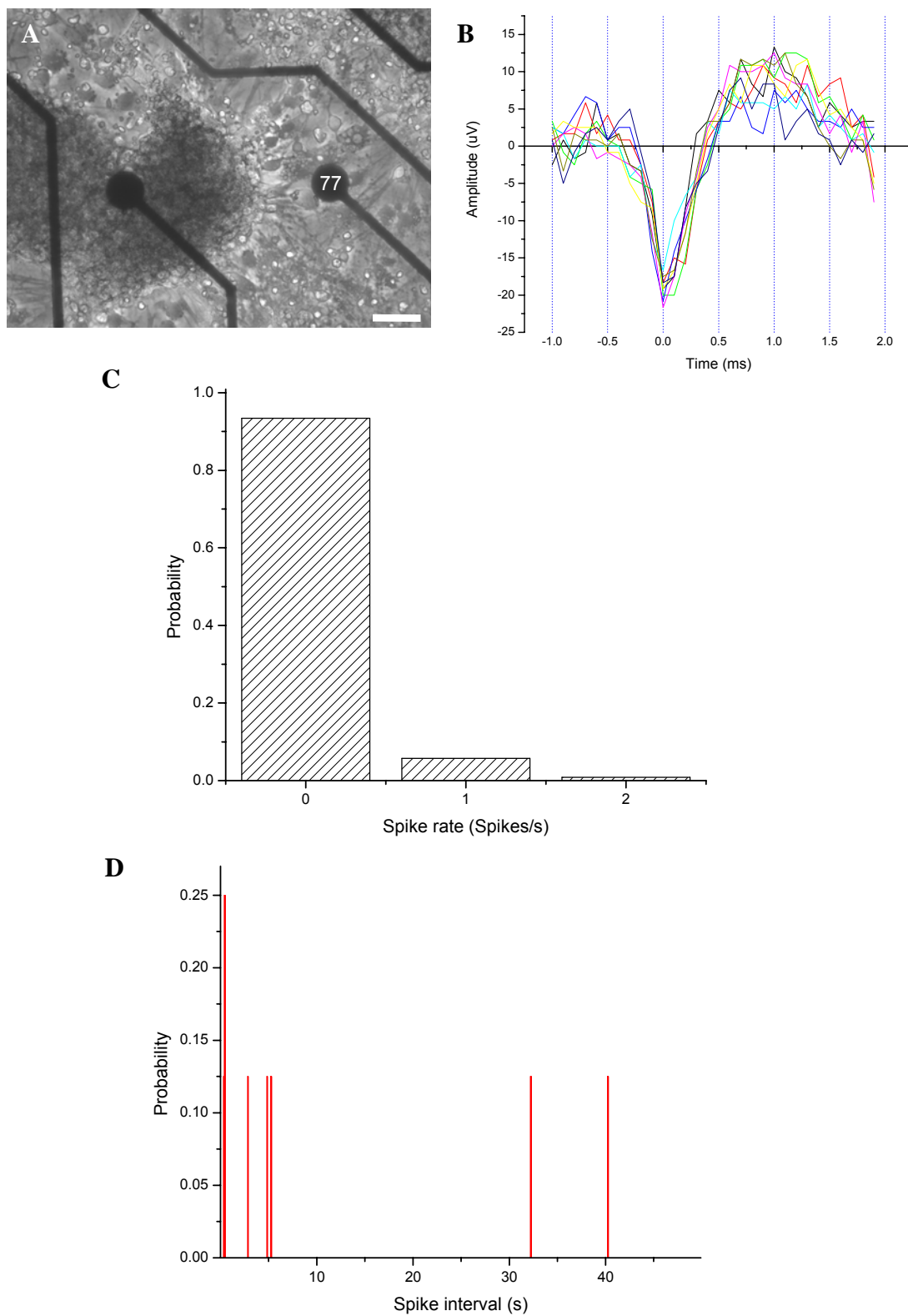
Figure 4.23 The highest activity was recorded from PEI-LN50K on the 22nd day post seeding. Recording from electrode 77, the most active electrode, was further analysed. (A) shows the cells surrounding electrode 77. (B) Waveform of spikes recorded from electrode 77, overlay of the last

**50 spikes. Probability of spike rate (C) and (D)  spike interval of electrode 77 over 2 minutes were plotted. (A) Bar, 50 $\mu$m**

electrodes increased significantly (Figure 4.24). Recordings could be obtained from 10 – 16 electrodes after 18 days post seeding for the 2 MEAs that were seeded at 150 000 cells/cm$^2$. Spontaneous synchronised activity was observed in PEI-LN150K cultures on the 17$^{th}$ day post seeding continuing into the 25$^{th}$ day of culture (Figure 4.25A). A recording from electrode 73 of PEI-LN150K cultures on the 20th day post seeding is shown in Figure 4.25.  The $V_{PP}$ of spikes recorded from electrode 73 on the 20th day post seeding averaged at 44.7 $\pm$ 9.9 $\mu$V ($\pm$ SD) (Figure 4.25B). The average $V_{min}$ obtained from the same electrode was -23.4 $\pm$ 3.3 $\mu$V ($\pm$ SD). The $V_{min}$ recorded across all active electrodes from PEI-LN150K cultures ranged from -18.9 to -32.7 $\mu$V on the 20$^{th}$ post seeding. The population of neurons growing on electrode 73 appeared to be inhomogenous as seen from the different spike forms with significant differences in amplitudes and temporal events (Figure 4.25B). Electrode 73 has a more random firing pattern compared to the other 10 electrodes (Figure 4.25A). The more homogenous waveform recorded from electrode 63 relative to electrode 73 is shown in Figure 4.26. A wider range of spike rate was recorded from electrode 73. The maximum spike rate recorded was 90 spikes/s (Figure 4.25C) with 25 % of the recording time of 2 minutes registering at 1 spike/s (Figure 4.25C insert). 87 % of the spikes occurring had a spike interval of less than 100 ms (Figure 4.25D).

Electrodes that were active in both PEI-LN50K and PEI-LN150K cultures were usually under cell clusters or in the close proximity of these cell clusters (Figure 4.23A, Figure 4.24). After 14 days post seeding PEI-LN150K cultures were especially confluent and many more cell clusters were observed dispersed randomly throughout the MEA surfaces as compared to PEI-LN50K cultures.

A



B
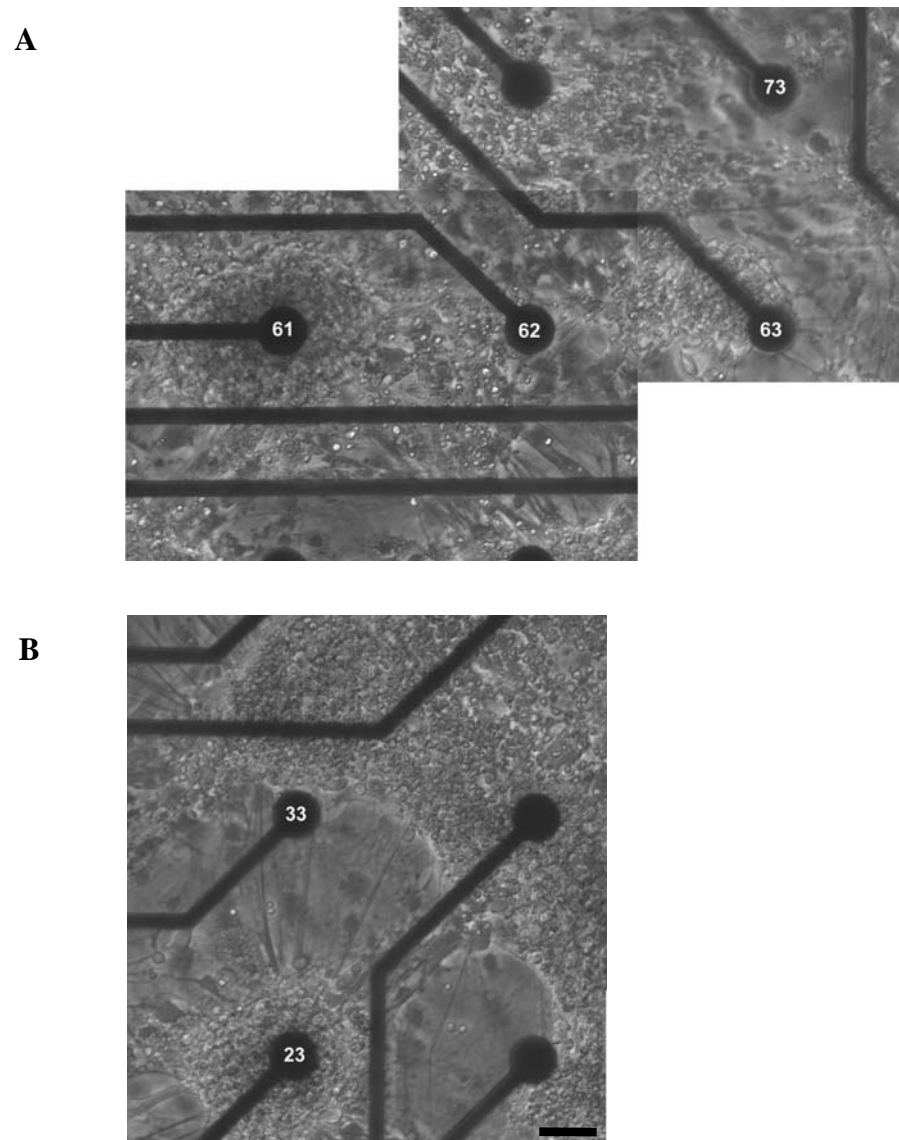


**Figure 4.24 Optical micrographs of PEI-LN150K cultures showing the cells surrounding some of the active electrodes after 20 days post seeding.  Bar 50 μm**

**A**



**B**



**C**

Electrode 73



**D**
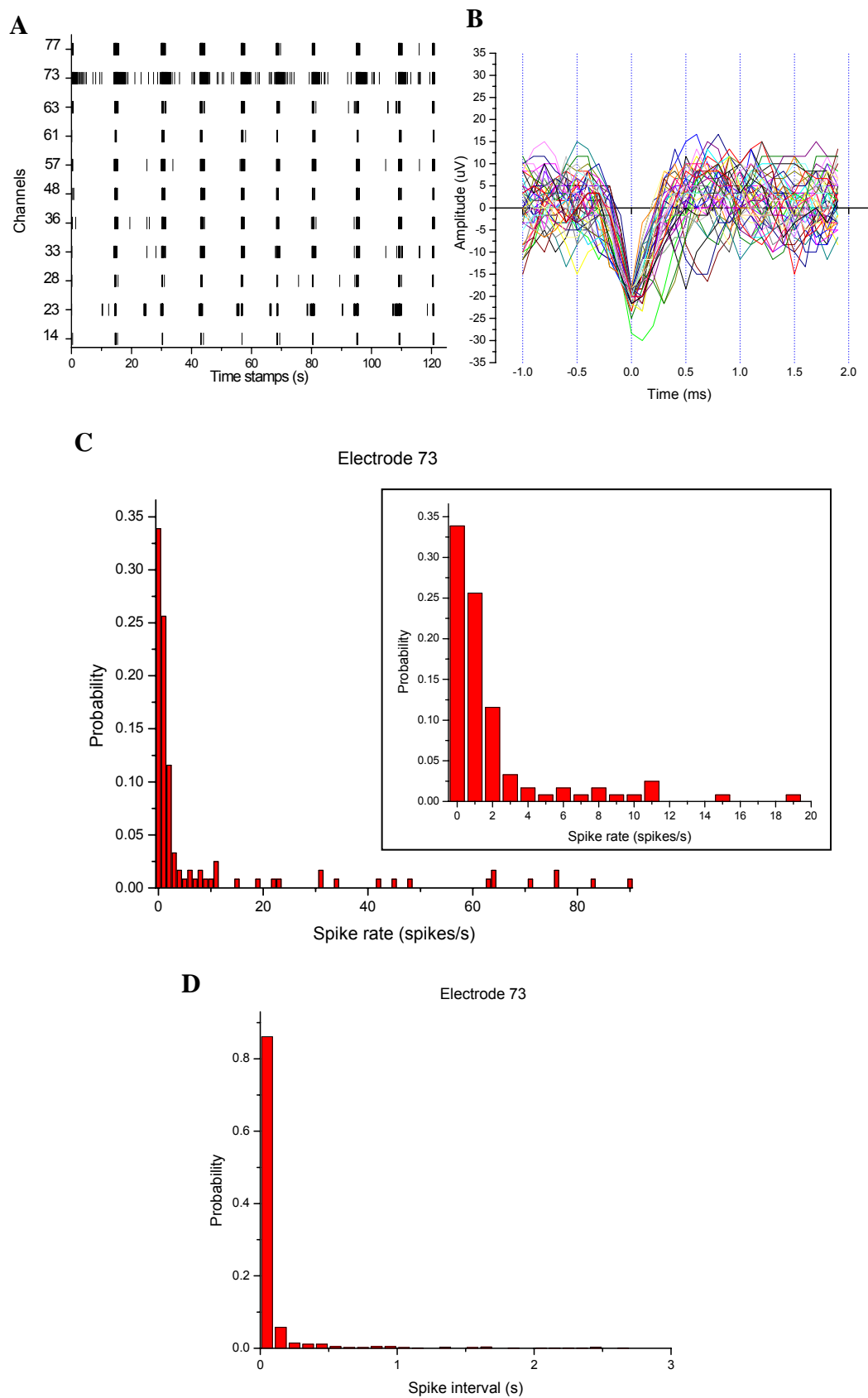
Electrode 73



**Figure 4.25 Raster plot of PEI-LN150K culture shown in figure 4.22 displaying the synchronised firing pattern of all active electrodes after 20 days post seeding (A). Recording from electrode 73**

**was further analysed and shown in (B) – (D). (B) Waveform of spikes recorded from electrode 73, overlay of the last 50 spikes. (C) Probability of spike rate recorded from electrode 73 over 2 minutes. Insert shows data from 0 – 20 spikes/s on the x-axis. (D) Probability of spike interval of electrode 73 over 2 minutes of recording.**
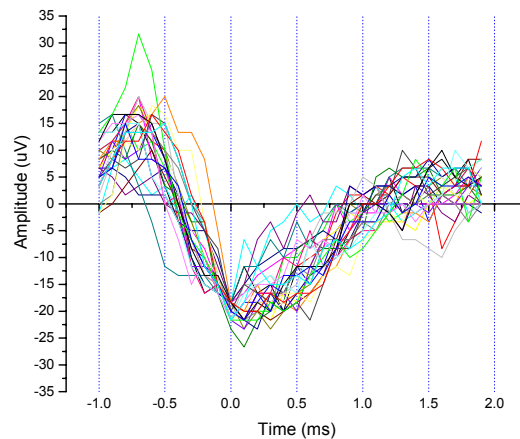


**Figure 4.26 Waveform of recording from electrode 63 in figure 4.23A. Scale of the axis is similar to that of figure 4.25B.**

P19-derived neurons that were seeded at 150 000 cells/cm$^2$ on PEI-LN coated MEAs were detected to start firing asynchronously between 6 – 9 days. Firing in the early stage of culture was usually irregular consisting of random isolated spikes. Different electrodes were observed to be active as the cultures matured until after 14 days post seeding. Along with the trend of increasing active electrodes, the amplitudes of the spikes were in general increasing as the MEA cultures progress. The minima of the spikes could reach a maximum of -200 µV.

After 14 days post seeding, the PEI-LN150 MEA cultures were more stable. The number of active electrodes was usually more than ten and there was lesser shift in the position of active electrodes. Most of the spike trains concerned single-unit activity, with stable amplitudes and waveforms (Figure 4.25B and Figure 4.26). The pattern of spontaneous firing was characterised at this time point by regular occurrences of short periods of synchronous firing at many of the recording sites, termed as network bursts.

The synchronised network activity lasts between 0.2 – 2 s. The duration of each synchronised activity was not observed to change significantly as the culture was prolonged. The raster plots and the total recorded activity of three PEI-LN150 MEA cultures between 17 – 20 days post seeding were shown in Figure 4.27. The number of active electrodes increased during network bursts. At 17 days post seeding, a pattern of firing including a phase of increased of firing activity leading to a short phase of synchronised firing and a phase of low level firing activity. As the cultures were prolonged, random firing between network bursts were drastically reduced after 17 days. The network activity of the P19-derived neurons developed into a recurrent pattern of firing with a repetition including a phase of low level firing activity, a short phase of synchronised firing and a silent network recovery phase. There was a general trend that the interval between successive network bursts increased as the culture matures (Figure 4.27, day 17 and day 18). The firing pattern of PEI-LN150 MEA cultures stabilised after 16 – 18 days post seeding.

17 days        18 days        20 days
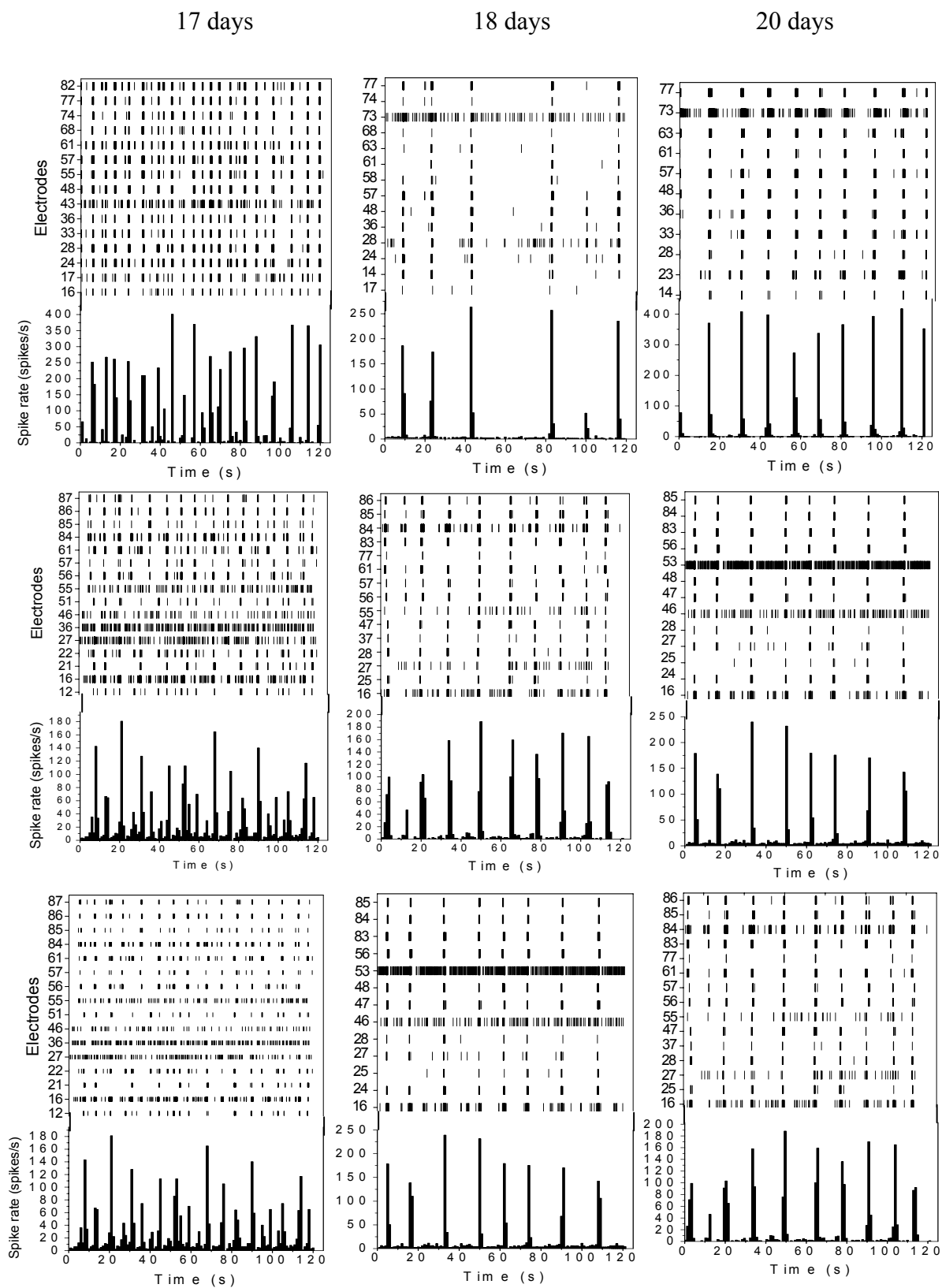


**Figure 4.27 Raster plots (above) of 3 MEA cultures after 17, 18 and 20 days post seeding. Total network firing rate profile (bottom) of the same MEA cultures.**

## 4.2 Response of P19-derived Neuronal Network to Neurotransmitters

P19 cells were induced to differentiate into neurons by suspending them for 4 days in 1 μM RA supplemented media. They were seeded as single cells at a density of 150 000 cells/cm$^2$ on PEI-LN coated MEAs. Robust spiking was observed usually between 17 – 26 days post seeding.

The major neurotransmitters of the central nervous system are γ-aminobutyric acid (GABA) and glutamate.  The effects of these neurotransmitters and their antagonists are investigated in the following sections.

### 4.2.1 Effects of neurotransmitters, their agonists and antagonists

P19-derived neurons do not form a monolayer culture since P19-derived neurons tended to form cell clusters. These cultures are shallow three dimensional layers in which glia are found below and above neural processes and may generate drug concentration gradients. Therefore, to observe the effects of different drugs on the three dimensional P19-derived neuronal network, continuous recording of between 2 to 3 hours would be necessary. After 12 -14 days post seeding, half of the media in the MEAs had to be changed daily due to the high metabolism of the cells as seen in the colour change of the pH-indicator within the media from orange-pink to yellow after 1 day indicating acidification of the medium. The media in the MEAs was changed 24 hours the day before recording was done. On the day recording was done the MEAs were removed from the incubator and connected to the amplifier and incubation unit. The native state of the MEA cultures was immediately recorded. A half medium change was done before the addition of drugs; this is referred to as the reference state. A complete measurement with the test substance comprised of the native state, reference state, the addition of test substance and wash state in order to exclude possible systematic baseline trends in electrophysiological activity during long-time measurements. Each state was measured for between 20 – 30 minutes. Half medium washes were performed to remove the test substances so as to minimise wash induced

damages to the cells. When the neuronal spontaneous activity was not returned to the reference state after washing of the test substance was performed their activity was then referred to as a new state. The native state was measured to compare with the reference state.

Before studying the responses of P19-derived neurons to the drugs, the stability of recording over a period of 2 hours and also after the addition of DMSO in which some of the drugs were dissolved was first investigated. Figure 4.28A shows the spike rate per second taken at 10s bins recorded continuously from six among thirteen active electrodes of one MEA culture after 17 days post seeding in the native state, reference state and for 60 minutes after the half medium change. The mean spike rate (MSR) for all active electrodes for one MEA culture represented the general activity of the culture, following closely the activity trend recorded at the individual electrode (Figure 4.28B). In the native state, the MSR of the network had a large variance. The larger standard deviation in MSR (1.09 spikes/s) in the native state was due to the synchronized network firing of MEA culture with little spontaneous activity in between the synchronized activity as seen in the raster plot in Figure 4.29A. Higher spike rates from twelve of the thirteen electrodes were obtained in the reference state. A decrease in spike rate was recorded from one electrode after the half medium change. There was an initial surge in spike rate directly after the half medium change which gradually decreased to a new state in the next 30 minutes. The initial surge in spike rate was due to the change in the ion concentration of the culture medium in the MEA. This sensitivity to sudden medium changes has been reported by Gross et al.[45] as well. They have shown that such sensitivity is not due to mechanical effect but by unknown factors in different media such as glucose levels, amino acid concentrations and hormones which affect the spontaneous activity. The MSR during the native state was $0.80 \pm 1.09$ spikes/s ($\pm$ standard deviation) and that 20 - 30 minutes after the half medium change was $1.18 \pm 0.39$ spikes/s which was not significantly different than that of the native state ($P > 0.05$, n = 13). The standard deviation of the MSR dropped from 1.09 to 0.39 spikes/s during that same period. The raster plot between $27 - 30$ minutes after the half medium change revealed that the firing pattern was random with some synchrony in the reference state (Figure 4.29B). At $30 - 40$ minutes after the half medium change, the MSR of $0.83 \pm 0.36$ spikes/s was similar to that of the native

state (P > 0.05, n = 13). The MSR was further maintained at the native state level between 40 – 50 minutes after the half medium change. The MSR 30 – 50 minutes after the half medium change was within 10 % of the MSR of the native state. Thereafter, the MSR continued to decrease at a slower rate until the recording was stopped after two hours. The recording of the MEA appeared to stabilise 30 minutes after the half medium change.
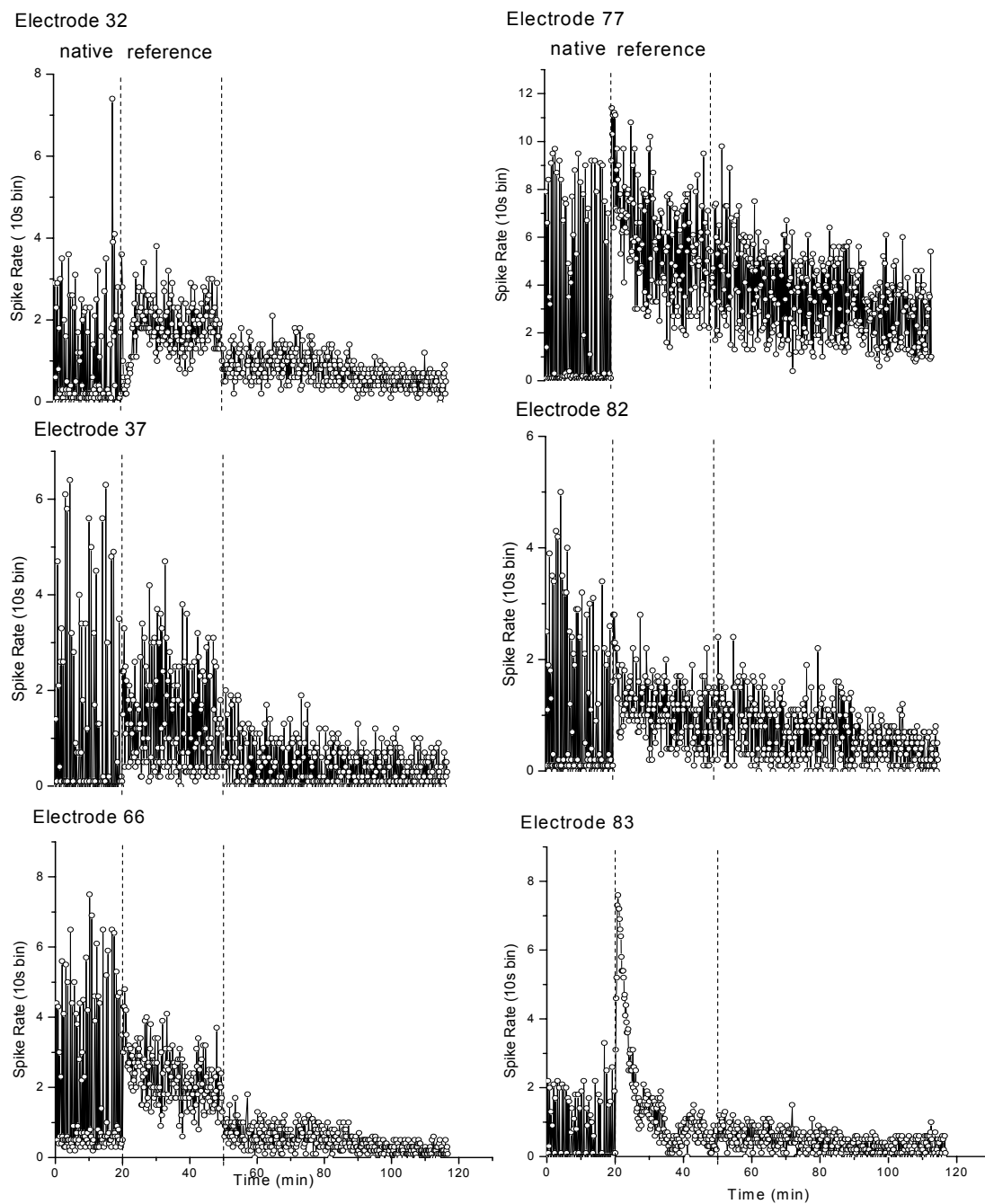
**Figure 4.28A Spike rate of P19-derived neurons over a period of 120 minutes in medium without the addition of drugs. Spike rate recorded from 6 among 13 active electrodes is shown here. A half medium change was performed at the 20th minute.**
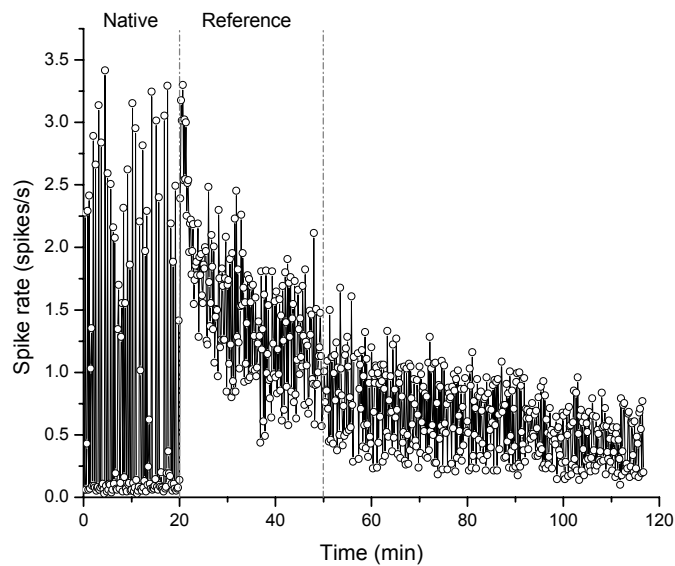
**Figure 4.28B Mean spike rate, MSR, (spike/s, 10s bins) of all thirteen electrodes during the 2 hours recording with a half medium change at the 20<sup>th</sup> minute. The MSR between the 50<sup>th</sup> – 70<sup>th</sup> minute of the recording, 30 – 50 minutes after the half medium change, was within 10 % of the mean spike rate of the native state. The recording of the MEA appeared to stabilise 30 minutes after the half medium change.**

10 % of the medium is removed from the MEA culture and 6 $\mu$l of DMSO (0.3 % of the culture medium), in which some of the drugs were dissolved, was added to it to examine the effect of DMSO on the cultures. There was no change in the spontaneous activity of the P19-derived neurons after the medium containing 6 $\mu$l DMSO was returned to the MEA culture even after 30 minutes (Figure 4.30). The MSR for all active electrodes in the period before and after the addition of 10 % medium containing 6 $\mu$l DMSO was 2.07 $\pm$ 2.29 and 2.19 $\pm$ 2.54 spikes/s respectively and they were not significantly different (P > 0.05, n = 16). It could therefore, be assumed that the return of the removed medium caused no activity artifacts by mechanical impact on the cells. Consequently, activity changes observed during the monitoring can be exclusively allocated to the action of test substances.

The network activity of the P19-derived neurons increased relative to the native state and appeared to stabilise between 20 - 30 minutes after the half medium change and returned to the native state after 30 minutes, remaining at the native state for the next 20 minutes. Test substances could hence be added to the cultures 30 minutes after the

reference state and the effects directly monitored after their addition. Half medium washes after the test substance addition were performed to check if activity might return to the reference state.
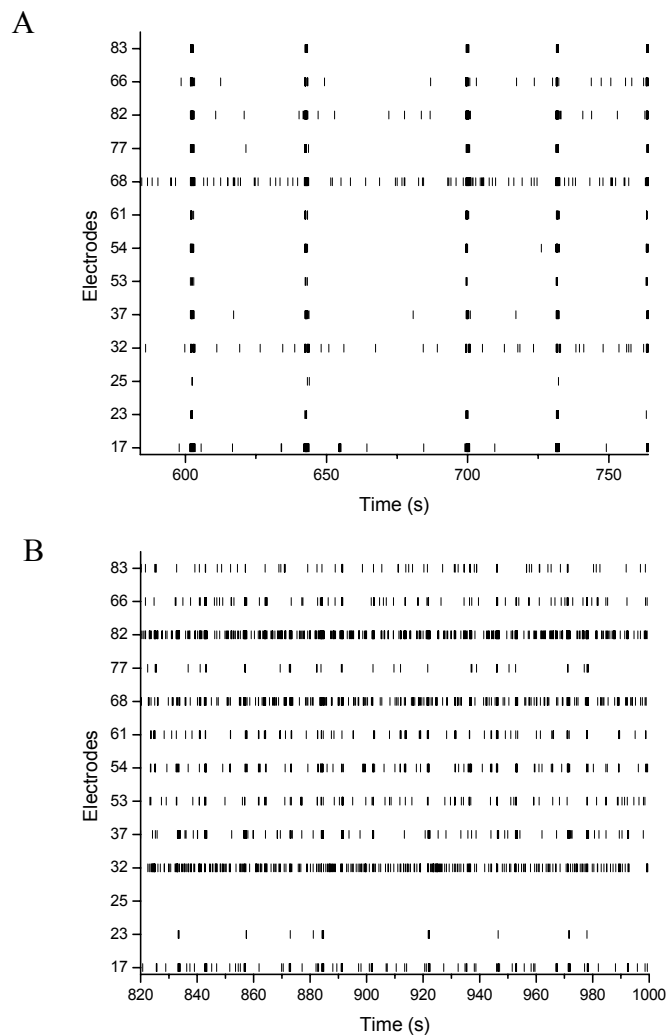


**Figure 4.29 Raster plots of the final three minutes recording of the native state (A) and reference state, 47th – 50th minute of the recording (B). (A) Synchronised network firing of MEA culture with little spontaneous activity in between the synchronized activity could be observed. (B) revealed that the firing pattern was random with some synchrony in the reference state.**
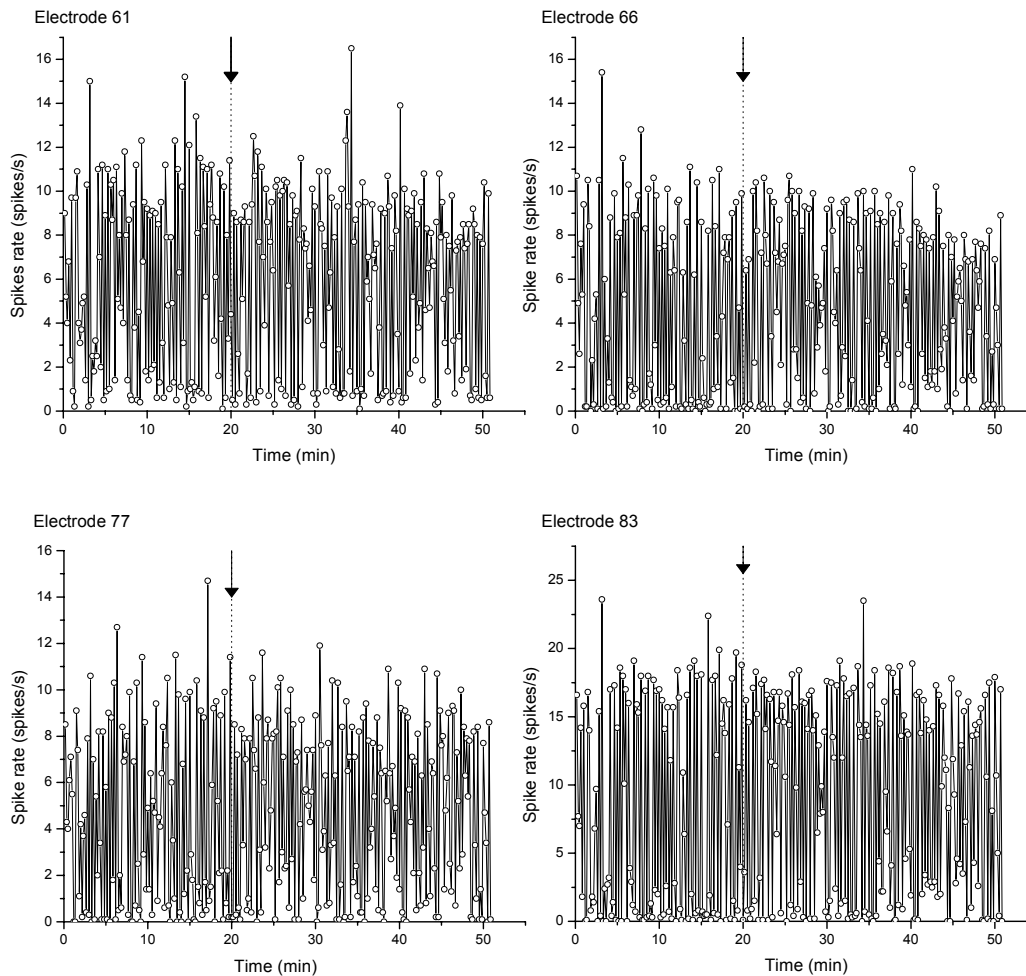
**Figure 4.30 Spike rate recorded from 4 electrodes. 6 µl of DMSO were added at the time point indicated by the arrows. The MSR for all active electrodes in the period before and after the addition of 10 % medium containing 6 µl DMSO was not significantly different.**

## 4.2.2 Application of inhibitory neurotransmitter, γ-aminobutyric acid (GABA) and antagonists

The addition of 20 µM bicuculline (BIC), a competitive GABA antagonist on the GABA$_A$ receptor, caused an increase in spike rate recorded from 54 % (7 of 13) of the electrodes, a decrease from 23 % (3 of 13) of the electrodes and no changes from 23 % (3 of 13) of the active electrodes of a MEA culture (MEA-N06-1) 21 days post seeding. Figure 4.31 displays the MSR of all electrodes that showed an increase in spike rate (BIC-positive) in 10s bins when BIC was first added. The MSR was 1.53 ±

1.58 spikes/s and 2.33 ± 2.10 spikes/s before and after the addition of 20 µM BIC (P < 0.05, n = 7), respectively. The MSR was 1.5 times that before BIC addition. The GABA disinhibition effect of BIC was found to last about 10 minutes; thereafter the activity of the P19-derived neurons appeared to revert back to the reference state 30 minutes after BIC application. Thirty minutes after the addition of 20 µM BIC the MSR dropped to 1.33 ± 1.29 spikes/s, similar to that of the reference state (P > 0.05, n = 7). In contrast, the MSR in the native state was 0.85 ± 0.78 spikes/s, not significantly lower than the reference state (P > 0.05, n = 7). A half medium wash (Wash 1) returned activity to the reference state after 30 minutes at MSR of 2.00 ± 1.68 spikes/s (P > 0.05, n = 7). Subsequent addition of a higher concentration of 50 µM BIC resulted in an increase in activity from only 23 % (3 of 13) of the active electrodes, a decrease in activity from 54 % (7 of 13) of the active electrodes and no change from 23 % (3 of 13) of the active electrodes. Out of the 7 electrodes that showed an increase in spike rate when 20 µM BIC was first added, the subsequent addition of 50 µM BIC resulted in an increase in spike rate in only 3 of them. The MSR 10 minutes after 50 µM BIC addition was 2.16 ± 1.68 spikes/s, not significantly higher than that of the reference state (P > 0.05, n = 7). One half wash thereafter resulted in a similar spike rate (2.07 ± 2.24 spikes/s) as the reference state (P > 0.05, n = 7).

Interpretation of the mean spike activity of all active electrodes gives a general trend in drug induced changes. Normalised data relative to the reference spike rate recorded from each individual electrode could reveal higher sensitivity to changes that was not detected with the computation of MSR. A higher significance in changes due to the addition of 20 µM BIC could be detected in the normalised data from BIC-positive electrodes (P < 0.01, n = 7) (Figure 4.32). The reference state's activity was also significantly different than that of the native state shown in the normalised data (P < 0.01, n = 7). The activity after the addition of 20 µM BIC and of the native state normalised to the reference activity was 1.70 ± 0.38 and 0.66 ± 0.16, respectively. The normalised spike rate after application of 50 µM BIC did not change significantly relative to both the spike rate at the reference and Wash 1 state (P > 0.05, n = 7). Although the reference activity was recovered after washing, the addition of the first

dose of BIC appeared to have changed the P19-derived neuronal network response to immediate subsequent BIC application.
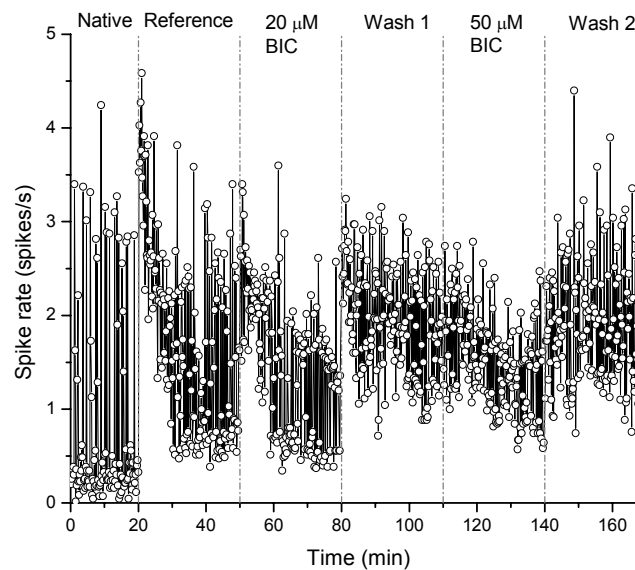


**Figure 4.31 MSR of the active electrodes from MEA-N06-1 (21 days post seeding) recorded at 10s bins that displayed an increase in spike rate when BIC was added. The initial addition of 20 $\mu$M BIC, a competitive GABA antagonist resulted in an increase in spike rate but the subsequent addition of 50 $\mu$M BIC did not cause an increase in activity. MSR after Wash 1 and Wash 2 returned to the reference level (P > 0.05, n = 7).**
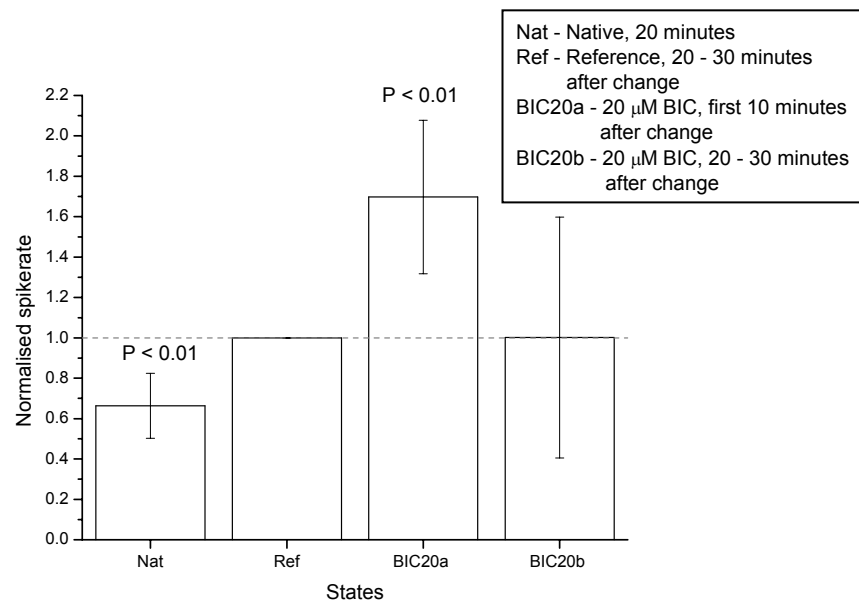


**Figure 4.32 Normalised spike rate relative to reference spike rate recorded from each BIC-positive electrode. A higher significance in changes due to the addition of 20 $\mu$M BIC could be**

detected in the normalised data (P < 0.01, n = 7). The grey dotted line at the level of the reference was drawn for comparing the other states.The legend indicates the state and time point of the recording.
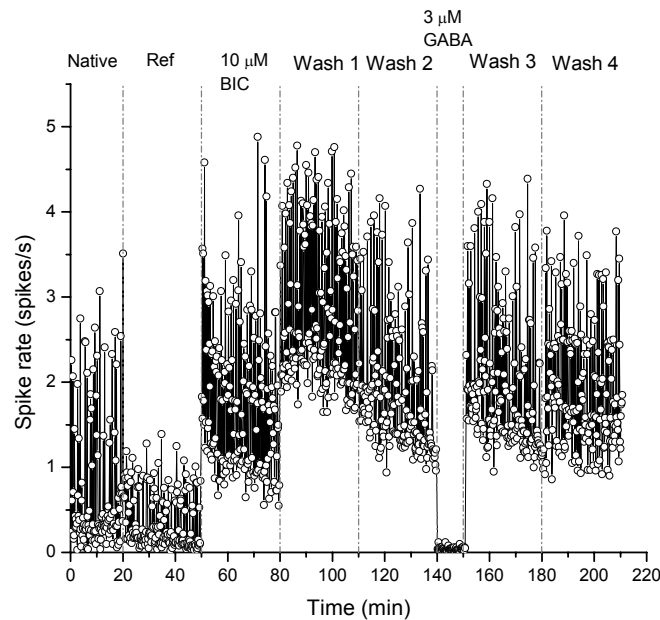


**Figure 4.33 MSR of all BIC-positive electrodes from MEA-N06-1 (23 days post seeding) recorded at 10s bins. The addition of 10 μM BIC resulted in the increase in spike rate from 67 % the active electrodes and subsequent addition of 3 μM GABA resulted in a complete inhibition of activity recorded from all but one electrode. Activity was recovered following wash steps.**

The addition of 10 μM BIC to MEA-N06-1 2 days later, 23 days post seeding, resulted in an increase in the proportion of active electrodes showing an augmentation in spike rate. There was an increase in spike rate after the addition of 10 μM BIC in 67 % (10 of 15) of the active electrodes (BIC-positive) while 20 % (3 of 15) and 13 % (2 of 15) had a decrease and no change in spike rate, respectively. Figure 4.33 displays the MSR of the 10 BIC-positive electrodes. The MSR of the reference state was not significantly different than that of the native state at $0.34 \pm 0.37$ and $0.75 \pm 0.85$ spikes/s respectively (P > 0.05, n = 10). With the addition of 10 μM BIC, the MSR increased to 5.7 times that of the reference state, $1.91 \pm 2.38$ and $0.34 \pm 0.37$ spikes/s, respectively (P < 0.05, n = 10). Thirty minutes after the addition of 10 μM BIC, MSR decreased slightly to $1.65 \pm 2.13$ spikes/s but did not return to the reference level. Thirty minutes after Wash 2 (2 x half medium wash), the MSR was similar to

that after 10 µM BIC at 1.63 ± 3.22 spikes/s (P > 0.05, n = 10). BIC seemed to have changed the firing activity of the P19-derived neurons after its addition since 2 half medium washes did not return activity to the reference state. The spontaneous firing recorded from all active electrodes except one was inhibited (MSR = 0.036 ± 0.051 spikes/s, n = 14) with the addition of 3 µM GABA at the 140th minute. That single electrode recorded an increase in spike rate when 3 µM GABA was added. Spontaneous activity recorded from all BIC-positive electrodes was inhibited when 3 µM GABA was added at the 140th minute (MSR = 0.041 ± 0.060 spikes/s, n = 10), indicating the presence of GABAergic neurons containing $GABA_A$ receptors. Subsequent wash (Wash 3) returned activity to MSR of 1.72 ± 3.30 spikes/s similar to the MSR prior to GABA treatment (P > 0.05, n = 10). MSR remained at this level until the 210th minute of recording.

Recording from a different MEA culture (MEA-A07-2) is shown in Figure 4.34. Muscimol, a GABA agonist at $GABA_A$ receptors, was added at 3 µM to two MEA cultures, MEA-A07-2 and MEA-A07-3, after18 days post seeding at the 40th minute. The MSR during the reference state for the MEA culture shown in Figure 4.34 was significantly higher (P < 0.01, n = 13) than that in the native state. The MSR for the native state and during the last 10 minutes of the reference state was 1.10 ± 0.90 and 1.89 ± 1.72 spikes/s, respectively. For both MEAs, spike rate from all active electrodes was reduced instantaneously after the addition of 3 µM muscimol which binds to high affinity sites on the $GABA_A$ receptors. This instantaneous decrease in spike rate was also observed with the addition of GABA in other cultures (Figure 4.33, Figure 4.38). For the MEA culture shown in Figure 4.34, the MSR was reduced from 1.89 ± 1.72 to 0.18 ± 0.32 spikes/s with the addition of 3 µM muscimol (P < 0.01, n = 13). The inhibition on network firing remained for the whole 20 minutes that muscimol was applied and activity was recovered when a half medium change was done, returning activity to an average spike rate of 1.90 ± 2.48 spikes/s after 30 minutes similar to that prior to muscimol addition (P > 0.01, n = 13). However, a half medium wash after muscimol application caused an instantaneous increase in MSR, not a gradual recovery as one might expect as washing would cause a slow dissociation of muscimol which binds to high affinity binding sites on the $GABA_A$

receptors. This indicates that the half medium wash performed induced activity artifacts due to mechanical impact on the cells during washing.

MEA-A07-2 in Figure 4.34 was tested with bicuculline (Figure 4.35) one day later at 19 days post seeding. 71 % (12 of 17) of the active electrodes had an increase in spike rate (BIC-positive) when 50 μM BIC was added while the spike rate for 6 % (1 of 17) and 24 % (4 of 17) had a decrease and no change in spike rate, respectively. The MSR of the active electrodes that had a spike rate increase upon addition of 50 μM BIC is shown in Figure 4.35. The MSR during the last 10 minutes of the reference state was similar to that of the native state at $1.58 \pm 1.32$ and $1.08 \pm 0.58$ spikes/s, respectively ($P > 0.05$, n = 12). Synchronised firing pattern was observed in the native state (Figure 4.36A) where many electrodes could be observed to detect coincidental events. Synchronised firing pattern was again observed in the reference state but with a higher frequency of non-synchronised events (Figure 4.36B). The addition of 50 μM BIC increased the MSR to $2.14 \pm 1.64$ spikes/s, 1.4 times that before the addition of BIC ($P < 0.001$, n = 12). The MSR then decreased to $1.47 \pm 1.58$ spikes/s, similar to that of the reference state ($P > 0.05$, n = 12). Synchronisation was increased in the firing pattern with a lower frequency of non-coincidental events between electrodes immediately after the addition of 50 μM BIC (Figure 4.36C) in contrast to the reference state. The addition of 3 μM muscimol during the application of 50 μM BIC resulted in the decrease of the spike rate in 76 % (13 of 17) of the active electrodes, an increase in 5 % (1 of 17) and no change in 18 % (3 of 17) of the active electrodes. Of the 12 electrodes that had an increase in spike rate with the addition of BIC, 9 had a decrease, 1 had an increase and 2 had no change in spike rate when 3 μM muscimol was added. The MSR decreased to $1.15 \pm 1.42$ spikes/s, 0.8 times that before muscimol addition. It gradually decreased further to $0.85 \pm 1.03$ spikes/s 30 minutes after the addition of 3 μM muscimol, 0.6 times that before muscimol addition (significantly different, $P < 0.05$, n = 12). The addition of 3 μM muscimol in the presence of 50 μM BIC did not completely inhibit network activity as was shown before (Figure 4.34). Due to the presence of the competitive antagonist of GABA on the $GABA_A$ receptor, the inhibition of network activity due to muscimol was less effective resulting in a more gradual spike rate reduction between the $80^{th}$ - $110^{th}$ minute. A half medium wash 30
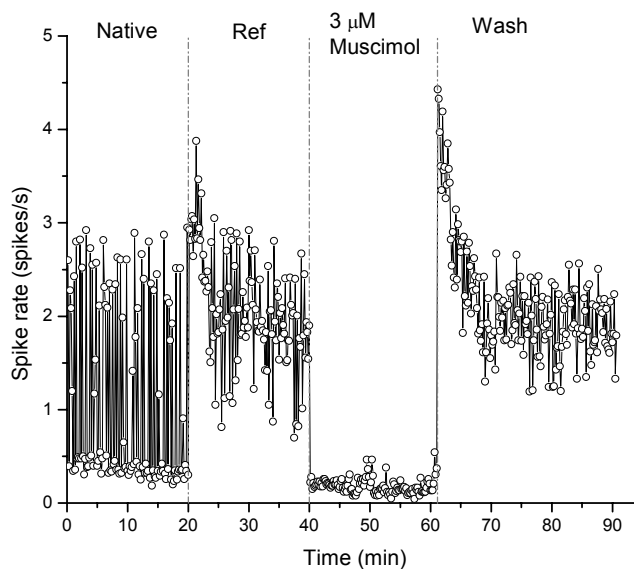
**Figure 4.34 Average spike rate of all active electrodes from MEA-A07-2 (18 days post seeding) at 10s bins. A lower spike rate was obtained for all electrodes when 3 μM muscimol was added.**
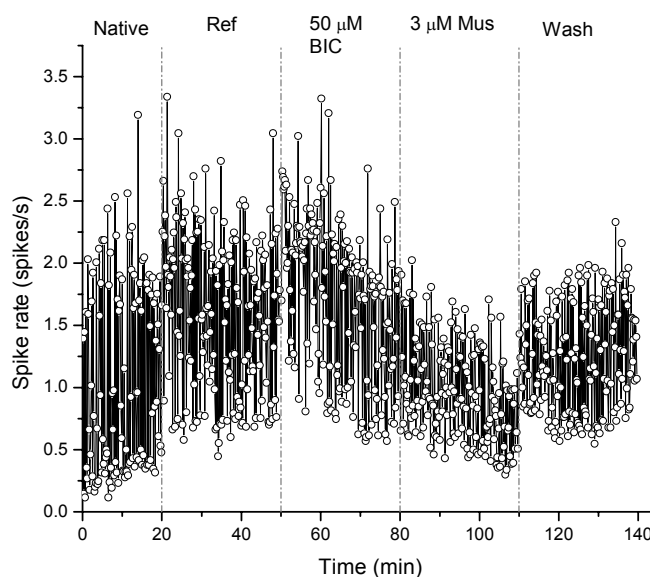


**Figure 4.35 MSR at 10s bins of BIC-positive electrodes from MEA-A07-2 (19 days post seeding). The addition of 50 μM BIC resulted in the increase in spike rate in 71 % of the active electrodes and the subsequent addition of muscimol (Mus), a GABA agonist resulted in the lowering of the spike rate from 76 % of the active electrodes. Due to the presence of BIC, the inhibition of network activity by muscimol was less effective resulting in a more gradual spike rate reduction. Spike rate was recovered following removal of the drugs.**
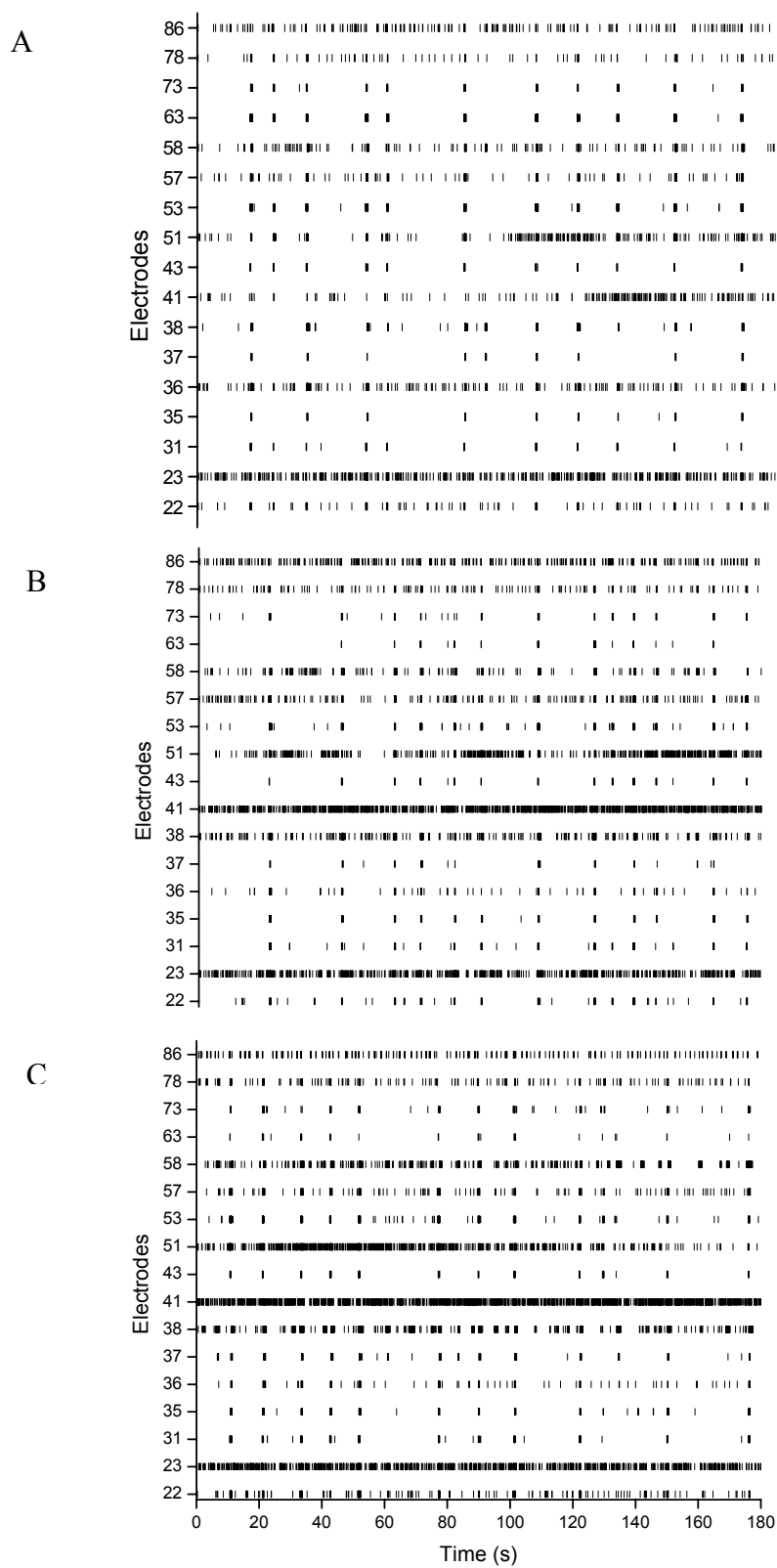
**Figure 4.36 Three minutes raster plots of the same MEA culture (MEA-A07-2) in Figure 4.35 at 19 days post seeding showing the native (A), reference (B) states just before and the state**

**immediately after the application of 50 μM BIC (C). Synchronised firing pattern was observed in the native state (A). Synchronised firing pattern was again observed in the reference state but with a higher frequency of non-synchronised events (B). The firing pattern was again more synchronised with a lower frequency of non-coincidental events between electrodes immediately after the addition of 50 μM BIC (C).**

minutes after the addition of muscimol returned the average spike rate to that of the reference state at $1.42 \pm 1.28$ spikes/s (P >0.05, n = 12).

The activity normalised to the reference activity from each electrode (Figure 4.37) upon 50 μM BIC application was $1.52 \pm 0.35$ (P < 0.001, n = 12). Figure 4.37 shows that as in the MSR data that the normalised activity of the native state, 30 minutes after BIC application and Wash state was not significantly different than that at the reference state. Without washing away BIC, the normalised activity due to the addition of 3μM muscimol (Mus 1 in Figure 4.37) and 20 – 30 minutes after muscimol application (Mus 2) was $0.69 \pm 0.40$ and $0.51 \pm 0.46$, respectively. Normalised activities at 'Mus 1' and 'Mus 2' periods were significantly lower than the reference state (P < 0.05, P < 0.01, respectively; n = 12). The rate of spike rate decrease during BIC application was different than that during muscimol application as can be seen from Figure 4.37. The spike rate decrease during muscimol application could therefore, be attributed to the action of muscimol. It appeared that the presence of BIC modulated the inhibitory activity of muscimol. Activity returned to the reference state after washing was performed to remove the drugs showing that the effects of both BIC and muscimol were reversible.
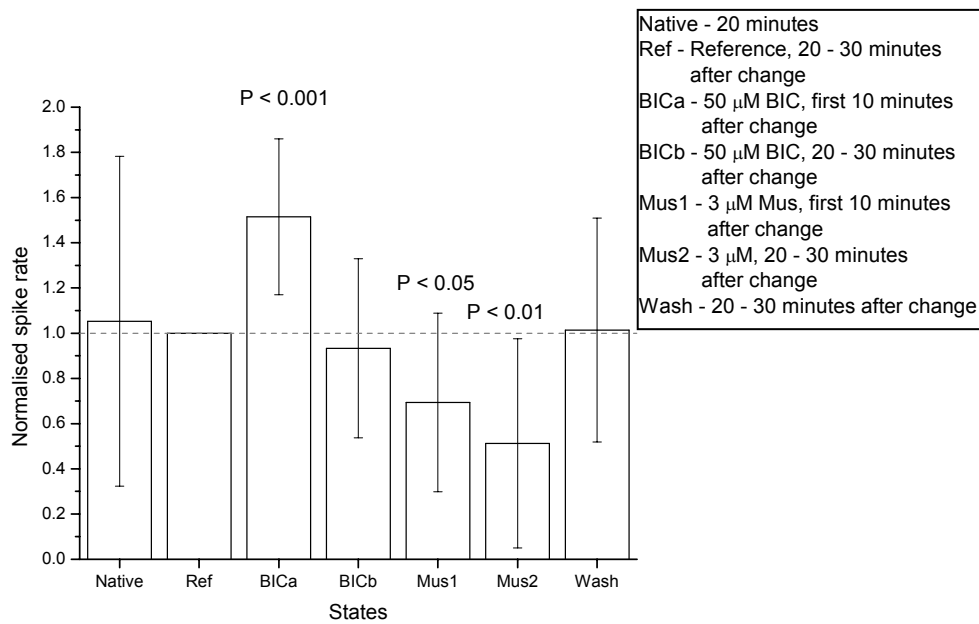
Figure 4.37 Normalised spike rate relative to reference spike rate recorded from each BIC-positive electrode in Figure 4.35. The grey dotted line at the level of the reference was drawn for comparing the other states. The legend indicates the state and time point of the recording.

## 4.2.3 Application of excitatory neurotransmitter, glutamate and antagonists

The responses of the MEA cultures to the excitatory neurotransmitter, glutamate, and its antagonists were not as consistent as to the inhibitory neurotransmitter, GABA, and its agonist and antagonist described in the previous section.

Higher concentrations of GABA and glutamate were added to MEA-N06-1 after 24 days post seeding. Figure 4.38 displayed the MSR recorded exclusively from electrodes that had an increase in spike rate when glutamate was added. The MSR of the reference state was not significantly different than that of the native state at $1.48 \pm 2.23$ and $1.11 \pm 1.63$ spikes/s, respectively (n = 13, $P > 0.05$). The addition of two different doses of GABA resulted in the complete inhibition of network activity in all 19 active electrodes. Two half washes was needed to restore the network activity. The addition of more than 10 times higher concentration of GABA appeared to silence the network activity of the P19-derived neurons. The addition of 10 µM glutamate

resulted in the increase in MSR in 13 of the 19 active electrodes (68 %), a decrease in 5 and no change in 1 of the 19 active electrodes. The MSR of all the electrodes that had an increase in spike rate when glutamate was applied was $3.10 \pm 3.54$ spikes/s in the first 5 minutes which was significantly different than that before glutamate application ($P < 0.01$, $n = 13$). This was quickly down regulated within the next 11 minutes to give an MSR of $1.28 \pm 2.29$ spikes/s between $20 - 30$ minutes after glutamate addition which was not significantly different to that just before glutamate addition at the $205^{th}$ minute ($P > 0.05$, $n = 13$). The rapid down regulation of the excitatory effect was interpreted to be the result of AMPA desensitisation or the uptake of glutamate by glial cells to control the extracellular glutamate concentration. Wash 5, thirty minutes after the addition of glutamate, resulted in an average spike rate of $0.81 \pm 1.78$ spikes/s, not significantly different than that of the reference state ($P > 0.05$, $n = 13$). The restoration of activity to the reference state after more than 4 hours of recording showed that P19-derived neuronal networks cultured on the MEAs was a robust system for long term recording.
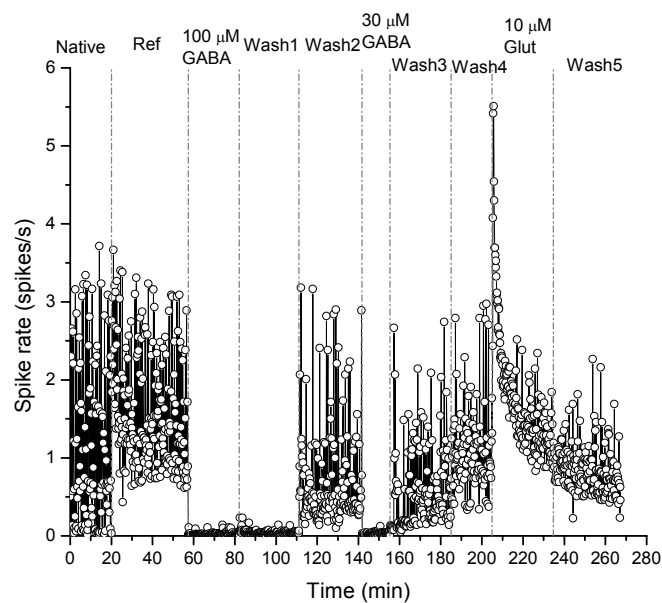


**Figure 4.38 MSR recorded from only electrodes of MEA-N06-1 (24 days post seeding) that had an increase in spike rate when glutamate was added. The addition of two different concentrations of GABA resulted in the complete inhibition of network activity in all 19 active electrodes. The addition of 10 μM glutamate resulted in the increase in a transient increase in MSR from 68 % of the active electrodes.**

A decrease in MSR was recorded from 71 % (10 of 14) of the active electrodes of MEA-A07-3 which was not previously treated with GABA when 10 µM cyclothiazide (CTZ), a potent blocker of AMPA desensitization, was added 23 days post seeding. A smaller proportion of the active electrodes (4 of 14) displayed higher spike rates when CTZ was added.

MSR of the four electrodes in MEA-A07-3 23 days post seeding increased to 4.85 ± 3.27 spikes/s from 3.17 ± 2.24 spikes/s in the reference state during the first 5 minutes of CTZ application (Figure 4.39A). The effect of CTZ application on MSR had the same characteristic trend as that of exogenous glutamate application seen in Figure 4.38 with an almost instantaneous overshoot which exponentially decreased to a stable baseline. This clearly shows the presence of endogenous glutamate in the P19-derived neuronal cultures. The average spike rate then decreased to 1.51 ± 1.44 spikes/s 24 minutes after CTZ application and was completely inhibited when glutamate was added thereafter.

CTZ acts as a positive modulator of AMPA receptors by stabilising the non-desensitised state of the activated AMPA receptor[36, 60]. However, the prolongation of the AMPA receptor activation in the P19-derived neuronal culture was not significant with 10 µM CTZ as expected. A higher dose of CTZ was not tested. When exogenous glutamate (10 µM) was added to MEA-A07-1 culture at 21 and 24 days post seeding the time it took for MSR to reduce by 1 spike/s ($\tau$) was 3.5 and 0.3 minutes, respectively. The $\tau$ value for MSR reduction during CTZ application in MEA-A07-3 23 days post seeding was 1.6 minutes. In comparison, cultures that were exposed previously to GABA had a more pronounced excitatory response to exogenous glutamate application such as MEA-N06-1 (Figure 4.38) which had a $\tau$ value of 2.7 minutes.

Most of the electrodes in MEA-A07-3 had an almost instantaneous reduction in MSR upon CTZ addition (Figure 4.39B), resulting in an exponential decrease in the MSR of most electrodes from 2.68 ± 3.88 spikes/s to a final of 1.04 ± 1.89 spikes/s 24 minutes after CTZ addition. The MSR during CTZ application was significantly lower than that of the reference state at 3.58 ± 3.33 spikes/s ($P < 0.05$, n = 10).

An addition of glutamate after CTZ application resulted unexpectedly in an inhibition of activity recorded from all electrodes (Figure 4.39). The instantaneous decrease of MSR upon the addition of glutamate at the $45^{th}$ minute of recording was an activity artifact due to the addition of the drug. However, the maintenance of this unexpected inhibition during the whole 30 minutes of glutamate application could be perhaps accounted for by the prominently GABAergic system shown previously. The excitatory inputs generated by the higher concentration of glutamate could activate the GABAergic neurons which in turn silenced the network.
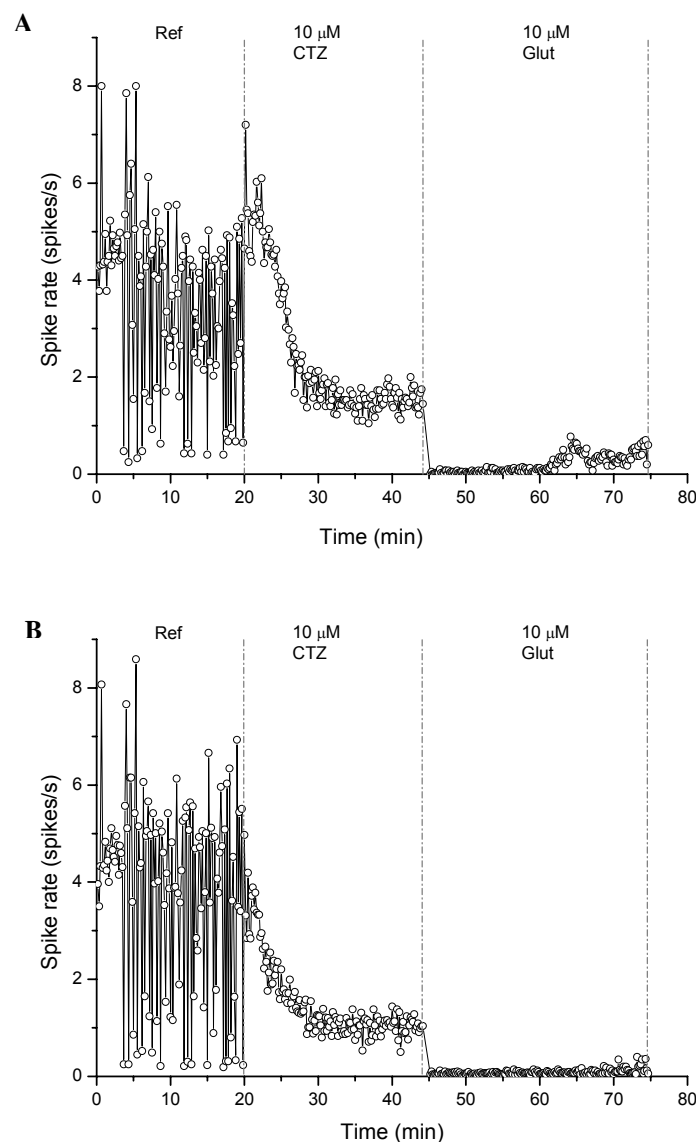


**Figure 4.39 MSR recorded from MEA-A07-3 (23 days post seeding) which was not previously treated with GABA. (A) Only 4 out of 14 active electrodes had an increase in MSR upon 10 μM CTZ application. The effect of CTZ application on MSR had the same characteristic trend as**

**that of exogenous glutamate application seen in Figure 4.38 with an almost instantaneous overshoot which exponentially decreased to a stable baseline. (B) MSR recorded from 71 % (10 of 14) of the active electrodes decreased when 10 μM CTZ was added.**

The addition of 0.3 μM TTX to MEA-A07-3 the next day eliminated all spikes and remained so during the period of 8 minutes that it was applied. Half medium wash was performed three times but the spike activity of the network was not recovered. Activity was increased the next day. The elimination of activity due to TTX showed that sodium channels were active during action potential generation.
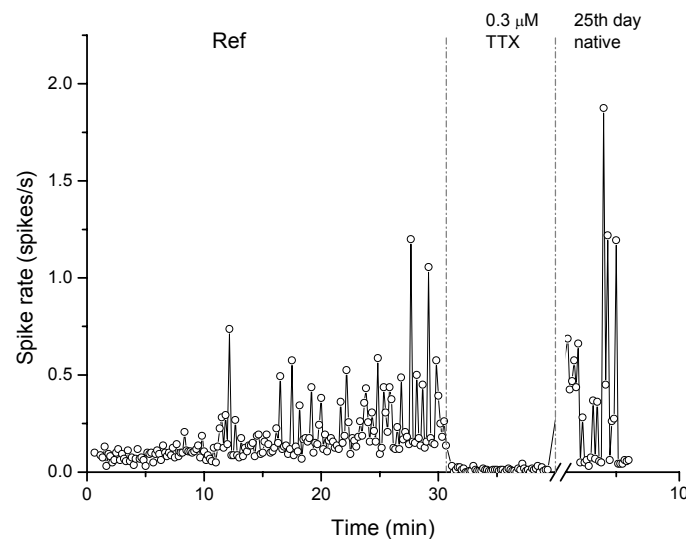


**Figure 4.40 MSR of 16 active electrodes in MEA-A07-3 (24 days post seeding). The addition of 0.3 μM TTX eliminated all spikes and remained so during the time of 8 minutes that it was applied.**

## 4.3     OR5 Transfection

Transfection of P19-derived neurons for the expression of OR5 receptor was performed via various ways, recombinant semliki forest virus (SFV) infection, electroporation and DNA / calcium phosphate coprecipitaion.

## 4.3.1     Viral infection

P19 cells were differentiated according to method IC2S and seeded on PEI-LN coated surfaces at 150 000 cells/cm$^2$. Spontaneous activity was detected after 7 days post seeding. P19-derived neurons cultured on MEAs and sibling culture flasks were infected with replication deficient SFV particles after 18 days post seeding, the time point when synchronised network activity was observed. MEA recording from SVF infected P19-derived neurons could not be obtained as the cells failed to spontaneously fire after the infection, although confocal laser microscopy of sibling cultures showed that OR5 receptors were detected (Figure 4.41). It was also observed that clusters of cells in the MEA cultures were floating off 15 hours after infection. Electron micrograph showed that there was active formation of receptors on the surface of infected cells (Figure 4.42). This was not observed in control cultures. The exocytosis of a vesicle containing membrane proteins could be seen in Figure 4.42B. The overexpression of OR5 receptor could have disrupted the process of action potential generation and transmission in the SFV infected P19-derived neurons.
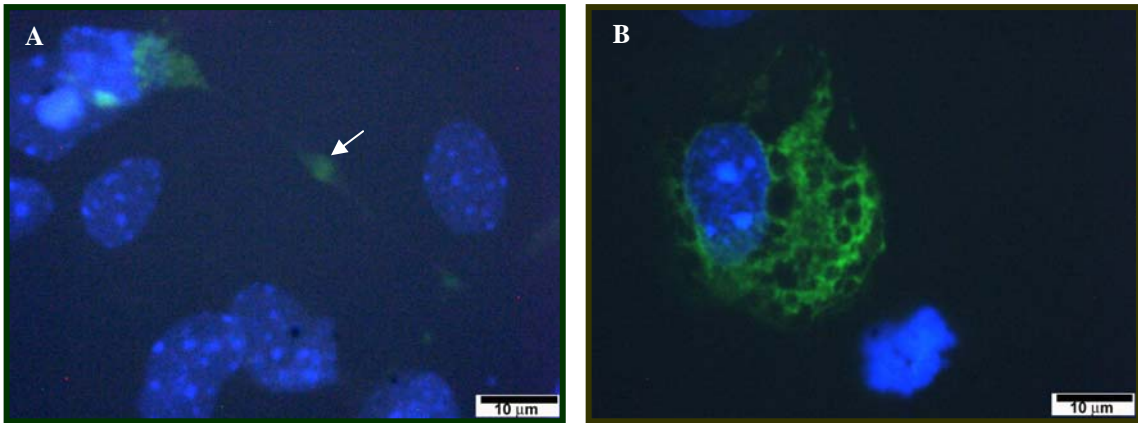
**Figure 4.41 Immunostaining of SFV infected RA treated P19 cells. DAPI stained nuclei (blue) and OR5 stained (green) neuron (arrow in A) and non neuronal cell (B) could be observed on the same day in sibling cultures when MEA recording was performed at the 18th day post seeding.**
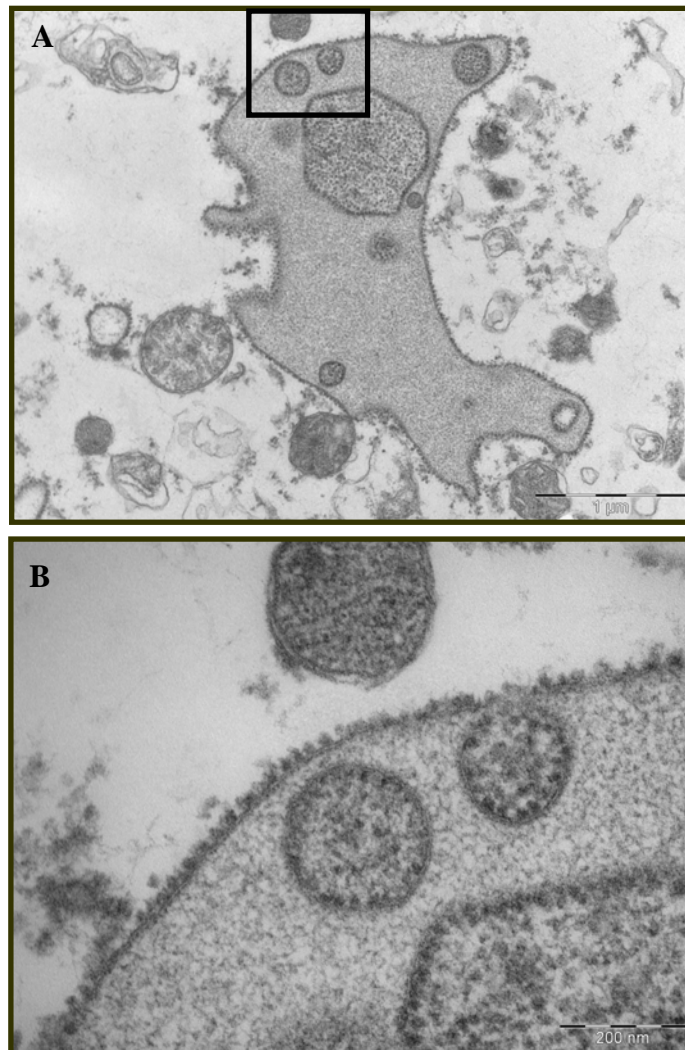


**Figure 4.42 Electron micrographs of infected cells showing active membrane bound receptor formation. (B) is an enlarged region indicated in (A). (A) Bar, 1 μm. (B) Bar, 200 nm.**

## 4.3.2    DNA cloning

T-Rex$^{TM}$ System, a tetracycline (Tet) regulated expression system for mammalian cells was used to express OR5 in P19-derived neurons. Tet regulation in the system is based on the binding of Tet to the Tet repressor and subsequent derepression of the promoter controlling expression of gene of interest. The expression of the gene of interest was controlled in this system by the strong human cytomegalovirus immediate-early (CMV) promoter and two tetracycline operator 2 (TetO$_2$) sites. Another plasmid, pcDNA6/TR$^©$, encoding for the Tet repressor under the control of the CMV promoter regulates the expression.

Plasmids pTNT-OR5 and pcDNA4/TO were double restricted by EcoRI and Not1 enzymes and ligated by DNA ligase. The recombinant plasmid pcDNA4/TO–OR5 had a size of 6057 base pairs. PCR of the recombinant plasmid showed that a product of 1000 bp was present (Figure 4.43) using OR5 reverse and forward primers. The OR5 encoding DNA sequence is 942 bp in size.
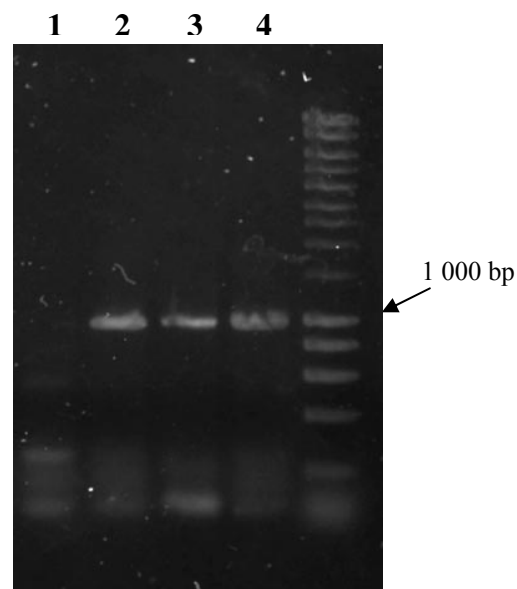


**Figure 4.43 1 % agarose gel showing a 1000 bp PCR product of recombinant pcDNA4/TO-OR5 in lanes 2 and 4. Lane 1 – without plasmid (negative control), lane 2 and 4 – pcDNA4/TO-OR5, Lane 3 – pTNT-OR5 (positive control).**
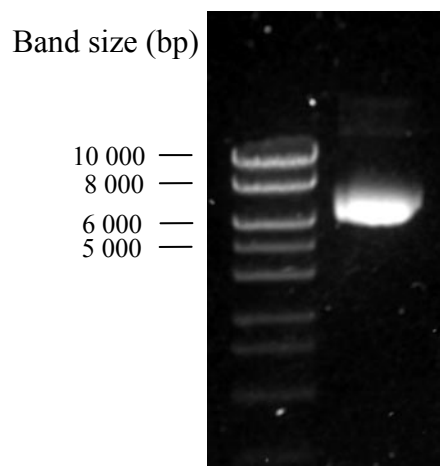
**Figure 4.44 Recombinant pcDNA4/TO-OR5 was linearised with Sap 1, desalted and ethanol precipitated. 1 % agarose gel showed that the 6057 bp plasmid was present after ethanol precipitation.**

Prior to transfecting the cells with the recombinant pcDNA4/TO-OR5 plasmids (Figure 4.44), the plasmids were sent for sequencing to verify that OR5 was correctly encoded. There was one mismatch at position 15 (Appendix), before the Kozak sequence (position 19 – 27). The recombinant plasmid was missing a thymine nucleotide at position 15. Since the mismatch was at an inconsequential site, the recombinant pcDNA4/TO-OR5 plasmid was transfected into the cells.

## 4.3.3    Electroporation and calcium phosphate precipitation

Transfection by both electroporation and calcium phosphate were performed on RA treated P19 cells to introduce the 2 plasmids into the cells. Three combinations of transfection methods were performed. Group 1 consisted of first electroporating pcDNA $^{TM}$ 4/TO/OR5 plasmids in to the RA treated P19 cells and then introducing pcDNA6/TR$^©$ plasmids by calcium phosphate method. Group 2 consisted of first electroporating pcDNA6/TR$^©$ plasmids, followed by transfecting with pcDNA $^{TM}$ 4/TO/OR5 plasmids via calcium phosphate method. Group 3 consisted of transfecting the cells first with pcDNA6/TR$^©$ plasmids and then pcDNA $^{TM}$ 4/TO/OR5 plasmids by calcium phosphate method. Controls for group 1 and group 3 stained for b-Gal were shown in Figure 4.45 and Figure 4.46. Transfection efficiency by both electroporation and calcium phosphate method appeared to be within 10 %.

Transfection of the RA treated P19 cells were performed within three days after RA induction, the time period when the cells still undergo mitotic division. Cultures that were first transfected with pcDNA $^{TM}$ 4/TO/OR5 appeared to be not as robust as cultures that were first transfected with pcDNA6/TR$^{©}$. There was more cell death in these cultures. The expression of OR5 in the P19-derived neurons without the repression mechanism of pcDNA6/TR$^{©}$ appeared to compromise growth and proliferation of the cells. Spontaneous activity of the sibling MEA cultures for all groups was not detected. The addition of OR5 ligand, lilial, to the MEA cultures between 17 – 19 days post seeding at concentrations of 0.5 μM up to 200 μM did not stimulate any firing the cultures. Immunostaining of the sibling glass coverslip cultures was difficult to perform as the cells were easily washed away during the process of staining. Few OR5 expressing cells could be detected in group 3 cultures (Figure 4.47B) and the neuronal morphology of group 3 cultures could be clearly seen (Figure 4.47D). Transfection of both plasmids into P19-derived neurons appeared to disrupt the inherent generation of firing activity.
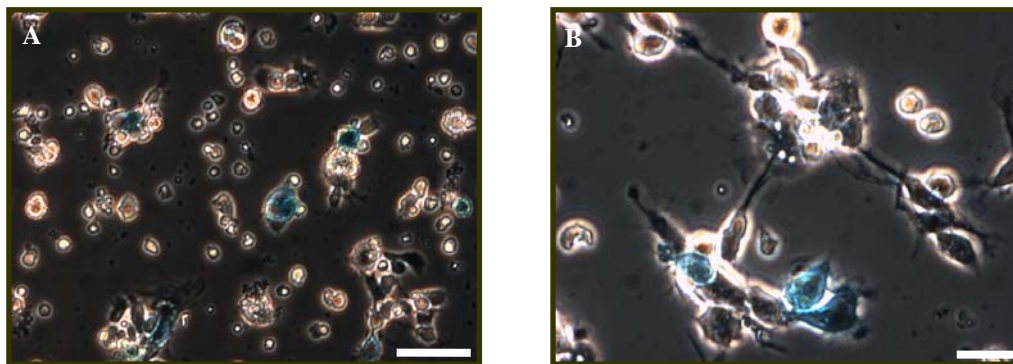


**Figure 4.45 RA treated P19 cells stained for β-Gal a day after electroporated with pcDNA $^{TM}$ 4/TO/lacZ plasmids. (A) Bar, 50 μm. (B) Bar, 20 μm.**
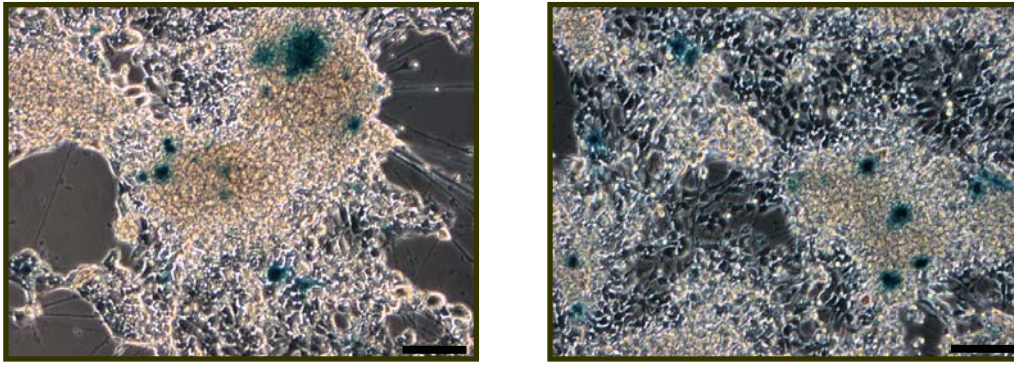
**Figure 4.46 Two different areas of P19-derived neuronal cultures stained for β-Gal 3 days post seeding. pcDNA6/TR© and pcDNA ™ 4/TO/lacZ plasmids were transfected into the P19-derived neurons by the calcium phosphate precipitation method. Bar, 100 μm.**
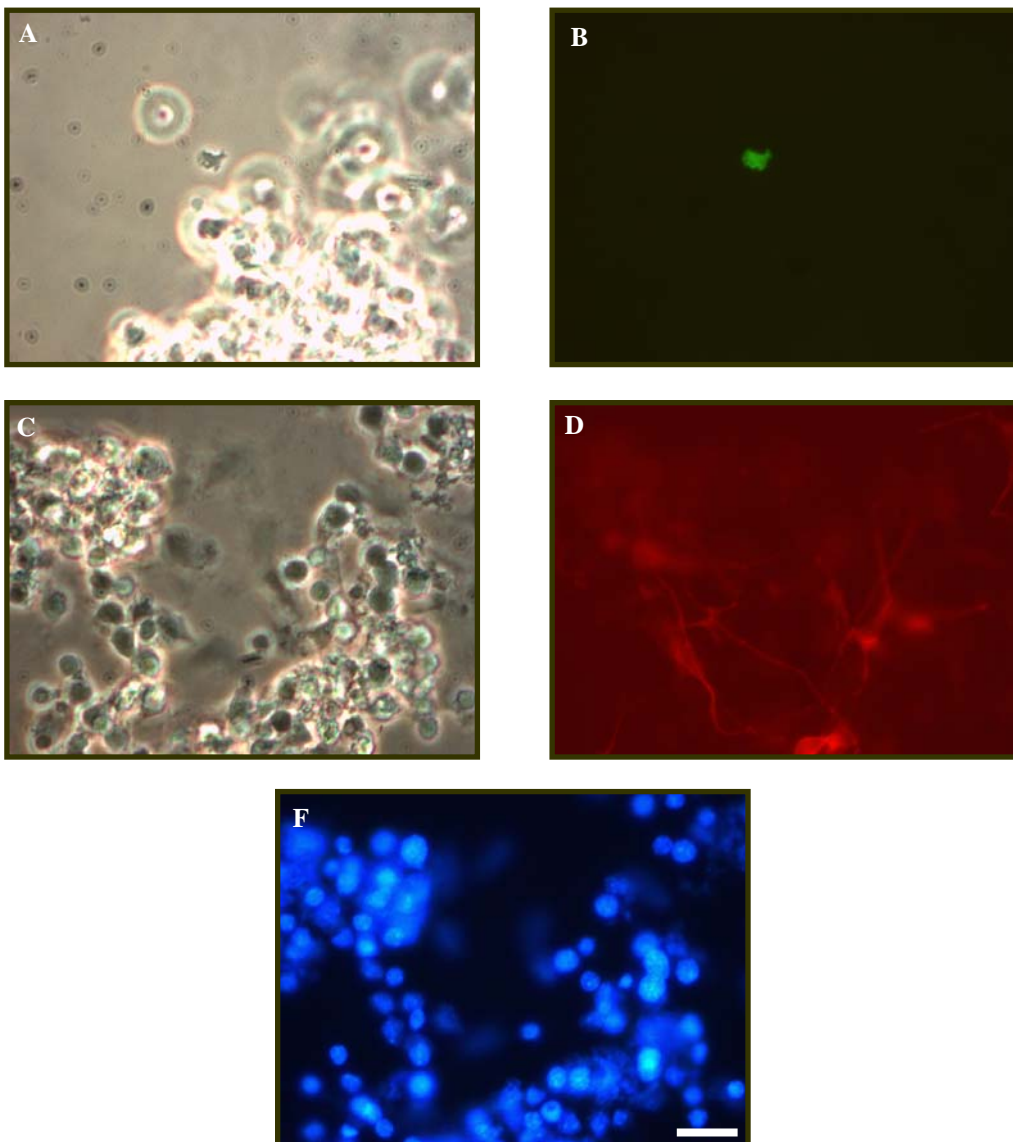


**Figure 4.47 P19-derived neurons stained against OR5 (green) and MAP2 (red) after 7 days post seeding (4 days after transfection). pcDNA ™ 4/TO/lacZ and pcDNA6/TR© plasmids were**

transfected into the P19-derived neurons by the calcium phosphate precipitation method. The nuclei were stained blue (DAPI). (A) and (B) show the same area. (C) - (F) show the same area. (A) – (F) Bar, 20 μm.

# 5. Discussion

## 5.1 Optimisation of Neuronal Differentiation of P19 EC Cells

### 5.1.1 Culture conditions

The population of P19-derived neurons was heterogeneous with respect to the morphology and neurotransmitters they synthesise as reported by others[11, 14, 16]. Up to five days culture on surfaces, RA treated P19 EC cells displayed characteristics of neuronal progenitor cells, maturing into post-mitotic neurons and glial cells after 5 days *in vitro*.[61] Therefore, these cells are sensitive to culture conditions before achieving the terminal differentiated phenotype. To perform reliable MEA recordings, P19-derived neurons need to be able form mature and stable neuronal networks.

The vitamin A derivative retinoic acid has been implicated to play a central role in several processes occurring during vertebrate development. Presence of this morphogen is believed to provide positional information necessary for the proper formation of the nervous system[62]. It can have a profound effect on cell proliferation and is a potent inducer of differentiation in several cell types. Although it was shown that differentiation of P19 EC cells was initiated after only one hour of RA treatment[12], differentiation into the neuronal lineage was not efficient after only one day in suspension as seen from the immature neuronal morphology and the low proportion of neurons. Jonk *et al*.[12] has shown that the expression of retinoic acid receptor mRNA was maximal after four days RA treatment. Aggregation in suspension culture helps to accelerate the rate of RA mediated retinoic acid receptor induction. Embryoid body-like aggregates were formed in the RA supplemented suspension cultures. Embryonal carcinoma cell lines are analogue of early embryo cells.[7, 63] When these cells are detached from the substratum, they form embryoid bodies consisting of an outer layer of endodermal cells surrounding an embryonic carcinoma cell core after four days in suspension. A variety of differentiated cells could be obtained when the embryoid bodies are attached to a substratum.[6, 7, 63] With the addition of RA, the appearance of neurons was accompanied by the disappearance of embryonal carcinoma cells. It was found that for RA concentrations above $5 \times 10^{-8}$

M, all of the aggregates contained cells with neuron-like processes after three days[10] and below $5 \times 10^{-8}$ M, the cultures resembled untreated controls and contained only embryonal carcinoma cells and small amounts of extraembryonic endoderm like cells. The effect of RA above $0.5 \times 10^{-6}$ M on the differentiation of P19 cells was found to be insignificant in agreement with the results of Jones-Villeneuve *et al.*[10]

Aggregated seeded cultures resulted in localised high density pockets of well developed neuronal populations that possessed long sinuous neuritic formations. A more homogeneous coverage of neuronal network on culture surfaces was naturally observed when RA treated P19 cells were dissociated and seeded as single cells. There was a range of distinct morphological types based on cell body size and dendritic morphology. Some neurons form clusters and give rise to fascicles of axons, suggesting that these cells might resemble those destined to become projection neurons. Other neurons were dispersed and might more closely resemble cells of the interneuronal type. Networks develop from isolated neurons into fully connected neuronal network, passing through phases of massive overproduction of synaptic connections and subsequent synaptic elimination and stabilisation.

Parnas *et al.*[64] have reported that increased culture density accelerates the coordinated maturation of P19-derived neurons in several aspects such as protein expression, basal release, neurotransmitter release, neurite outgrowth and segregation of cytoskeletal elements. Similarly, enhanced acquisition of neuronal polarity was also observed in high cell density cultures. Many factors such as higher growth factor density and increased cell to cell contracts contribute to the enhanced neuronal maturation in denser cultures. Cell density affects many cellular aspects such as gene expression, cell growth and cell morphology. One of the classical effects of increased cell density is the inhibition of cell growth and proliferation. Increased cell density has been known to affect the expression of several receptors, mainly receptor protein tyrosine kinases.[34, 65]

MAP2 is expressed in P19-derived neurons but not in undifferentiated P19 EC cells. It was shown that when MAP2 expression was blocked in differentiating P19 cells by antisense RNA, these cells did not extend neurites nor withdraw from the cell cycle events which occur during terminal differentiation of P19 cells[56]. Dendrites containing

MAP2 were detected early in P19-derived neurons and axons containing NF160 developed later *in vitro*.

The most complex form of regulated secretion occurs perhaps in the nervous system where neurotransmitter release is tightly regulated both temporally and spatially.[66] Synaptic vesicles are the storage organelles which are found in all synapses participating in quantal release of classical neurotransmitters. The expression of synaptophysin correlates with synapse formation.[67] Neurons overexpressing synaptophysin has been reported to show increased frequency of spontaneous release which in turn stimulates the maturation of synapses.[66]

It has been reported than the proportion of GAD positive neurons in P19-derived neuronal population is 10 % regardless of the cell density.[16] A small proportion of MAP2 stained P19-derived neurons was stained also for GAD.

A mix population consisting of neurons and glial cells was obtained after the differentiation of RA treated P19 cells. It is known that glial cells play an important role in ensuring brain development and function.[68-72] They guide the migration of neurons, promote the survival and differentiation of neurons, insulate and nourish neurons as well as enhance neuronal synaptic efficacy[70, 71]. However, due to a concern that the overgrowth of non-neuronal cells could result in interference of neuron-electrode coupling since the non-neuronal cells consisting largely of glial cells grow and proliferate beneath the neuronal network. The monolayer of non-neuronal cells could result in an insulating layer between the electrodes and neurons causing a reduction in the detection of neuronal firing and hence the low number of active electrodes. The reduction of the still mitotic non-neuronal cells was performed by the addition of Ara-C, an anti-metabolic agent. P19-derived neurons was observed to survive longer when Ara-C was added later *in vitro*. Mitotic neuronal progenitor cells have been reported to be initially present early in the culture[15] were affected by the presence of Ara-C. However, the addition of Ara-C later in culture still resulted in the death of the neuronal culture. A co-culture of spatially separated glial cells either isolated from day 18 embryos of pregnant CD rats or purified from RA treated P19 cells with P19-derived neurons was attempted to reduce the non-neuronal cells in P19-derived neuronal cultures. The co-culture method neither decreased the

proportion of non-neuronal cells nor increased the number of firing events in P19-derived neuronal culture. Direct glial-neuron contacts were found to be necessary for growth and maturation of neurons as reported by others[73].

## 5.1.2    Cell culture surface coating

The cell membrane is composed of a lipid bilayer associated with integral and peripheral proteins and polysaccharides. Communication and interaction of a cell with its environment thus take place principally through the particular characteristics of each of these species as well as through their combination.[74, 75] Two major types of phenomena, both of which involve various types of forces (i.e. electrostatic, electrodynamic), may be distinguished: specific and non-specific interactions. In the former, where ligand/receptors are involved, the complex structure of these molecules and also the charges associated with them allows very precise recognition and binding. In the latter, however, interaction is less precise and does not depend on complex charge specificity.

Presence of specific charges on the biomaterial surface may induce electrostatic and/or electrodynamic interaction with cell membrane components. Polylysine is a basic poly-amino acid with a net positive charge that is frequently used to cover the surface to which neurons attach. It is often used in cell studies to augment the attachment of cells to tissue culture flasks. It is believed that polylysine enhances cell adhesion to substrates by means of electrostatic interaction between anionic sites located on lipids, proteins and/or polysaccharides of plasma membranes and cationic sites of polylysine molecules.[76] Polyethyleneimine is an organic polymer that has a high density of amino groups that can be protonated. It has been frequently used in the built up of polyelectrolyte layers and some of the applications of such multilayered polyelectrolyte films were for cell attachment[77, 78]. Similar to PDL coatings, pre-coating with PEI was also found to enhance cell attachment[79]. Laminin is an extracellular matrix protein found in basement membranes of human brains. Its function is to activate focal adhesion proteins for neuronal development.[10, 80] Laminin may stimulate the development of longer neuronal processes than polylysine.[10, 81] The binding of neurons on laminin could be more specific physiologically than it does on polylysine. Several synthetic peptides based on laminin sequences have been

described as similar to those of the whole laminin molecule.[57-59, 82] Laminin based peptides that have biological activity include the well known Arg-Gly-Asp (RGD) sequence from the short arm of the A chain and the Ile-Lys-Val-Ala-Val (IKVAV) containing peptide from the long arm of the A chain. IKVAV containing peptides were observed to promote neurite outgrowth.[83]

The laminin fragment is electrostatically attracted to the positively charged layer of PEI or PDL which is first adsorbed to the substrate.[77, 84] The P19-derived neurons were found to be able to produce synaptophysin earlier when grown on PEI-LN coated surfaces as compared to those growing on PDL coated surfaces. The formation of a higher concentration of synaptophysin in localized areas in PEI-LN cultures is associated with improved synapse maturation and the ability of P19-derived neurons to release neurotransmitters 14 days post seeding. P19-derived neurons appeared to show a more mature phenotype when cultured on PEI-LN surfaces compared to PDL-LN surfaces. The PDL used had a much higher molecular weight than the PEI applied. The higher molecular weight molecule has more attachment sites for the laminin fragment perhaps resulting in a stronger electrostatic adsorption of the laminin fragment. Extracellular matrix proteins that were found to be strongly attached to the surface were found to reduce cellular motility and proliferation as remodeling of the extracellular environment is impeded.[74, 75, 85]

Appropriate cell-adhesive substrates, diffusible neurotrophic activity and cell bound signals and their synergistic interactions were essential requirements for maturation and long term survival of P19-derived neurons.

## 5.1.3    Extracellular Recording with Microelectrode Array

Micro-electrode array technology initiated by Pine and Gross[86, 87] have now become a reliable interfacing technique capable of establishing a bi-directional communication between a population of neurons and the external world.[5, 43, 47, 48, 50] Cultured neuronal networks are a well accepted experimental model in neuroscience research. They have been successfully utilised for studying pharmacological effects[48-50], for investigating

synapse formation and change in connectivity during development[88] and for studying learning and plasticity mechanisms at the network level[89].

MEA biosensor (8X8) from Multi Channel Systems® has a square recording area of 4500 μm with 64 flat TiN electrodes of 30 μm diameter and 200 μm inter-electrode distance. Spike activity can be detected at distances up to 100 μm from a neuron in an acute brain slice. Typically, signal sources are within 30 μm radius around the electrode center. The smaller the distance the higher are the extracellular signals.

### 5.1.3.1   Spontaneous activity

Differences in amplitude and shape of spikes recorded from the neurons were observed due to the distance between the source and electrode and due to the mechanisms of the coupling between cell membrane and electrode in single-cell contacts, respectively. Spikes recorded from spontaneously firing P19-derived neurons in all culture conditions studied typically have characteristics of the first derivative of the intracellular action potential indicating that voltage gated ion currents in these neurons operate properly independent of the culture conditions exposed to. Once neuronal differentiation was initiated, the neurons derived from P19 EC cells were able to generate action potential. Spontaneous activity is expected to have an important structuring role especially during early development.[88] Although P19-derived neurons were capable of generating action potentials in the sub-optimal culture conditions, the firing pattern did not develop beyond asynchronised single spikes pattern unlike in the PEI-LN150K cultures. Neuronal network maturation reflect changes in synaptic efficacy[90]. The observation that PEI-LN precoated cultures produced a more mature neuronal network activity coincides with the observation that a higher density of synaptophysin was detected in PEI-LN cultures.

Low density neuronal cultures of between 20 000 to 50 000 cells/cm$^2$ showed little if any synchronized network activity although the P19-derived neurons in these cultures showed a very significant development and maturation in neuronal phenotype. Neuronal cultures developed from aggregate seeded cultures on the other hand, have the capability of developing neuronal networks that have synchronous firing ability although the number of active electrodes remained low. Asynchronous single spike

firing activity usually indicates reduced synaptic efficacy caused by incomplete development of functional synapses for example in immature cortical neurons.[90] Such reduced synaptic efficacy results in a higher failure probability that an action potential would be communicated between neurons. Networks with high cell densities often show a spontaneous, partly synchronised, activity pattern. Higher neuronal densities of above 100 000 cells/cm$^2$ have been shown to promote long term neuronal survival.[73] This survival enhancement of neurons at high density cultures could not be simply explained for by the concomitant increase in endogenous glial cells as coculture of low density neurons with increased glial cell population did not prolong neuronal survival significantly[73]. The increased in number of neurons in such high density culture also leads to more effective self-conditioning of the culture medium by diffusible neuron derived autocrine factors.

Randomly cultured neurons form multiple connections yielding a largely intractable network. Increasing the cell density to 150 000 cells/cm$^2$ on the MEAs resulted in an improved synchronization of spike activity. However, high density P19-derived neuronal cultures studied here still exhibit a lower frequency of spike activity and of synchronised network activity in comparison to primary cultures of embryonic rat cortical neurons[91]. The frequency of synchronised spontaneous bursts is thought to indicate the excitability of cells due to the number of functional synapses per cell and their synaptic density which affect the probability of successful signal propagation over the whole network.[92]

Although the number of active electrodes and the signal to noise ratios achieved varied from culture to culture and are influenced by neuronal cell density, glial density and size of the adhesion island over the recording matrix there is no change in these two variables after 17 days post seeding as the individual cultures progressed *in vitro* showing the stability of cell electrode coupling. The increase in the amplitude of recorded spikes suggested a progressive increase in the degree of electrical coupling between electrodes and overlying neurons in addition to the rising expression of the voltage-dependent inward channels underlying the spike.

Spikes were first recorded usually on the 7$^{th}$ day post seeding on the MEAs. 1-3 active electrodes were obtained early in the culture of the P19-derived neurons. It was not

until after 14 days post seeding that more robust and multiple recordings could be obtained from more than 10 active electrodes. A sufficient time, in this case after 14 days post seeding, must be allowed for neurite promoting activity and spontaneous activity related to the development of glutamate receptors. The development of neuronal electrophysiological properties has been found by others to plateau between 15 and 28 days *in vivo*[19, 40] which was also observed with MEA recordings performed here.

Spontaneous firing activity in the cultured P19-derived neuronal network displayed a characteristic time structure with the regular occurrence of short phases of synchronised firing (network burst activity) later *in vitro*. The spontaneous firing activity, developed from random firing from single neurons into a pattern of firing including a phase of increased firing activity leading to a short phase of synchronised firing and a phase of low level firing activity. As the cultures were prolonged, the network activity of the P19-derived neurons developed into a recurrent pattern of firing with a repetition including a phase of low level firing activity, a short phase of synchronised firing and a silent network recovery phase. During such network bursts the number of active electrodes as well as spike rate was increased. Analysis of the network burst activities in the P19-derived neuronal cultures was attempted with a self made program (MEA-SPAT) developed for primary cultures of embryonic rat cortical neurons[93]. The program was unable to detect reliably the network bursts observed in the P19-derived neuronal cultures due to their larger deviations in bursts activity than in the primary cortical neuronal cultures.

It has been reported that spontaneously bursting networks are recommended for applications as biosensors because pattern changes can be more readily identified.[46, 47, 94] Dissociated cortical neurons grown on MEAs similarly show activities that undergo changes as the cultures develop *in vitro*.[92, 95, 96, 88, 88] The dissociated cortical neurons go through a first stage of development at 7 days *in vitro* (DIV) characterized by the absence of organized activity and the occurrences low frequency randomly generated spikes. At 14 DIV, the mean firing rate for all active recording electrodes increased. Their usual behaviour was made up of local spiking and bursts. At 21 DIV, the network showed a different behaviour where sporatic bursts were preceded and followed by nearly silent periods. The maturation of network electrophysiology

appeared to coincide with the formation and maturation of synapses in dissociated cortical neurons shown by Ichikawa *et al.*[90]. They showed that the number of synapses per neuron increased with DIV until the 4th or 5th week. During the 4th and 5th week in these cortical cultures, the network reaches a stable condition of maturation exhibiting a richer and elaborate temporal pattern of bursting activity suggesting an accommodation of the synaptic connections and a balance between excitatory and inhibitory components[92].

## 5.2    Responses to Neurotransmitters

P19 cells have been reported to differentiate into populations of diverse neuronal cell types expressing a variety of neurotransmitters similar to the neocortical neurons. Responses to neurotransmitters and their antagonists or agonists were performed after 18 days post seeding when spontaneous activity was stabilised. Extracellular recordings of P19-derived neurons exposed to two major neurotransmitters in the neocortex, the inhibitory GABA and excitatory glutamate, and their antagonists or agonists were not similar across the whole population of active electrodes. Recording from the electrodes reveals the summation of the simultaneous activity of a population of cells.

### 5.2.1    Response to inhibitory neurotransmitter, GABA and its agonist and antagonist

In general, a larger proportion of active electrodes were showing higher spike rates when BIC was added, causing a disinhibition of $GABA_A$ receptors. The presence of endogenous GABA in the P19-derived neuronal cultures was clearly shown by the disinhibitory effect of BIC. BIC, a plant convulsant, is known to compete with GABA for binding to $GABA_A$ receptors and reduce $GABA_A$ receptor currents by decreasing open frequency and mean duration of the receptor.[97] BIC could elicit a higher rate of activity in the P19-derived neurons which also show temporary increased partial synchronisation. The higher spike rate induced dropped 10 minutes after BIC application. A second addition of BIC directly after mostly did not increase the spike rate in comparison to the previous wash state even when the BIC concentration was

increased. The proportion of active electrodes with a higher spike rate increased significantly in the same MEA culture when exposed to BIC the next day. The initial addition of BIC could cause activity induced modulation of firing activity resulting in the changed sensitivity to BIC.

P19-derived neurons were shown to possess functional GABA receptors and specifically GABA$_A$ receptors[4, 17], showing responses to GABA via intracellular recordings.[19, 98] It was reported that GABA induced depolarisation in immature P19-derived neurons[19, 61] while in mature P19-derived neurons either had a biphasic depolarizing/hyperpolarizing[19] or a completely inhibitory response to GABA[4, 17]. GABA induced responses in P19-derived neurons were shown to be sensitive to BIC, a GABA$_A$ receptor antagonist.[19, 61, 98]

The silencing of all spontaneous activity across the MEAs when GABA was applied although the application of BIC affected only a subpopulation of P19-derived neurons indicated that other subtypes of GABA receptors exist in the cultures. Firing activity of P19-derived neurons was also completely inhibited with the addition of the selective GABA$_A$ receptor agonist, muscimol which is a conformationally restricted GABA analogue. Although not all populations of neurons in the proximity of the electrodes were sensitive to BIC most of them showed spontaneous activity that was inhibited when muscimol was applied. This could be an indication of the presence of GABA$_C$ receptors since muscimol is also a partial agonist of the GABA$_C$ receptor[24]. Virtually all neurons in the adult mammalian CNS respond to GABA although only approximately 30 % of the total neurons in the adult mammalian CNS are GABAergic. GABA$_A$ receptors have been known to mediate the bulk of fast inhibitory neurotransmission in the mammalian brain.[99]

The inhibitory effectiveness of muscimol on the P19-derived neurons was reduced in the presence of BIC. BIC is a competitive GABA antagonist on the GABA$_A$ receptors directly competing for the same ligand site as muscimol. The spontaneous activity of the P19-derived neurons was only reduced when the same concentration of muscimol was added in the presence of BIC unlike when only muscimol was added to the cultures causing an instantaneous inhibition of spontaneous activity. However, the instantaneous increase in spike activity during removal of BIC and muscimol

indicated that the mechanical effect of washing caused activity artifacts. A slow recovery of the activity after muscimol application would be expected as muscimol binds to $GABA_A$ receptors with high affinity. The installation of a perfusion system to the MEA setup would get rid of activity artifacts due to washing.

## 5.2.2 Response to excitatory neurotransmitter, glutamate and antagonists

P19-derived neurons that were treated previously with GABA appeared to have well developed responses to the major excitatory neurotransmitter later on *in vitro*. Glutamate had an excitatory effect on many of the neurons that were exposed previously to GABA. GABA receptors are predominantly present in the early stages of the development of the mammalian cortical neurons mediating excitatory responses which subsequently shapes the maturation of the neuronal system.[22, 23] The later development of NMDA type glutamate receptors take over the excitatory role of the neuronal system and GABA receptors switch to its well known inhibitory function. Synaptic connections have been known to undergo use dependent modifications leading to strengthening or weakening of their efficacy.[89] The increased synaptic efficacy also increased probability of glutamate release which stimulates the trafficking of AMPA receptors into initially silent synapses consisting of only NMDA receptors, thus strengthening excitatory synaptic contacts[8, 30]. P19-derived neurons possess functional NMDA and AMPA receptors that exhibit excitatory post-synaptic currents that respond to NMDA and non-NMDA antagonists[19, 20, 98, 100], although Morley *et al.*[100] reported that $Ca^{2+}$ surges due to non-NMDA receptors were not detected in P19-derived neurons which could mean that the non-NMDA receptors do not mediate $Ca^{2+}$ permeable channels. The exponential decrease in average spike rate after a brief upsurge in average spike rate during glutamate application in these cells seemed to demonstrate that the fast acting AMPA type of glutamate receptors were predominant. The long term extracellular recordings of the P19-derived neurons were in B27 supplemented Neurobasal medium that contained 0.8 mM $Mg^{2+}$. Extracellular concentrations of $Mg^{2+}$ inhibits NMDA receptors which could explain why the response of the neuronal spontaneous activity to glutamate had a predominantly

AMPA type characteristic. It would be interesting in this case to perform the recording in $Mg^{2+}$ deficient medium to examine the full range of glutamate responses. Arnold et al.[89] reported that NMDA receptor is a key regulator of activity dependent change in network activity by increasing $Ca^{2+}$ entry though NMDA receptors which in turn triggers downstream signal regulated kinases. Gene transcription responses triggered by $Ca^{2+}$ flux are important for the sustenance of synchronous bursting. In the developing brain, self sustaining (input independent) recurrent network activity is crucial to network maturation.

In contrast, glutamate had a prominently inhibitory effect on cultures that were not previously exposed to exogenous application of GABA. Only a small population of P19-derived neurons in cultures not previously treated with GABA showed excitatory responses to glutamate in these cultures.

Similar to glutamate response, the addition of CTZ, a potent blocker of AMPA desensitisation, caused an exponential decrease after an initial rise in average spike rate. The addition of CTZ however, did not cause a significant prolongation of the period of excitation of endogenous glutamate. In fact, in cultures that were exposed to doses of GABA glutamate could elicit a more robust excitatory response in terms of the high proportion of active electrodes that recorded increased activity and the longer period of excitation before desensitisation. In cultures that were not exposed to GABA previously the subsequent addition of glutamate after CTZ application inhibited network activity. This smaller excitatory response was an indication of a low density of glutamate receptors present in P19-derived neurons that were not exposed to exogenous dose of GABA.

AMPA receptors have a lower affinity for glutamate than NMDA receptors. Network activity might require highly controlled activation of glutamate ionotropic receptors and the neuron excitability might depend on short term activation of the receptor. The finding would be consistent with the crucial role played by the neuronal and glial uptake mechanisms, keeping low extracellular glutamate concentrations in the functioning of glutamatergic transmission at central synapses.

The spontaneous activity of these cells as in the mammalian central nervous system (CNS) was controlled by a delicate balance of inhibitory and excitatory neurotransmitters. Extracellular recordings with MEAs are a result of integration of synaptic inputs. It appeared that P19-derived neuronal network was a predominantly GABAergic system with low excitatory inputs. P19-derived neuronal networks on MEAs were able to show reasonable physiological response to the drugs added.

## 5.3     OR5 Transfection

Postmitotic cells such as neurons have been proven to be notoriously difficult to transfect. A range of methods such as Semliki Forest virus vectors, electroporation and calcium phosphate-DNA coprecipitation have been applied to P19-derived neurons for the expression of OR5 in this study. Lemker[54] had been able to show by Real-Time PCR that P19-derived neurons possess the components essential for the olfactory signaling cascade. She showed a four times increase in fluorescence due to the influx of $Ca^{2+}$ ions when OR5 ligand, lilial, was added to OR5-SFV infected cultures proving the functional incorporation of OR5 in the plasma membrane of P19-derived neurons.

However, extracellular recording of OR5 transfected cultures 17 days post seeding did not detect an increase in activity due to the addition of the OR5 ligand. The reason for the apparent discrepancy of the result could lie in the time frame of the transfection. Lemker[54] performed the infection with OR5-SFV vectors and calcium imaging within 1 week after RA treatment. It has been reported that immature P19-derived neurons had excitatory responses to GABA[19, 61] showing that intracellular concentration of $Cl^-$ were higher than the extracellular environment. Such a higher intracellular $Cl^-$ concentration would be necessary too for the activation of the olfactory receptor signaling cascade in the olfactory receptor neurons of the olfactory epithelium. However, robust network activities were recorded by MEA only 17 days after RA treatment due to the increased maturation of the P19-derived neuronal network which was necessary for robust neuronal firing activities. Application of GABA to the network during this time had a complete inhibitory effect on the spontaneous activity, showing that intracellular $Cl^-$ concentration is lower than the extracellular

environment in the mature P19-derived neurons. Therefore, although OR5 was expressed in mature P19-derived neurons as shown by immunostaining, changes in activity could not be detected in MEA cultures when the OR5 ligand was added. Moreover, the OR5 transfection of P19-derived neurons appeared to impede the generation of spontaneous activity as seen by the cessation of signals after OR5-SFV vectors infection of cultures 18 days post seeding and no spontaneous activity was detected in cultures transfected by both electroporation and calcium phosphate precipitation method.

# 6.    Conclusions and Outlook

Culture conditions were optimised to obtain a high efficiency of neuronal differentiation of P19 EC cells for extracellular recordings with MEAs. The highest efficiency of neuronal differentiation from pluripotent P19 EC cells were obtained when the undifferentiated cells were treated for four days in suspension cultures in the presence of retinoic acid. Rapid and increased maturation of P19-derived neurons were observed when the neurons were dissociated and plated at high cell density on PEI-LN coated surfaces.

The improved neuronal maturation observed morphologically coincided with the increased firing activity of the P19-derived neurons detected by extracellular recording with microelectrode array. Extracellular recording of spontaneous firing activity was detected one week post seeding. Synchronised network activity of the P19-derived neurons was detected two weeks post seeding. Such spontaneously synchronised networks are recommended for applications as biosensors because pattern changes can be more readily identified. Network activities of the P19-derived neurons were reproducible and robust over a two to three hour recording period.

Mature P19-derived neuronal network display synchronised network activities that were controlled by a balance of excitatory and inhibitory neurotransmitters. Extracellular recordings due to the addition of two major neurotransmitters in the central nervous system, GABA and glutamate, and their agonists and antagonists showed the presence of endogenous GABA and glutamate in the cultures. P19-derived neurons displayed heterogeneous responses to the two major neurotransimitters, GABA and glutamate, due to the presence of a heterogeneous population of neurons. Signal induced changes in network activity could be observed showing that P19-derived neurons have the capability to undergo synaptic plasticity. This suggests that P19-derived neurons could be applied as a model for the study of synaptic plasticity.

Extracellular recording with microelectrode array showed the presence of GABA and glutamate receptors in P19-derived neurons. GABA$_A$ receptors and non-NMDA type glutamate receptors were also shown to be present in these cultures. P19-derived neuronal networks formed on microeletrode arrays were predominantly GABAergic.

Extracellular recording with microelectrode array of OR5 transfected P19-derived neurons could not be obtained although OR5 was found to be expressed in culture. It would be interesting to transfect P19-derived neurons with "alternative" transmembrane receptors such as acetylcholine receptors and observe the network responses on microelectrode arrays.

P19-derived neurons grown on microelectrode arrays have reasonably good physiological responses to the drugs that were added. P19-derived neuronal networks grown on MEAs could be used as a platform for biosensor application.

# Acknowledgements

I would like to thank many people who have in one way or another helped me to come so far as to writing the final chapter of this thesis.

First of all, I would like to thank Prof. Knoll for giving me an opportunity and the resources to work and learn in his group at the Max Planck Institute for Polymer Research in Mainz.

To my supervisor, Dr. Eva-Kathrin Sinner, I could never have done it without her infectious optimism and her continuous encouragement and support. It has been a joy working in her group.

To the former group members, Dr. Mark Pottek and Dr. Melanie Jungblut, for which their friendship and experience in the field of neurobiology I cannot do without. I am grateful for the time and discussion we had during the last phase of the experiments, although they were no longer present in the institute.

I appreciate the friendliness and help in scanning electron microscopy and transfection of the cells from the people of Prof. Wolfrum's group at the Johannes Gutenberg-University Mainz, namely, Elisabeth Sehn, Dr. Andreas Giessl and Tobias Goldmann.

Of course, without the company of colleagues in the institute, my experience in Germany would not be half as fun. There are two people particularly, who I would like to thank, Danica Christensen and Mi-Kyoung Park, for their cooking, among many things, especially during the period of writing this thesis where they made sure I got a good meal in between.

Lastly, my parents and my partner, Maik, who are always there for me. I caused much worries to my parents during my whole thirty years and I cannot hope to repay them for their care and concern in my lifetime. And of course to Maik, for dreaming and sharing this journey with me, and for waiting in Singapore these last five long months.

# References

1.  Pancrazio, J. J.; Whelan, J. P.; Borkholder, D. A.; Ma, W.; Stenger, D. A., Development and application of cell-based biosensors. *Annals of Biomedical Engineering* **1999,** 27, (6), 697-711.
2.  Stenger, D. A.; Gross, G. W.; Keefer, E. W.; Shaffer, K. M.; Andreadis, J. D.; Ma, W.; Pancrazio, J. J., Detection of physiologically active compounds using cell-based biosensors. *Trends in Biotechnology* **2001,** 19, (8), 304-9.
3.  Hales, T. G.; Tyndale, R. F., Few cell lines with GABAA mRNAs have functional receptors. *Journal of Neuroscience* **1994,** 14, (9), 5429-36.
4.  Reynolds, J. N.; Prasad, A.; Gillespie, L. L.; Paterno, G. D., Developmental expression of functional GABAA receptors containing the gamma 2 subunit in neurons derived from embryonal carcinoma (P19) cells. *Brain Research. Molecular Brain Research* **1996,** 35, (1-2), 11-8.
5.  Stett, A.; Egert, U.; Guenther, E.; Hofmann, F.; Meyer, T.; Nisch, W.; Haemmerle, H., Biological application of microelectrode arrays in drug discovery and basic research. *Analytical & Bioanalytical Chemistry* **2003,** 377, (3), 486-95.
6.  Hogan, B. L.; Taylor, A.; Adamson, E., Cell interactions modulate embryonal carcinoma cell differentiation into parietal or visceral endoderm. *Nature* **1981,** 291, (5812), 235-7.
7.  Martin, G. R.; Evans, M. J., Differentiation of clonal lines of teratocarcinoma cells: formation of embryoid bodies in vitro. *Proceedings of the National Academy of Sciences of the United States of America* **1975,** 72, (4), 1441-5.
8.  Isaac, J. T.; Ashby, M.; McBain, C. J., The role of the GluR2 subunit in AMPA receptor function and synaptic plasticity. *Neuron* **2007,** 54, (6), 859-71.
9.  MacPherson, P. A.; McBurney, M. W., P19 embryonic carcinoma cells: a source of cultured neurons amenable to genetic manipulation. *Methods: A Companion to Methods in Enzymology* **1995,** 7, 238-252.
10. Jones-Villeneuve, E. M.; McBurney, M. W.; Rogers, K. A.; Kalnins, V. I., Retinoic acid induces embryonal carcinoma cells to differentiate into neurons and glial cells. *Journal of Cell Biology* **1982,** 94, (2), 253-62.
11. McBurney, M. W.; Reuhl, K. R.; Ally, A. I.; Nasipuri, S.; Bell, J. C.; Craig, J., Differentiation and maturation of embryonal carcinoma-derived neurons in cell culture. *Journal of Neuroscience* **1988,** 8, (3), 1063-73.
12. Jonk, L. J.; de Jonge, M. E.; Kruyt, F. A.; Mummery, C. L.; van der Saag, P. T.; Kruijer, W., Aggregation and cell cycle dependent retinoic acid receptor mRNA expression in P19 embryonal carcinoma cells. *Mechanisms of Development* **1992,** 36, (3), 165-72.
13. Levine, J. M.; Flynn, P., Cell surface changes accompanying the neural differentiation of an embryonal carcinoma cell line. *Journal of Neuroscience* **1986,** 6, (11), 3374-84.
14. Staines, W. A.; Morassutti, D. J.; Reuhl, K. R.; Ally, A. I.; McBurney, M. W., Neurons Derived from P19 Embryonal Carcinoma Cells Have Varied Morphologies and Neurotransmitters. *Neuroscience* **1994,** 58, (4), 735-751.
15. Liour, S. S.; Kapitonov, D.; Yu, R. K., Expression of gangliosides in neuronal development of P19 embryonal carcinoma stem cells. *Journal of Neuroscience Research* **2000,** 62, (3), 363-73.

16.     Parnas, D.; Linial, M., Cholinergic Properties of Neurons Differentiated from an Embryonal Carcinoma Cell-Line (P19). *International Journal of Developmental Neuroscience* **1995,** 13, (7), 767-781.

17.     Reynolds, J. N.; Ryan, P. J.; Prasad, A.; Paterno, G. D., Neurons Derived from Embryonal Carcinoma (P19) Cells Express Multiple Gaba(a) Receptor Subunits and Fully Functional Gaba(a) Receptors. *Neuroscience Letters* **1994,** 165, (1-2), 129-132.

18.     Macpherson, P. A.; Jones, S.; Pawson, P. A.; Marshall, K. C.; McBurney, M. W., P19 Cells Differentiate into Glutamatergic and Glutamate-Responsive Neurons in Vitro. *Neuroscience* **1997,** 80, (2), 487-499.

19.     Magnuson, D. S. K.; Morassutti, D. J.; McBurney, M. W.; Marshall, K. C., Neurons Derived from P19 Embryonal Carcinoma Cells Develop Responses to Excitatory and Inhibitory Neurotransmitters. *Brain Research Developmental Brain Research* **1995,** 90, (1-2), 141-150.

20.     Turetsky, D. M.; Huettner, J. E.; Gottlieb, D. I.; Goldberg, M. P.; Choi, D. W., Glutamate Receptor-Mediated Currents and Toxicity in Embryonal Carcinoma Cells. *Journal of Neurobiology* **1993,** 24, (9), 1157-1169.

21.     Kandel, E. R.; Siegelbaum, S. A., Overview of synaptic transmission. In *Principles of Neural Science*, Fourth ed.; Kandel, E. R.; Schwartz, J. H.; Jessell, T. M., Eds. McGraw-Hill: New York, United States of America, 2000; pp 175-186.

22.     Miles, R., Neurobiology. A homeostatic switch.[comment]. *Nature* **1999,** 397, (6716), 215-6.

23.     Choi, D. W.; Mauluccigedde, M.; Kriegstein, A. R., Glutamate Neurotoxicity in Cortical Cell-Culture. *Journal of Neuroscience* **1987,** 7, (2), 357-368.

24.     Bormann, J., The 'ABC' of GABA receptors. *Trends in Pharmacological Sciences* **2000,** 21, (1), 16-9.

25.     Pickard, L.; Noel, J.; Henley, J. M.; Collingridge, G. L.; Molnar, E., Developmental changes in synaptic AMPA and NMDA receptor distribution and AMPA receptor subunit composition in living hippocampal neurons. *Journal of Neuroscience* **2000,** 20, (21), 7922-7931.

26.     Choi, D. W., Glutamate Neurotoxicity in Cortical Cell-Culture Is Calcium Dependent. *Neuroscience Letters* **1985,** 58, (3), 293-297.

27.     Olney, J. W.; Price, M. T.; Samson, L.; Labruyere, J., The Role of Specific Ions in Glutamate Neurotoxicity. *Neuroscience Letters* **1986,** 65, (1), 65-71.

28.     Kandel, E. R.; Siegelbaum, S. A., Synaptic integration. In *Principles of Neural Science*, Fourth ed.; Kandel, E. R.; Schwartz, J. H.; Jessell, T. M., Eds. McGraw-Hill: New York, United States of America, 2000; pp 207-228.

29.     Collingridge, G. L.; Isaac, J. T.; Wang, Y. T., Receptor trafficking and synaptic plasticity. *Nature Reviews Neuroscience* **2004,** 5, (12), 952-62.

30.     Malinow, R.; Malenka, R. C., AMPA receptor trafficking and synaptic plasticity. *Annual Review of Neuroscience* **2002,** 25, 103-26.

31.     Rao, V. R.; Finkbeiner, S., NMDA and AMPA receptors: old channels, new tricks. *Trends in Neurosciences* **2007,** 30, (6), 284-291.

32.     Dingledine, R.; Borges, K.; Bowie, D.; Traynelis, S. F., The glutamate receptor ion channels. *Pharmacological Reviews* **1999,** 51, (1), 7-61.

33.     Barnes-Davies, M.; Forsythe, I. D., Pre- and postsynaptic glutamate receptors at a giant excitatory synapse in rat auditory brainstem slices. *Journal of Physiology* **1995,** 488, (Pt 2), 387-406.

34. Ishikawa, T.; Takahashi, T., Mechanisms underlying presynaptic facilitatory effect of cyclothiazide at the calyx of Held of juvenile rats. *Journal of Physiology* **2001,** 533, (Pt 2), 423-31.

35. Mennerick, S.; Zorumski, C. F., Presynaptic influence on the time course of fast excitatory synaptic currents in cultured hippocampal cells. *Journal of Neuroscience* **1995,** 15, (4), 3178-92.

36. Hays, S. J.; Boxer, P. A.; Taylor, C. P.; Vartanian, M. G.; Robichaud, L. J.; Nielsen, E. O., N-Sulfonyl Derivatives of 6,7-Dichloro 3,4-Dihydro-3-Oxo-Quinoxalinecarboxylate as Glycine-Site Nmda and Ampa Antagonists. *Bioorganic & Medicinal Chemistry Letters* **1993,** 3, (1), 77-80.

37. Deng, L.; Chen, G., Cyclothiazide potently inhibits gamma-aminobutyric acid type A receptors in addition to enhancing glutamate responses. *Proceedings of the National Academy of Sciences of the United States of America* **2003,** 100, (22), 13025-9.

38. Qi, J. S.; Wang, Y.; Jiang, M.; Warren, P.; Chen, G., Cyclothiazide induces robust epileptiform activity in rat hippocampal neurons both in vitro and in vivo. *Journal of Physiology-London* **2006,** 571, (3), 605-618.

39. Matthews, H. R.; Reisert, J., Calcium, the two-faced messenger of olfactory transduction and adaptation. *Current Opinion in Neurobiology* **2003,** 13, (4), 469-75.

40. Magnuson, D. S. K.; Morassutti, D. J.; Staines, W. A.; McBurney, M. W.; Marshall, K. C., In Vivo Electrophysiological Maturation of Neurons Derived from a Multipotent Precursor (Embryonal Carcinoma) Cell Line. *Brain Research Developmental Brain Research* **1995,** 84, (1), 130-141.

41. Morassutti, D. J.; Staines, W. A.; Magnuson, D. S.; Marshall, K. C.; McBurney, M. W., Murine embryonal carcinoma-derived neurons survive and mature following transplantation into adult rat striatum. *Neuroscience* **1994,** 58, (4), 753-63.

42. Krantz-Rulcker, C.; Stenberg, M.; Winquist, F.; Lundstrom, I., Electronic tongues for environmental monitoring based on sensor arrays and pattern recognition: a review. *Analytica Chimica Acta* **2001,** 426, (2), 217-226.

43. Connolly, P.; Clark, P.; Curtis, A. S.; Dow, J. A.; Wilkinson, C. D., An extracellular microelectrode array for monitoring electrogenic cells in culture. *Biosensors & Bioelectronics* **1990,** 5, (3), 223-34.

44. Gross, G. W.; Wen, W. Y.; Lin, J. W., Transparent indium-tin oxide electrode patterns for extracellular, multisite recording in neuronal cultures. *Journal of Neuroscience Methods* **1985,** 15, (3), 243-52.

45. Gross, G. W.; Kowalski, J. M., Experimental and theoretical analysis of random nerve cell network dynamics. In *Neural Networks: Concepts, Applications, and Implementations*, Antognetti, P.; Milutinovic, V., Eds. Prentice-Hall: New Jersey, 1991; Vol. 4, pp 47-110.

46. Gross, G. W.; Rhoades, B.; Jordan, R., Neuronal Networks for Biochemical Sensing. *Sensors and Actuators B-Chemical* **1992,** 6, (1-3), 1-8.

47. Gross, G. W.; Rhoades, B. K.; Azzazy, H. M.; Wu, M. C., The use of neuronal networks on multielectrode arrays as biosensors. *Biosensors & Bioelectronics* **1995,** 10, (6-7), 553-67.

48. Chiappalone, M.; Vato, A.; Tedesco, M. B.; Marcoli, M.; Davide, F.; Martinoia, S., Networks of neurons coupled to microelectrode arrays: a neuronal sensory system for pharmacological applications. *Biosensors & Bioelectronics* **2003,** 18, (5-6), 627-634.

49.	Martinoia, S.; Bonzano, L.; Chiappalone, A.; Tedesco, A.; Marcoli, A.; Maura, G., In vitro cortical neuronal networks as a new high-sensitive system for biosensing applications. *Biosensors & Bioelectronics* **2005,** 20, (10), 2071-2078.

50.	Morefield, S. I.; Keefer, E. W.; Chapman, K. D.; Gross, G. W., Drug evaluations using neuronal networks cultured on microelectrode arrays. *Biosensors & Bioelectronics* **2000,** 15, (7-8), 383-396.

51.	Fromherz, P., Electrical interfacing of nerve cells and semiconductor chips. *Chemphyschem* **2002,** 3, (3), 276-284.

52.	Plonsey, R., Action potential sources and their volume conductor fields. *Procedures of IEEE* **1977,** 65, 601-611.

53.	Brewer, G. J.; Torricelli, J. R.; Evege, E. K.; Price, P. J., Optimized Survival of Hippocampal-Neurons in B27-Supplemented Neurobasal(Tm), a New Serum-Free Medium Combination. *Journal of Neuroscience Research* **1993,** 35, (5), 567-576.

54.	Lemker, E. S. Expression, Isolierung und Funktionanalyse des OR5 Reruchsrezeptors: einem Vertreter der G-Protein gekoppelten Rezeptor. PhD Thesis, Ludwig-Maximilians-Universität München, München, 2005.

55.	Potter, S. M.; DeMarse, T. B., A new approach to neural cell culture for long-term studies. *Journal of Neuroscience Methods* **2001,** 110, (1-2), 17-24.

56.	Dinsmore, J. H.; Solomon, F., Inhibition of MAP2 expression affects both morphological and cell division phenotypes of neuronal differentiation. *Cell* **1991,** 64, 817-826.

57.	Massia, S. P.; Rao, S. S.; Hubbell, J. A., Covalently immobilized laminin peptide Tyr-Ile-Gly-Ser-Arg (YIGSR) supports cell spreading and co-localization of the 67-kilodalton laminin receptor with alpha-actinin and vinculin. *Journal of Biological Chemistry* **1993,** 268, (11), 8053-9.

58.	Sephel, G. C.; Tashiro, K.; Sasaki, M.; Kandel, S.; Yamada, Y.; Kleinman, H. K., A laminin-pepsin fragment with cell attachment and neurite outgrowth activity at distinct sites. *Developmental Biology* **1989,** 135, (1), 172-81.

59.	Sephel, G. C.; Tashiro, K. I.; Sasaki, M.; Greatorex, D.; Martin, G. R.; Yamada, Y.; Kleinman, H. K., Laminin A chain synthetic peptide which supports neurite outgrowth. *Biochemical & Biophysical Research Communications* **1989,** 162, (2), 821-9.

60.	Atassi, B.; Glavinovic, M. I., Effect of cyclothiazide on spontaneous miniature excitatory postsynaptic currents in rat hippocampal pyramidal cells. *Pflugers Archiv-European Journal of Physiology* **1999,** 437, (3), 471-478.

61.	Lin, P. X.; Kusano, K.; Zhang, Q. L.; Felder, C. C.; Geiger, P. M.; Mahan, L. C., GABA(A) receptors modulate early spontaneous excitatory activity in differentiating P19 neurons. *Journal of Neurochemistry* **1996,** 66, (1), 233-242.

62.	Durston, A. J.; Timmermans, J. P.; Hage, W. J.; Hendriks, H. F.; de Vries, N. J.; Heideveld, M.; Nieuwkoop, P. D., Retinoic acid causes an anteroposterior transformation in the developing central nervous system. *Nature* **1989,** 340, (6229), 140-4.

63.	Damjanov, I.; Solter, D., Experimental teratoma. *Current Topics in Physiology* **1974,** 59, 69-130.

64.	Parnas, D.; Linial, M., Acceleration of Neuronal Maturation of P19 Cells by Increasing Culture Density. *Brain Research Developmental Brain Research* **1997,** 101, (1-2), 115-124.

65.	Rizzino, A.; Kazakoff, P.; Nebelsick, J., Density-Induced down Regulation of Epidermal Growth-Factor Receptors. *In Vitro Cellular & Developmental Biology* **1990,** 26, (5), 537-542.

66.	Linial, M.; Parnas, D., Deciphering neuronal secretion: Tools of the trade. *Biochimica Et Biophysica Acta-Reviews on Biomembranes* **1996,** 1286, (2), 117-152.

67.	Schilling, K.; Barco, E. B.; Rhinehart, D.; Pilgrim, C., Expression of Synaptophysin and Neuron-Specific Enolase during Neuronal Differentiation Invitro - Effects of Dimethyl-Sulfoxide. *Journal of Neuroscience Research* **1989,** 24, (3), 347-354.

68.	Brown, D. R., Neuronal release of vasoactive intestinal peptide is important to astrocytic protection of neurons from glutamate toxicity. *Molecular and Cellular Neuroscience* **2000,** 15, (5), 465-475.

69.	Hatton, G. I., Dynamic neuronal-glial interactions: an overview 20 years later. *Peptides* **2004,** 25, (3), 403-411.

70.	Oliet, S. H. R.; Piet, R.; Poulain, D. A., Control of glutamate clearance and synaptic efficacy by glial coverage of neurons. *Science* **2001,** 292, (5518), 923-926.

71.	Pfrieger, F. W.; Barres, B. A., Synaptic efficacy enhanced by glial cells in vitro. *Science* **1997,** 277, (5332), 1684-1687.

72.	Rozovsky, I.; Wei, M.; Morgan, T. E.; Finch, C. E., Reversible age impairments in neurite outgrowth by manipulations of astrocytic GFAP. *Neurobiology of Aging* **2005,** 26, (5), 705-715.

73.	Schmalenbach, C.; Muller, H. W., Astroglia Neuron Interactions That Promote Long-Term Neuronal Survival. *Journal of Chemical Neuroanatomy* **1993,** 6, (4), 229-237.

74.	Juliano, R. L.; Haskill, S., Signal transduction from the extracellular matrix. *Journal of Cell Biology* **1993,** 120, (3), 577-85.

75.	Kaverina, I.; Krylyshkina, O.; Small, J. V., Regulation of substrate adhesion dynamics during cell motility [Review]. *International Journal of Biochemistry & Cell Biology* **2002,** 34, (7), 746-761.

76.	Santini, M. T.; Cametti, C.; Indovina, P. L.; Morelli, G.; Donelli, G., Polylysine induces changes in membrane electrical properties of K562 cells. *Journal of Biomedical Materials Research* **1997,** 35, (2), 165-74.

77.	He, W.; Bellamkonda, R. V., Nanoscale neuro-integrative coatings for neural implants. *Biomaterials* **2005,** 26, (16), 2983-2990.

78.	Vodouhe, C.; Schmittbuhl, M.; Boulmedais, F.; Bagnard, D.; Vautier, D.; Schaaf, P.; Egles, C.; Voegel, J. C.; Ogier, J., Effect of functionalization of multilayered polyelectrolyte films on motoneuron growth. *Biomaterials* **2005,** 26, (5), 545-554.

79.	Vancha, A. R.; Govindaraju, S.; Parsa, K. V. L.; Jasti, M.; Gonzalez-Garcia, M.; Ballestero, R. P., Use of polyethyleneimine polymer in cell culture as attachment factor and lipofection enhancer. *Bmc Biotechnology* **2004,** 4, -.

80.	Liesi, P.; Dahl, D.; Vaheri, A., Neurons cultured from developing rat brain attach and spread preferentially to laminin. *Journal of Neuroscience Research* **1984,** 11, (3), 241-51.

81.	Lein, P. J.; Banker, G. A.; Higgins, D., Laminin Selectively Enhances Axonal Growth and Accelerates the Development of Polarity by Hippocampal-Neurons in Culture. *Developmental Brain Research* **1992,** 69, (2), 191-197.

82. Urano, Y.; Iiduka, M.; Sugiyama, A.; Akiyama, H.; Uzawa, K.; Matsumoto, G.; Kawasaki, Y.; Tashiro, F., Involvement of the mouse Prp19 gene in neuronal/astroglial cell fate decisions. *Journal of Biological Chemistry* **2006,** 281, (11), 7498-7514.

83. Kanemoto, T.; Reich, R.; Royce, L.; Greatorex, D.; Adler, S. H.; Shiraishi, N.; Martin, G. R.; Yamada, Y.; Kleinman, H. K., Identification of an Amino-Acid-Sequence from the Laminin-a Chain That Stimulates Metastasis and Collagenase-Iv Production. *Proceedings of the National Academy of Sciences of the United States of America* **1990,** 87, (6), 2279-2283.

84. Huber, M.; Heiduschka, P.; Kienle, S.; Pavlidis, C.; Mack, J.; Walk, T.; Jung, G.; Thanos, S., Modification of glassy carbon surfaces with synthetic laminin-derived peptides for nerve cell attachment and neurite growth. *Journal of Biomedical Materials Research* **1998,** 41, (2), 278-288.

85. Wood, W.; Martin, P., Structures in focus - filopodia. *International Journal of Biochemistry & Cell Biology* **2002,** 34, (7), 726-730.

86. Gross, G. W.; Williams, A. N.; Lucas, J. H., Recording of Spontaneous Activity with Photoetched Microelectrode Surfaces from Mouse Spinal Neurons in Culture. *Journal of Neuroscience Methods* **1982,** 5, (1-2), 13-22.

87. Pine, J., Recording Action-Potentials from Cultured Neurons with Extracellular Micro-Circuit Electrodes. *Journal of Neuroscience Methods* **1980,** 2, (1), 19-31.

88. Corner, M. A.; van Pelt, J.; Wolters, P. S.; Baker, R. E.; Nuytinck, R. H., Physiological effects of sustained blockade of excitatory synaptic transmission on spontaneously active developing neuronal networks - an inquiry into the reciprocal linkage between intrinsic biorhythms and neuroplasticity in early ontogeny. *Neuroscience and Biobehavioral Reviews* **2002,** 26, (2), 127-185.

89. Arnold, F. J. L.; Hofmann, F.; Bengtson, C. P.; Wittmann, M.; Vanhoutte, P.; Bading, H., Microelectrocle array recordings of cultured hippocampal networks reveal a simple model for transcription and protein synthesis-dependent plasticity. *Journal of Physiology-London* **2005,** 564, (1), 3-19.

90. Ichikawa, M.; Muramoto, K.; Kobayashi, K.; Kawahara, M.; Kuroda, Y., Formation and Maturation of Synapses in Primary Cultures of Rat Cerebral Cortical-Cells - an Electron-Microscopic Study. *Neuroscience Research* **1993,** 16, (2), 95-103.

91. Jungblut, M. Detektion neuroaktiver Substanzen durch Modifikation des Aktivitätsmusters neokortikaler Netzwerke auf Multielektrodenarrays-Charakterisierung und Optimierung eines neuronalen Biosensors. PhD Dissertation, Johannes Gutenberg-University Mainz, Mainz, 2006.

92. Maeda, E.; Robinson, H. P. C.; Kawana, A., The Mechanisms of Generation and Propagation of Synchronized Bursting in Developing Networks of Cortical-Neurons. *Journal of Neuroscience* **1995,** 15, (10), 6834-6845.

93. Kujawski, P. Klassifikation neuronaler Netzwerkaktivität kortikaler Kulturen auf Mikroelektrodenarrays mithilfe von Hidden-Markov-Modellen. Master Thesis, Fachhochschule Darmstadt, Darmstadt, 2005.

94. Selinger, J. V.; Pancrazio, J. J.; Gross, G. W., Measuring synchronization in neuronal networks for biosensor applications. *Biosensors & Bioelectronics* **2004,** 19, (7), 675-683.

95. Chiappalone, M.; Bove, M.; Vato, A.; Tedesco, M.; Martinoia, S., Dissociated cortical networks show spontaneously correlated activity patterns during in vitro development. *Brain Research* **2006,** 1093, 41-53.

96.     Jimbo, Y.; Kawana, A.; Parodi, P.; Torre, V., The dynamics of a neuronal culture of dissociated cortical neurons of neonatal rats. *Biological Cybernetics* **2000,** 83, (1), 1-20.

97.     Macdonald, R. L.; Rogers, C. J.; Twyman, R. E., Kinetic-Properties of the Gabaa Receptor Main Conductance State of Mouse Spinal-Cord Neurons in Culture. *Journal of Physiology-London* **1989,** 410, 479-499.

98.     Finley, M. F. A.; Kulkarni, N.; Huettner, J. E., Synapse Formation and Establishment of Neuronal Polarity by P19 Embryonic Carcinoma Cells and Embryonic Stem Cells. *Journal of Neuroscience* **1996,** 16, (3), 1056-1065.

99.     Korpi, E. R.; Grunder, G.; Luddens, H., Drug interactions at GABA(A) receptors. *Progress in Neurobiology* **2002,** 67, (2), 113-159.

100.    Morley, P.; MacPherson, P.; Whitfield, J. F.; Harris, E. W.; McBurney, M. W., Glutamate receptor-mediated calcium surges in neurons derived from P19 cells. *Journal of Neurochemistry* **1995,** 65, (3), 1093-9.

# List of Figures

## List of Tables

# Appendix

## *Recombinant pcDNA/TO-OR5 plasmid*

## *DNA sequence of part of the pcDNA4/TO-OR5 plasmid*

```
           EcoRI                  NcoI
           ~~~~~                  ~~~~~~
     1     AATTCTTTTT TTTTTAAACC ACCATGGGAT ACACCGACAT CGAGATGAAC CGGCTGGGCA AGACAGAAAG GAACCAAACT GTCATCTCCC AGTTCCTTCT
           TTAAGAAAAA AAAAATTTGG TGGTACCCTA TGTGGCTGTA GCTCTACTTG GCCGACCCGT TCTGTCTTTC CTTGGTTTGA CAGTAGAGGG TCAAGGAAGA
   101     CCTGGGCCTG CCCATTCCCC CAGAGCACCA GCACGTGTTC TACGCCCTGT TCCTGTCCAT GTACCTCACC ACTGTTCTAG GGAACCTCAT CATCATCATC
           GGACCCGGAC GGGTAAGGGG GTCTCGTGGT CGTGCACAAG ATGCGGGACA AGGACAGGTA CATGGAGTGG TGACAAGATC CCTTGGAGTA GTAGTAGTAG
   201     CTCATTCTAC TGGATTCCCA TCTCCACACA CCCATGTACT TGTTTCTCAG CAACTTGTCC TTCTCTGACC TCTGCTTTTC CTCTGTTACG ATGCCCAAGT
           GAGTAAGATG ACCTAAGGGT AGAGGTGTGT GGGTACATGA ACAAAGAGTC GTTGAACAGG AAGAGACTGG AGACGAAAAG GAGACAATGC TACGGGTTCA
                                                                                                        AvaI
                                                                                                        ~~~~~~~
   301     TGTTGCAGAA CATGCAGAGC CAAGTTCCAT CCATCCCCTA TGCAGGCTGC CTGTCACAAA TATACTTCTT TCTGTTTTTT GGAGACCTCG GGAACTTCCT
           ACAACGTCTT GTACGTCTCG GTTCAAGGTA GGTAGGGGAT ACGTCCGACG GACAGTGTTT ATATGAAGAA AGACAAAAAA CCTCTGGAGC CCTTGAAGGA
                     NcoI
                     ~~~~~~~
   401     GCTTGTGGCC ATGGCCTATG ACCGCTATGT GGCCATCTGC TTCCCCCTTC ATTACATGAG CATCATGAGC CCCAAGCTCT GTGTGAGTCT GGTGGTGCTG
           CGAACACCGG TACCGGATAC TGGCGATACA CCGGTAGACG AAGGGGGAAG TAATGTACTC GTAGTACTCG GGGTTCGAGA CACACTCAGA CCACCACGAC
   501     TCCTGGGTGC TGACTACCTT CCATGCCATG CTGCACACCC TGCTCATGGC CAGATTGTCA TTCTGTGAGG ACAATGTGAT CCCCCACTTT TTCTGTGACA
           AGGACCCACG ACTGATGGAA GGTACGGTAC GACGTGTGGG ACGAGTACCG GTCTAACAGT AAGACACTCC TGTTACACTA GGGGGTGAAA AAGACACTGT
   601     TGTCTGCTCT GCTGAAGCTG GCCTGCTCTG ACACCCGTGT TAATGAGGTT GTGATATTTA TTGTGGTCAG CCTCTTTCTT GTCCTTCCAT TTGCCCTCAT
           ACAGACGAGA CGACTTCGAC CGGACGAGAC TGTGGGCACA ATTACTCCAA CACTATAAAT AACACCAGTC GGAGAAAGAA CAGGAAGGTA AACGGGAGTA
   701     TATCATGTCC TATGTAAGAA TTGTGTCTTC CATTCTCAAG GTCCCTTCTT CTCAAGGTAT CTACAAAGCC TTTTCCACAT GTGGATCTCA CCTGTCTGTA
           ATAGTACAGG ATACATTCTT AACACAGAAG GTAAGAGTTC CAGGGAAGAA GAGTTCCATA GATGTTTCGG AAAAGGTGTA CACCTAGAGT GGACAGACAT
   801     GTGTCACTGT TCTATGGGAC AGTCATTGGT CTCTATTTAT GTCCTTCCAG TAATAATTCT ACTGTGAAGG AGACTGTCAT GTCTTTGATG TACACAGTGG
           CACAGTGACA AGATACCCTG TCAGTAACCA GAGATAAATA CAGGAAGGTC ATTATTAAGA TGACACTTCC TCTGACAGTA CAGAAACTAC ATGTGTCACC
   901     TGACTCCCAT GCTGAACCCC TTTATCTACA GCCTGAGGAA TAGAGATATA AAGGGAGCAA TGGAAAGAAT CTTTTGCAAA AGAAAAATTC AACTAAACCT
           ACTGAGGGTA CGACTTGGGG AAATAGATGT CGGACTCCTT ATCTCTATAT TTCCCTCGTT ACCTTTCTTA GAAAACGTTT TCTTTTTAAG TTGATTTGGA
                     NotI
                     ~~~~~~~~~
                          AvaI
                          ~~~~~~
  1001     ATAAGCGGCC GCTCGAGTCT
           TATTCGCCGG CGAGCTCAGA
```

136

# Curriculum Vitae

## Education

01/2004 - present  Max Planck Institute for Polymer Research, Johannes Gutenberg-University, Mainz, Germany, Ph.D. from Biology department (Dr. rer. nat.), degree expected 12/2007

07/2000 - 06/2003  National University of Singapore, Master of Engineering, Singapore, Singapore

07/1996 - 08/2000  National University of Singapore, Degree of Bachelor of Engineering (Mechanical) Second Class Honours (Lower Division) with a minor in Law, Singapore

## Research Experience

01/2004 - present  Max Planck Institute for Polymer Research, Ph.D. dissertation

- Thesis: Neurons derived from P19 embryonic carcinoma cells as a platform for biosensor applications – optimisation and characterisation
- Investigating the effect of self assembled monolayer on the growth of cells

10/2002 - 11/2003  National University of Singapore, Department of Materials Science, Faculty of Science, Research Assistant

- Investigation of the effects of nanopatterns on the proliferation and growth of osteoblasts, fibroblasts and mesenchymal progenitor cells
- Differentiation of human mesenchymal progenitor cells in PCL-PEG scaffolds

07/2000 - 08/2002  National University of Singapore, Faculty of Engineering, Master thesis

- Thesis: Development of skin substitute using polycaprolactone based membrane as epidermal substitute

07/1999 - 05/2000  National University of Singapore, Department of Mechanical Engineering, Faculty of Engineering, Final year project

- Thesis: The chemical characterisation of three-dimensional bioresorbable scaffolds for tissue engineering applications

## Awards

2006  Best paper award in the Journal of Materials Science-Materials in Medicine

## Training Certificates

2003  Responsible care and use of laboratory animals program, Office of life sciences, NUS laboratory animals centre

## Technical Expertise

Cell biology, biochemistry, molecular biology, in vivo experiments, tissue engineering, neurobiology, cell-based biosensor, surface modification, material surface characterisation, polymer characterisation

## Languages

First language: English, mother tongue: Mandarin, fluent in German

## Selected Publications in International Journals

1. **Khor, H. L.**; Kuan, Y.; Kukula, H.; Tamada, K.; Knoll, W.; Moeller, M.; Hutmacher, D. W., Response of cells on surface-induced nanopatterns: Fibroblasts and mesenchymal progenitor cells. *Biomacromolecules* **2007,** 8, (5), 1530-1540.
2. Ng, K. W.; **Khor, H. L.**; Hutmacher, D. W., In vitro characterization of natural and synthetic dermal matrices cultured with human dermal fibroblasts. *Biomaterials* **2004,** 25, (14), 2807-2818.
3. **Khor, H. L.**; Ng, K. W.; Htay, A. S.; Schantz, J. T.; Teoh, S. H.; Hutmacher, D. W., Preliminary study of a polycaprolactone membrane utilized as epidermal substrate. *Journal of Materials Science-Materials in Medicine* **2003,** 14, (2), 113-120.